Tasmania Department Of Resources and Energy

Division of Mines and Mineral Resources

REPORT 1991/10

Revocation report on the Melba Flats Exempt Area, SR 1987, No 216 of 11 km^2

by A. V. Brown

with contributions from R. G. Richardson and R. S. Bottrill and an Appendix by G. Thomas.

Two other Appendices are by B. D. Goscombe and A. V. Brown, These are also separate Division of Mines and Mineral Resources reports.

DIVISION OF MINES AND MINERAL RESOURCES, PO BOX 56, ROSNY PARK, TASMANIA 7018

2/63

CONTENTS

FIGURES

TABLES

3/63

ABSTRACT

Information gained from a diamond drill hole, and associated surface mapping, has proven that the western margin of the Serpentine Hill Ultramafic Complex has been thrust over a succession of andesitic, volcaniclastic wacke and interbedded graphitic mudstone. The thrust surface dips approximately 40° to 45° to the east. In places the mudstone units are highly mineralised. The mineralisation is mainly pervasive and consists of fine to medium-grained pyrrhotite with subsidiary pyrite, sphalerite, galena and chalcopyrite, with background values of gold and silver. Minor, thin, cross-cutting veins of quartz and calcite, containing fine to medium-grained cassiterite, are also present.

Because the underlying succession consists of andesitic, volcaniclastic wacke and graphitic mudstone, this succession is considered to be a correlate of the Rosebery Group sequences, as found in the Rosebery–Hercules–South Comet area to the east, rather than a continuation of the Crimson Creek Formation from the north.

Distribution of Platinum Group Elements (PGE) within samples obtained from six shallow drill holes within the ultramafic-mafic rocks, covered by the Exempt Area, are consistent with an earlier study which used surface samples. Analyses indicate that the majority of the rocks within the Serpentine Hill Ultramafic Complex are relatively enriched in PPGE (Pt-Pd-Rh) in comparison to IPGE (Os-I-Ru).

The Exempt Area also contains the Five-Mile or Cuni copper-nickel field, from which minor PGE values have also been recorded; two 'silver-lead-zinc' vein deposits, the McKimmie and Lead Blocks; and the Serpentine Hill asbestos deposits. Historical and background reviews of geological and geophysical projects over these deposits are presented.

INTRODUCTION

Exempt Area SR 1987 No 216, of 11 square kilometres, is enclosed by the corners CP650680, CP690680, CP690660, CP680660, CP680650 and CP650650 (fig. 1). The eastern side of the area is underlain by rocks belonging to the Serpentine Hill Ultramafic Complex and the western side by a succession of volcaniclastic lithic and quartz wacke with interbedded mudstone and siltstone. In the past this sequence has been mapped as being part of the Crimson Creek Formation, but because of the nature of the sequence obtained in the drill hole at Melba Flats and from railway cuttings to the south-west, this assumption must be re-evaluated. The rock successions cropping out in the south-eastern corner of the area belong to the Dundas Group, while outcrops of Crotty Sandstone occur in the south-western corner (fig. 2).

The area was exempted from the Mining Act so that follow-up work to an earlier project could be carried out on the Platinum Group Element (PGE) potential of the area. The earlier study (Brown *et al.*, 1988) consisted of mapping and surface sampling for later PGE analysis of the different ultramafic, gabbroic and basaltic rocks which comprise the Serpentine Hill Complex.

Initially, the follow-up programme consisted of six shallow drill holes, with the idea of obtaining samples for analysis from every 20 m, over a stratigraphic depth of 100 m, to check PGE distribution over a stratigraphic depth for each of the different rock types. Before this programme had been completed a decision was taken to revise the old (1962) Zeehan 1:63 360 scale geological map sheet and to produce an up-dated 1:50 000 scale geological map sheet. Because of the revision and information gathered in the lower 50 m of drill hole DDH-SH1 at Melba Flats, it was decided to deepen this drill hole to 500 m to see if the base of the ultramafic complex could be penetrated, and to ascertain the nature of the underlying sequence.

Deepening DDH-SH1 proved that the base of the ultramafic complex was a thrust fault along which the complex had over-ridden a previously unknown sequence of mineralised volcano-sedimentary rocks. Further deepening of the drill hole to 670 m was then undertaken to gather more information, so as to allow characterisation of this sedimentary sequence and associated mineralisation.

SUMMARY OF THE REGIONAL GEOLOGY

The exempt area is covered by the Zeehan 1:63 360 (1":1 mile) scale geological map (Blissett and Gulline, 1962). Numerous early reports, listed in the Bibliography, contain schematic geological maps and geophysical data. Differentiation of the ultramafic-mafic rocks of the Serpentine Hill Ultramafic Complex was carried out by Rubenach (1967, 1974). More recent regional mapping can be found in Brown (1986), and Brown *et al.*, (1988) contains detailed information on part of the complex.

The ultramafic complex on the eastern side of the Exempt Area consists of serpentinite sheaths around and between blocks of serpentinised peridotite, low-Ti quartz tholeiite lavas, and associated gabbroic rocks (Rubenach, 1967, 1974; Brown, 1986; Brown *et al.*, 1988).

Rubenach (1967; 1974) reported two lenses of foliated amphibolite, one on the western boundary and one on the northern boundary of the ultramafic complex. He considered these lenses to have been formed by deformation of the ultramafic rocks during tectonic emplacememt. The lense on the northern boundary, which crops out at the mouth of the Argent Tunnel, has recently been re-examined, and it is described as a mylonitic amphibolite lense having "... a strong foliation dipping moderately to the southeast" (Berry, 1988).

The diamond-drill hole at Melba Flats (SH1) encountered an amphibolite zone between approximately 50 and 277 metres. Preliminary analysis of this zone has been undertaken (Goscombe, 1991, Appendix 4). In summary, the amphibolite zone represents a packet of ductile shear zones which formed coincident with amphibolite facies metamorphism. A bare minimum lateral displacement of 200 m to 250 m occurred during ductile shear. The early ductile shear fabric was reactivated by thin, discrete shear bands and later-stage, brittle deformation with accompanying influx of retrogressive fluids. Total lateral displacement during both the ductile and later brittle episodes is unknown, but could have been on a kilometre-scale (Goscombe, 1991, Appendix 4).

Until the recent (1990) remapping of the area was undertaken, the volcaniclastic lithicwacke/mudstone succession had been considered as the southern extent of the Crimson Creek Formation. However wacke samples from the Melba Flats drill hole, and from railway and track cuttings to the west of Melba Flats, contain detritus from an andesitic volcanic source and the interbedded, mineralised mudstone horizons consist, in places, of in excess of 50% amorphous carbon (XRD analysis, sample Z.380/1, from SH1-381.5 m, Appendix 2). Neither the type of volcanism, nor the carbonaceous mudstone and associated mineralisation, are characteristic of sedimentary rocks from the Crimson Creek Formation in the type area, suggesting that the succession in the drill hole, and to the west, belongs to a different rock sequence. Further mapping will be undertaken to to try and resolve the problem.

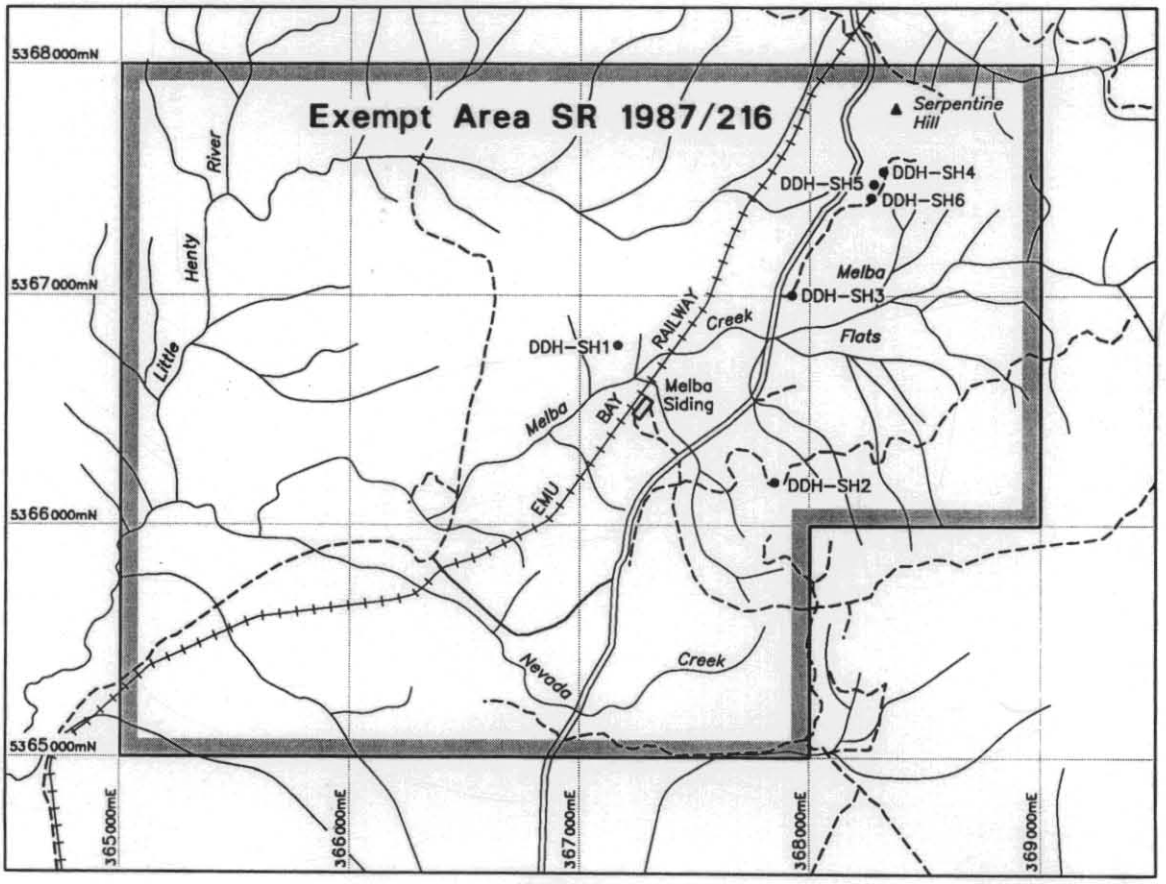

FIGURE 1
Location of Exempt Area SR 1987/216

5 cm

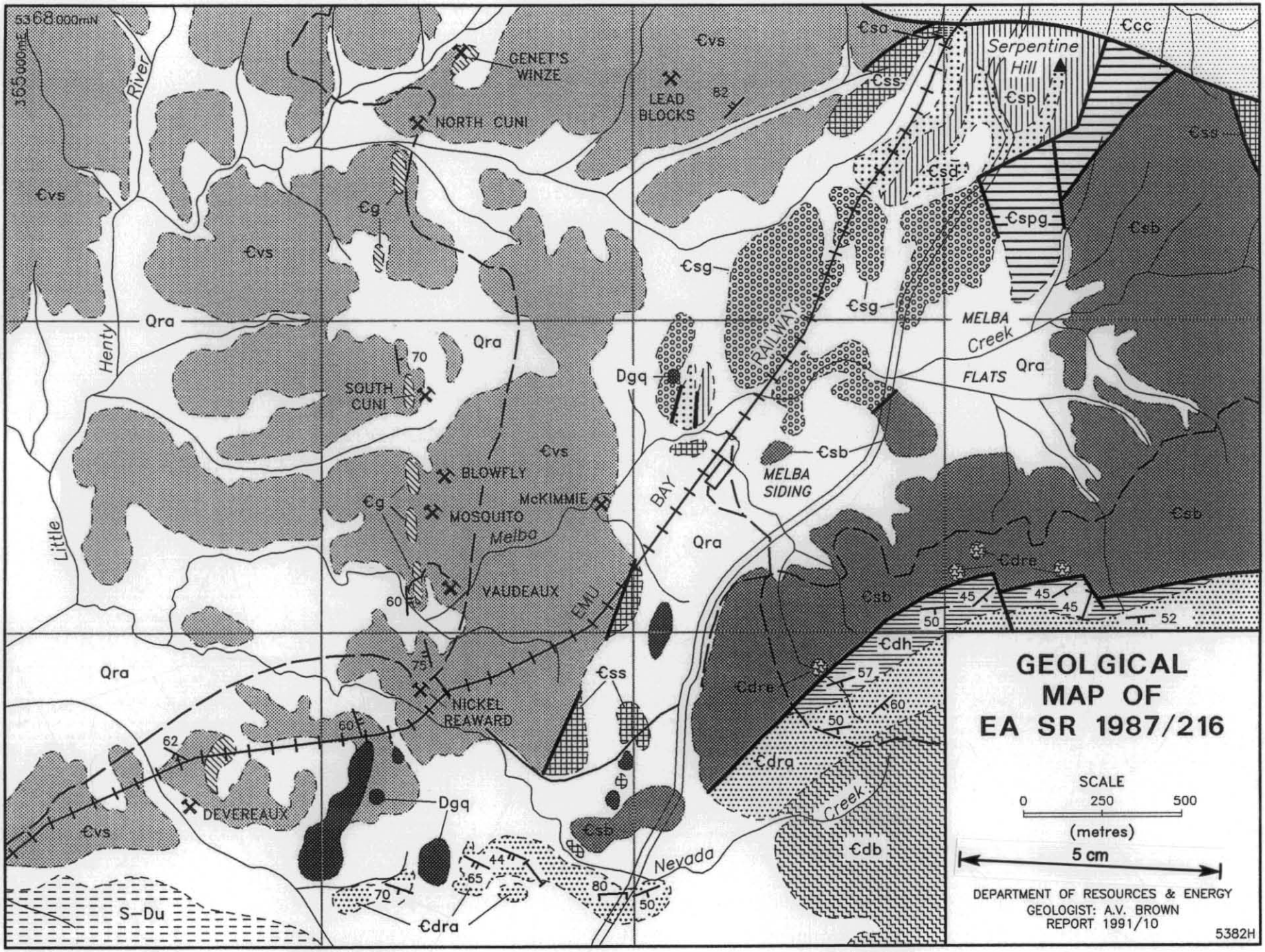
5368.000mN
365.000mE
River
Henty
Little
Melba
Creek
Nevada
Creek
BAY
EMU
RAILWAY
MELBA
FLATS
MELBA
SIDING
Serpentine
Hill
GENET'S
WINZE
NORTH CUNI
LEAD
BLOCKS
SOUTH
CUNI
BLOWFLY
McKIMMIE
MOSQUITO
VAUDEAUX
NICKEL
REAWARD
DEVEREAUX
Qra
Cvs
Cg
Csa
Ccc
Css
Csp
Csd
Cspg
Csb
Csg
Dgq
Cdre
Cdh
Cdra
Cdb
S-Du
82
70
60
75
62
44
65
80
50
45
52
57
GEOLGICAL
MAP OF
EA SR 1987/216
SCALE
0 250 500
(metres)
5 cm
DEPARTMENT OF RESOURCES & ENERGY
GEOLOGIST: A.V. BROWN
REPORT 1991/10
5382H

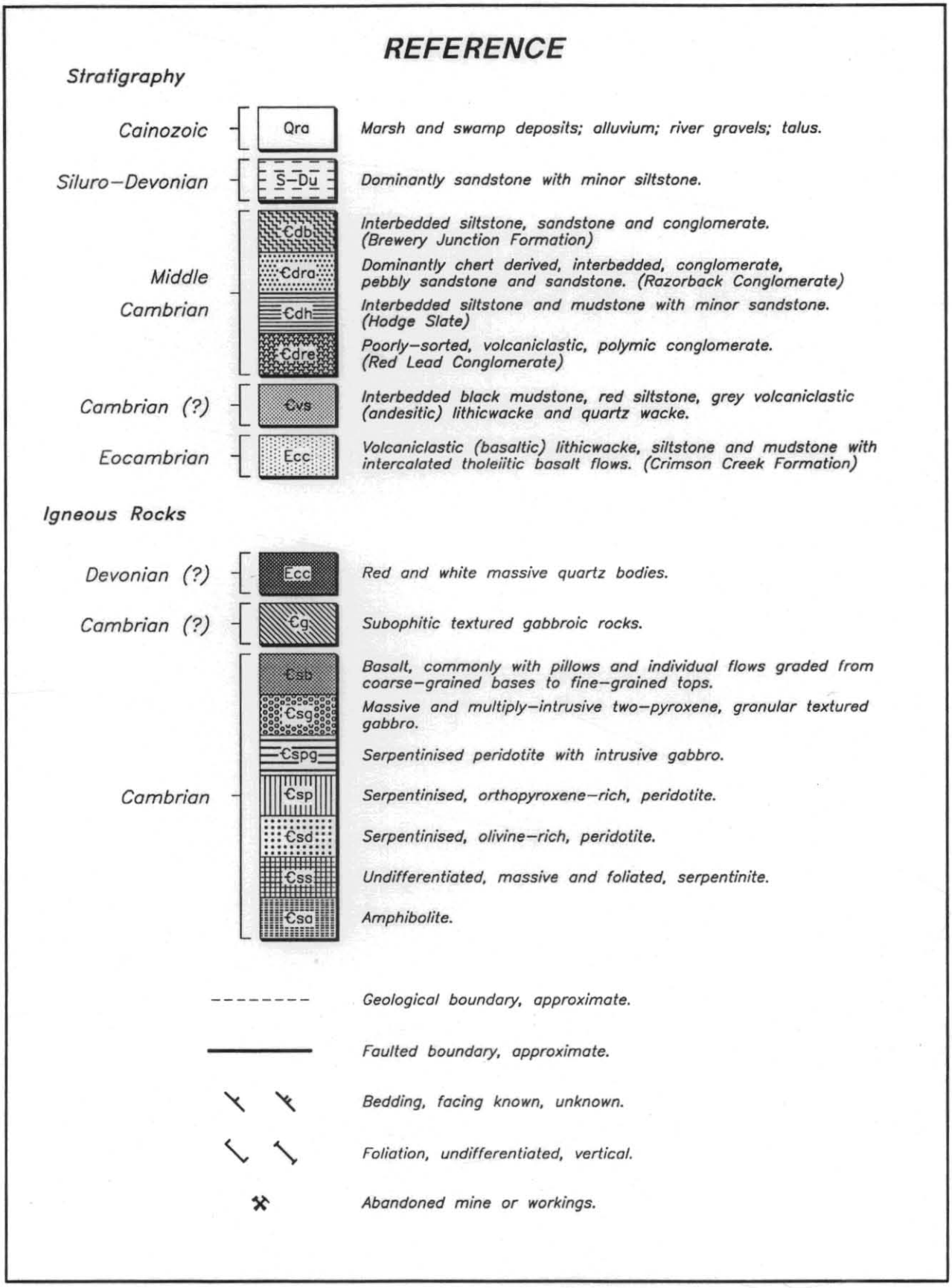

FIGURE 2

Geological map of Exempt Area SR 1987/216

SUMMARY OF THE RESULTS OBTAINED FROM THE DRILL HOLE PROGRAMME

Whole rock major and trace element analyses of representative samples from the six drill holes are included as Appendix 3. The following summary of the information obtained from the programme has been broken into sections based on mineralisation type, i.e. PGE, nickel, and precious and base metals.

Platinum Group Element (PGE) mineralisation

A comparison of the results obtained from a study of the various rock types within the Serpentine Hill Ultramafic Complex for Platinum Group Elements (PGE) (Brown *et al.*, 1988), and the results from samples of drill core from this study, show that although absolute values vary, the same overall trend occurs. Combining the data from both studies show that there are three diferent ultramafic lithologies, each with a different chrome spinel composition and each with different PGE values (Table 1).

The most chrome-rich spinels, measured by the ratio Cr* = Cr/Cr + Al and using electron microprobe analytical data, came from the Melba Flats area (Table 1). These spinels have a Cr* of ~84 and an Mg* = (Mg/Mg + Fe^{2+}) of ~50, and occur in serpentinised orthopyroxene-bearing dunite, which also contains a high concentration (up to approximately 5%) of disseminated and ponded chrome spinel grains.

Drill Hole SH1 was collared at the spot where a surface sample with reasonable PGE values (Pt – 1240 ppb; Pb – 4 ppb; Rh – 54 ppb; Ir – 70 ppb; Ru – 180) was obtained during the original study (Brown *et al.*, 1988). A 20 mm thick chromitite band was encounted in the drill hole at a depth of eight metres. This band contained spinel grains with Cr* of 84.6 and Mg* of 52 and gave lower overall values for PGE (SH1/2, Table 1, fig. 3), especially for PPGE (Pt, Pd, Rh), but gave reasonable IPGE (Os, Ir, Ru) values.

The main problem with the Melba Flats area is that ultramafic rock types change rapidly in both surface outcrop and in the drill hole. The high chrome spinel (Cr* ~84) dunite sequence, constituting the surface outcrop, is faulted out at approximately 10 m below the surface. Below this is approximately 50 m of an olivine-rich peridotite sequence with chrome spinel grains which have Cr* ~68; approximately 10 m of an orthopyroxene-rich peridotite with Cr* ~56; and then another 15–20 m slice of serpentinite with Cr* ~84 occurs before the main part of the amphibolite zone is reached.

In the area of drill holes SH4, 5 and 6 (fig. 1), the surface outcrops and the upper parts of the drill holes consist of serpentinised olivine-rich peridotite which contains lenses and zones with high concentrations of disseminated chrome spinel, with Cr* ~68 and Mg* ~38 (fig. 3), the Mg values being low because of alteration. Surface chromitite

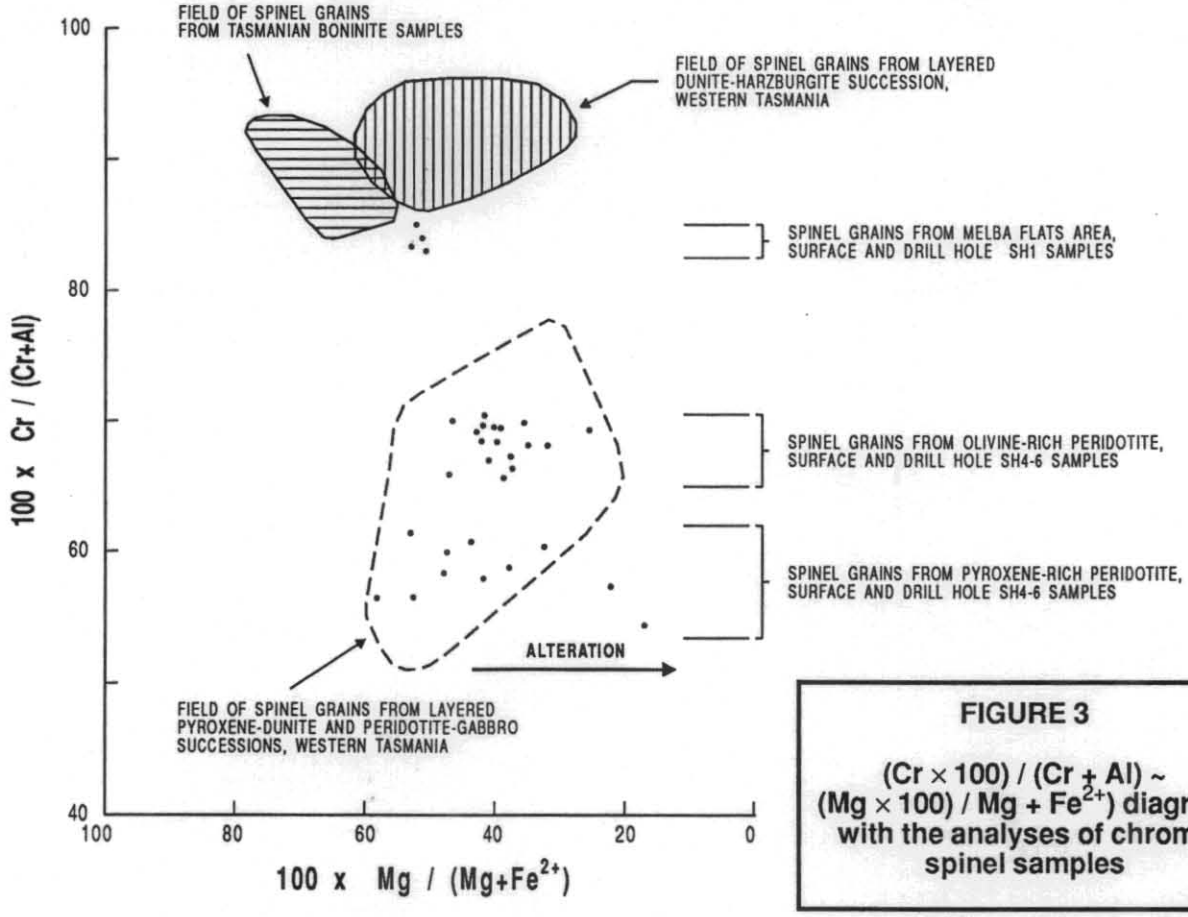

FIGURE 3

(Cr × 100) / (Cr + Al) ~ (Mg × 100) / Mg + Fe^{2+}) diagram with the analyses of chrome spinel samples

5 cm

8/63

TABLE 1

Composition of chrome spinel grains and analyses for gold and Platinum Group Elements of samples from the Serpentine Hill drill holes (SH1–6)

Sample No.	Depth (m)	Rock type	Cr*	Mg*	Au	Ir	Os	Pd	Pt	Ru	Pt*
Detection Limits					1	0.5	5	10	20	20	2
SH1/11	1.0	Serpentinised dunite	84.1	51.7	-	-	-	-	-	-	-
SH1/2	8.0	Chromitite	83.2	51.5	20	51	58	<	32	220	19
SH1/3	20.0	Serpentinised pyroxene-bearing dunite	66.1	46.5	34	<	<	<	<	<	6
SH1/5	62.5	Amphibolitised, serpentinised peridotite	54.4	15.5	17	<	<	<	<	<	7
SH1/6	78.5	Serpentinised dunite	84.8	51.1	13	1.0	<	<	<	<	3
SH1/8	104.5	Amphibolitised, serpentinised peridotite	57.5	21.3	4	1.0	<	22	<	<	7
SH2/1	62	Basaltic breccia	-	-	220	<	<	28	<	<	14
SH2/3	113	Fine-grained basalt	-	-	17	<	<	15	21	<	14
SH2/5	148	Fine-grained basalt	-	-	21	<	<	<	<	<	5
SH3/1	46.5	Gabbro	-	-	44	<	<	<	<	<	8
SH3/2	66.0	Gabbro	-	-	23	<	<	<	<	<	5
SH3/3	91.5	Gabbro	-	-	22	<	<	<	<	<	10
SH3/4	114.5	Gabbro	-	-	41	<	<	<	<	<	5
SG3/5	138.5	Gabbro	-	-	11	<	<	<	<	<	6
SH4/1	15.5	Serpentinised peridotite	70.1	34.9	15	<	<	<	<	<	3
SH4/2	33.0	Serpentinised peridotite	69.5	40.8	17	0.9	<	<	<	<	<
SH4/4	66.0	Serpentinised peridotite	56.3	58.4	21	0.5	<	<	<	<	<
SH4/6	92.0	Serpentinised peridotite	-	-	40	<	<	<	<	<	10
SH4/7	100.0	Serpentinised peridotite	-	-	380	1.8	<	<	<	<	<
SH5/1	22.5	Serpentinised pyroxene-dunite	66.4	36.3	10	<	<	<	<	<	2
SH5/2	41.5	Serpentinised pyroxene-dunite	67.1	36.0	37	<	<	<	<	<	2
SH5/3	54.5	Serpentinised pyroxene-dunite	70.2	40.7	5	2.2	4	7	18	<	2
SH5/4	65.0	Serpentinised pyroxene-dunite	67.0	39.8	13	1.1	<	<	<	<	5
SH5/5	86.5	Serpentinised pyroxenite	62.6	40.0	-	-	-	-	-	-	12
SH5/6	100.0	Serpentinised pyroxenite	-	-	9	1.1	<	<	<	<	6
SH6/1	11.5	Serpentinised pyroxene-dunite	65.7	37.7	43	3.4	<	<	<	<	23
SH6/2	34.5	Serpentinised pyroxene-dunite	68.4	39.2	43	5.0	<	<	<	<	6
SH6/3	47.5	Serpentinised pyroxene-dunite	69.3	38.9	30	3.0	<	<	<	<	4
SH6/5	81.5	Serpentinised pyroxene-dunite	68.5	40.9	14	2.9	<	<	<	<	3
SH6/6	101.0	Serpentinised pyroxenite	59.1	37.2	48	1.6	<	43	<	<	10

– = Not determined < = Less than detection limits

Cr* = Cr / (Cr + Al) Mg* = Mg / (Mg + Fe^{2+})

Values for Au, Ir, Os, Pd, Pt and Ru in parts per billion

Pt* by XRF, Division of Mines and Mineral Resources laboratory

Ir, Os, Pd, Pt and Ru by Neutron Activation Analyses, Becquerel Laboratories Pty Ltd, Lucas Heights, NSW

samples from this zone (Table 3, Brown *et al.*, 1988) contain detectable PPGE (Pt ~35 ppb; Pd ~2.5 ppb; Rh ~5 ppb). Samples from the drill holes have detectable Au (10–43, av. ~23 ppb) as well as values for Ir (1–5 ppb) and Pt (up to 23 ppb).

The lower parts of the three drill holes pass into orthopyroxene-rich peridotite, characterised by chrome spinel grains with Cr* ~59 and Mg* ~39 (fig. 3). These rocks usually have very low to undetectable values of PGE (Table 1), however, one sample (SH4/7) is anomalously high in Au (380 ppb) and another sample (SH6/6) anomalously high in Pd (43 ppb). A third sample (SH1/8), which has as an anomalously high value for Pd (23 ppb), is petrographically similar to a sample from the lower part of the Melba Flats drill hole (SH6/6), which also has a high Pd Value (43 ppb).

Surface samples of both the low-Ti tholeiitic basalt and two-pyroxene granular gabbro gave detectable Pt (~37 ppb for basalt and ~36 ppb for gabbro) and Pd (~25 ppb for basalt and ~10 ppb for gabbro) values (Brown *et al.*, 1988). In comparison, samples from DDH-SH2 and DDH-SH3 (Table 1) gave lower values for both Pt (basalt ~11 ppb; gabbro ~7 ppb)) and Pd (basalt ~20 ppb; gabbro below detection limit). All basaltic and gabbroic samples from the drill holes have Au values, with one sample of basalt (SH2/1), containing 220 ppb.

Overall, the ultramafic rocks at the top of the Melba Flats drill hole (SH1) having the higher IPGE (Os-Ir-Ru) values contain the spinel grains with a chemical signature (Cr* ~84) which is close to that of spinel grains within the 'osmiridium'-bearing ultramafic lithologies of western Tasmania (Cr* ~90), and probably represent a variation of this group of ultramafic rocks. These ultramafic rocks formed as a magma chamber cumulate from the magma which also produced the boninitic lavas found in the Heazlewood and Stonehenge areas of western Tasmania (Brown and Jenner, 1989).

The rocks with the higher PPGE (PT-Pd-Rh) in drill holes SH4–6 are associated with the low-Ti tholeiitic basalt and two-pyroxene granular gabbro (drill holes SH2 and SH3 respectively). This group of ultramafic rocks was formed by multiple magma intrusions into a magma chamber, producing an early orthopyroxene-rich peridotite, characterised by spinel grains with Cr* ~59, followed by a later olivine-rich peridotite, characterised by spinel grains with Cr* ~68 (Table 1).

In summary, the results of both the earlier and present surveys are consistent, even though absolute PGE values vary. The combined results are also consistent with the fact that 'osmiridium' is found in western Tasmania in association with ultramafic rocks with high IPGE, the Layered Dunite-Harzburgite succession (LDH), and the ultramafic rocks with the higher PPGE values belong to the Layered Peridotite-Gabbro (LPG) and Layered Pyroxene-Dunite (LPD) successions of Brown (1986).

Nickel mineralisation within the ultramafic rocks

Some of the drill hole samples of serpentinised peridotite from the Serpentine Hill area (e.g. DDH 5 and 6) are pervaded by small (5–10 μm), anhedral grains of cobalt-bearing pentlandite, minor cobalt-bearing millerite, and subsidiary nickeliferous chalcopyrite. These grains occur in fractures within the primary mineral grains or are pervasively throughout the serpentinitic matrix.

The source of this mineralisation is unknown, however it is secondary and contains similar nickel minerals to those found in the Cuni area to the west.

Analyses of grains of the above-mentioned minerals were obtained by use of the Electron Microprobe, Central Science Laboratory, University of Tasmania (AVB) and are listed in Table 2.

Table 2

Sample No.	Grains*	Cu	Ni	Fe	Co	S
Pentlandite						
SH5/2	(5)		0.3247	0.1666	0.0413	0.4679
SH5/3	(5)		0.3237	0.1585	0.0494	0.4683
SH5/4	(5)		0.3192	0.1864	0.0242	0.4702
SH6/3	(5)		0.3239	0.1572	0.0521	0.4681
SH6/5	(8)		0.3220	0.1732	0.0358	0.4688
SH6/6	(10)		0.2977	0.2096	0.0240	0.4687
Millerite						
SH5/1	(5)	0.4292	0.0107	0.0468	0.5133	
SH6/3	(2)	0.4759	0.0048	0.0151	0.5042	
Ni-Chalcopyrite						
SH6/3	(1)	0.1901	0.1970	0.1061	0.0025	5.043

* The numbers in brackets are the number of grains analyses in each sample, the results presented are an average of these analyses.

Polished thin section descriptions of samples SH5/1–4 and SH6/3–6 have been examined for nickel-bearing minerals by R. S. Bottrill. He summarised the presence of the following minerals:

Pentlandite

Traces to ~0.5% (especially SH5/2, SH5/3 and SH6/6). The grains occasionally appear euhedral but most commonly are irregular, anhedral and are typically interstitial or intergrown with serpentinite or magnetite. Grains are usually ~50 μm across but some rare skeletal crystals up to 350 μm (in SH6/3) do occur. Some alteration to millerite is commonly present, and inclusions of chalcopyrite and galena also occur (especially in SH6/3).

Millerite

Traces, much less common that pentlandite, noted in SH5/1, SH5/2 and SH6/3. Grains are usually anhedral and somewhat smaller than pentlandite, which it is partially replacing. Disseminated throughout the groundmass in a similar manner to pentlandite.

Chalcopyrite

Traces, similar in abundance to millerite. Noted in SH5/3, SH5/4, SH6/3, SH6/5 and SH6/6. Grains usually ~10 μm.

Galena

Faint traces, rarer than chalcopyrite. Noted in SH5/3, SH5/4, SH6/3, grains usually <10 μm. Usually associated with pentlandite and chalcopyrite as fine inclusions or rimming grains.

Precious and base metal values from the sedimentary succession in the lower part of DDH-SH1

Numerous zones of mineralised, black, graphitic mudstone were encountered throughout the lower 400 m of DDH-SH1 (core log, Appendix 2). These zones contained pyrrhotite ± pyrite ± sphalerite ± galena ± chalcopyrite.

Eighteen (18) samples were selected, at random, over the interval and analysed for precious (Au and Ag) and base (Cu, Pb, Zn, and Sn) metals. The values obtained are presented in Table 3.

All samples analysed contained copper and zinc as well as background values for gold and silver. Most samples also contain lead and a few, tin (Table 3). Two samples, Z491 (297 m) and Z508 (671 m), gave good lead and zinc values as well as containing tin.

In places, these zones are cut by thin, mineralised, quartz veins which contain sphalerite, galena and minor cassiterite. So far none of these veins have been analysed, however polished thin section descriptions were undertaken by R. S. Bottrill:

- Sample Z380/2 from 296.05 m — mineralised quartz vein. Polished section reveals sphalerite with inclusions of pyrrhotite and chalcopyrite; galena; fine blebs of pyrrhotite; chalcopyrite; and traces of bornite. Most of the sulphides are intergrown and cogenetic with each other and the host. The sphalerite with pyrrhotite and chalcopyrite is late stage exsolution and/or replacement.

- Sample Z382 from 463.5 m — mineralised mudstone. Polished thin section shows that the black mudstone is strongly replaced and veined by carbonate and sulphides. The shale itself is strongly graphitic, but the graphite is mostly very fine-grained. Fine- to medium-grained sulphides are disseminated throughout. These consist predominantly of pyrrhotite with minor to rare sphalerite and chalcopyrite. The grains appear epigenetic or vein-related. Some fine- to medium-grained cassiterite is also present, as is rare leucoxene.

  The veins are mostly carbonate with rare quartz and micas, and minor to abundant sulphide grains. The dominant sulphide is again pyrrhotite, but sphalerite and pyrite are more abundant. The pyrite is porous and appears to be replacing pyrrhotite, as is minor fine-grained marcasite. The sphalerite is iron-rich and contains inclusions of pyrrhotite and chalcopyrite. Galena is very rare and fine grained.

Down-hole magnetic susceptibility survey of DDH-SH1

A down-hole magnetic susceptibility survey was carried out on DDH-SH1 as a test excercise using new equipment. Four runs were undertaken. Zero metres for the runs was plus one metre above ground level. Run 1 went to a depth of 260 m before meeting a blockage in the hole. Runs 2–4 were undertaken after the blockage was removed and the hole finished. Run 2 went down to 590 m and was used for meter adjustments. Run 3 was up hole from 590 m. These results are presented as Figure 4. Run 4 resurveyed the zone between 145 m and 190 m on a less sensitive scale. Original data for all or any of these runs can be obtained from the Division on request.

A number of zones of high readings were obtained. Preliminary work has identified a reason for most of these but further work is needed. A number of spikes were recorded during the runs, especially those at 218 m, 279 m, and 325 m; so far, however, these have not been resolved.

Four zones of high readings were obtained:

(i) The peak at 8.0 m corresponds to a 20 mm thick lense of chromitite.

(ii) The peaks from 10 to 30 m and 70 to 100 m correspond to serpentinised peridotite with varying amounts of secondary magnetite.

(iii) Three high areas between 150 m and 190 m (~154 m; 164–166 m, and 182–185 m) coincide with banded amphibolite containing varying amounts of magnetite.

(iv) The zone between ~350 m and 360 m contains sedimentary rocks dominated by foliated quartz wacke with minor graphitic mudstone. Along most foliation planes sulphide mineralisation, dominated by pyrrhotite, is abundant.

The 18 areas from which mineralised mudstone samples were taken for metal analyses gave readings of between 200 and 400 SI units.

5 cm

FIGURE 4

Magnetic susceptibility results, DDH-SH1, Run 3.

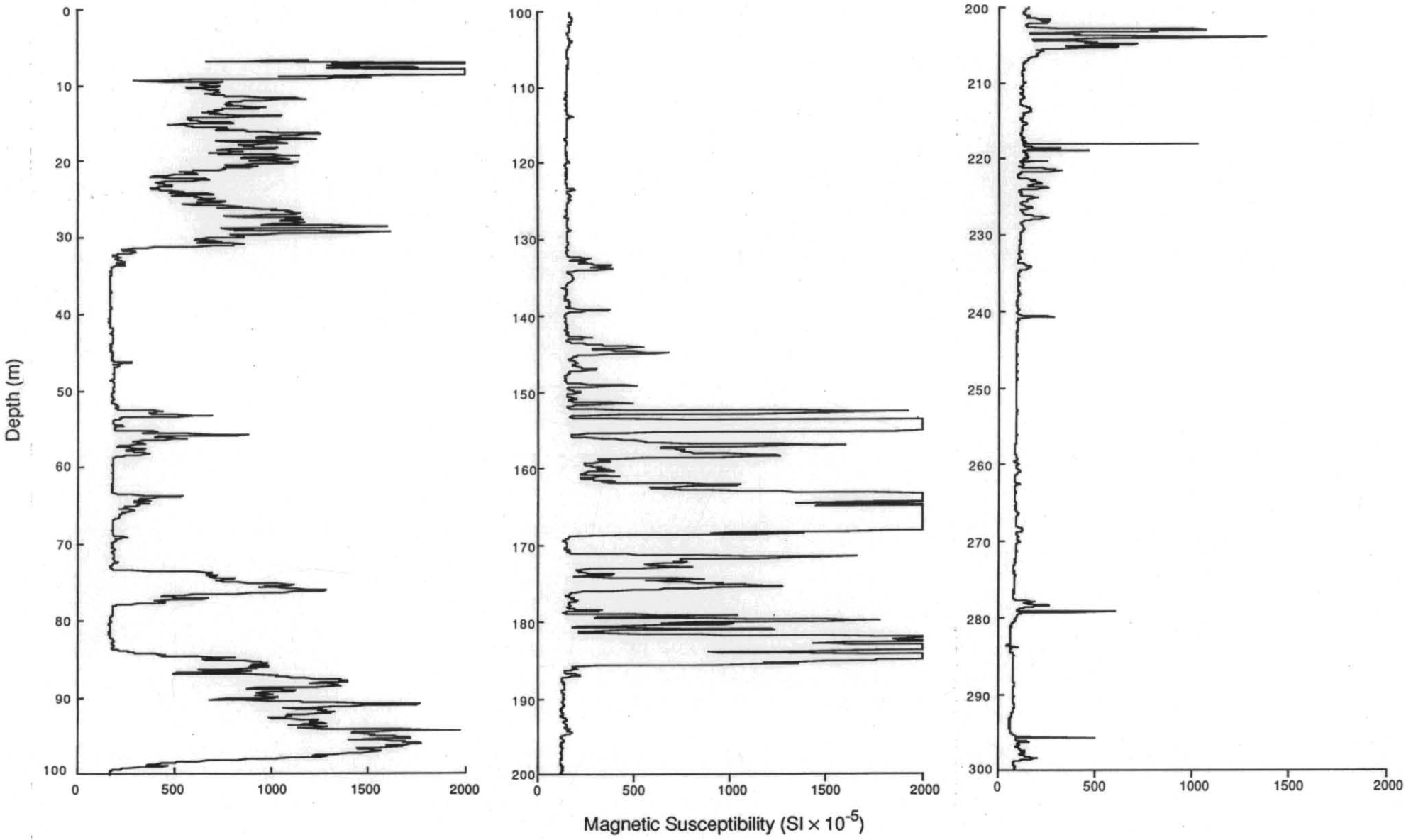

11/63

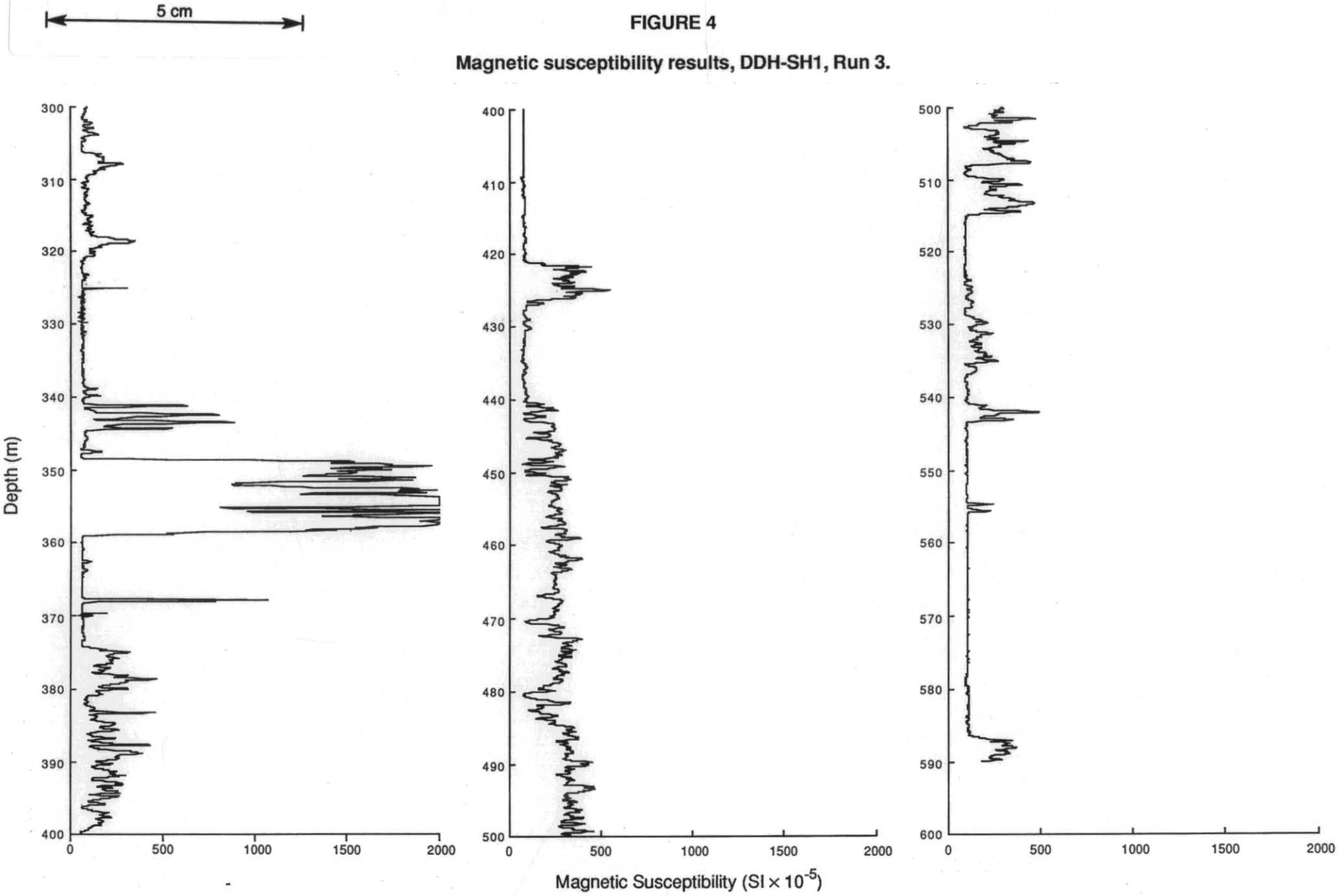

FIGURE 4

Magnetic susceptibility results, DDH-SH1, Run 3.

12/63

TABLE 3

Analyses of samples for precious and base metals, DDH-SH1

Sample No.	Depth (m)		Au ppb	Ag ppb	As ppm	Cu ppm	Pb ppm	Zn ppm	Sn ppm
		D.L.	0.1	0.05	20	5	10	5	10
Z.491	297.0		1.3	6.0	<	240	2200	7300	22
Z.492	319.8		1.8	3.2	<	145	46	220	<
Z.493	369.4		7.2	5.3	22	430	440	780	38
Z.494	377.2		12.6	5.2	<	165	115	150	<
Z.495	389.2		7.2	0.2	<	115	26	150	13
Z.496	393.2		1.6	0.2	<	240	10	135	<
Z.497	425.3		0.3	2.8	<	140	16	60	<
Z.498	442.2		1.4	1.5	<	250	67	88	<
Z.499	453.0		7.5	5.2	<	210	50	410	<
Z.500	484.9		1.8	3.4	<	160	45	83	<
Z.501	492.2		1.7	4.6	<	145	<	130	<
Z.502	504.0		13.0	0.5	<	195	<	82	<
Z.503	543.8		2.4	0.2	<	190	110	150	<
Z.504	590.5		2.0	2.4	<	220	11	45	<
Z.505	607.1		1.4	0.3	<	230	40	75	<
Z.506	612.1		1.3	0.8	<	39	<	69	<
Z.507	642.4		1.7	3.7	<	82	15	81	<
Z.508	670.6		7.0	4.4	<	38	3800	6600	38

D.L. Detection limits < Less than detection limit

Au & Ag analysed using aqua-regia digest/Carbon Furnace Atomic Absorption Spectro-Photometry
As, Cu, Pb, Zn, & Sn — analysed by XRF
Analyses by Department of Resources and Energy Laboratories, Rosny Park

14/63

REVIEW OF THE FIVE MILE OR CUNI COPPER-NICKEL FIELD

Introduction

Included within the Exempt Area is the North Dundas/Five Mile/Cuni Copper-Nickel Field, and two stringer vein lead-zinc deposits, the Lead Blocks and McKimmie prospects.

Parallel with, but to the west of, the line of Cu-Ni mineralisation at Cuni is a thick (50 m+) gabbroic dyke, the Cuni Dyke. This dyke contains secondary sulphide mineralisation. On preliminary chemical and petrographic characteristics it is different to the gabbroic bodies associated with the ultramafic rocks of the Serpentine Hill Ultramafic Complex, and from literature descriptions, different to the dykes associated with the Cu-Ni mineralisation.

Data from old reports (summarised in Taylor and Burger, 1952) and later drilling (Hovarth, 1957; Robinson, 1959) indicate that the Cu-Ni mineralisation occurs within an "ultrabasic/basic dyke" system. The ore bodies occurred around the footwall of these 'dykes'. Some of the old drill holes intersected small veins of galena and siderite cutting the Cu-Ni mineralisation. The highest values of nickel and copper were obtained from samples collected from near the footwall of the 'dykes', or within the sedimentary rock just below the contact.

The history and a detailed description of the different lodes in the Five-Mile/Cuni Copper-Nickel Deposits are contained in Taylor and Burger (1952). Detailed work on the mineralogy of the deposits can be found in Williams (1958), and the area is included in a review by Hughes (1965).

Williams (1958) distinguished two different ore groups from the five main mines within the Cuni area. These associations he listed as:

"(1) High grade pentlandite-pyrrhotite ore at North and South Cuni and at the Vaudeau Mine", and

"(2) High grade millerite ore at the Nickel Reward and Devereaux prospects, together with low grade millerite mineralisation at North Cuni."

Petrographic, XRD, and spectroscopic descriptions of samples of the copper-nickel ore from various workings in this field can be found in Stillwell (1946*b*) and McAndrew (1956). Descriptions of mineragraphic examination (Edwards, 1957; Williams, 1957) and flotation tests on tailings (Stillwell, 1946*a*) are also available.

Historical background

Four periods of exploration and mining have occurred in the Five-Mile/Cuni field. The histories of the different lease areas are included in Appendix 1.

In their summary, Taylor and Burger (1952) reported that four leases were pegged in the vicinity of Nickel Junction on 20 June 1893. One of these, 1925/91M, was granted as a reward claim for copper and a second, 1926/91M, was granted as a reward claim for nickel. With the exception of a shaft being sunk to an unknown depth on the latter lease during 1894, no other work is recorded on any lease issued during 1893–94, and the last of this early batch of leases became void during August 1898.

A second period of activity started during 1909 and continued until 1914. A bulk sample of ore obtained from the field during 1912 was assayed in England, and gave 17.00% Ni and 6.45% Cu. During the 1909–1914 period average assays from trial shipments of ore were 8–11% Ni and 4–14% Cu (Taylor and Burger, 1952).

Between 1928 and 1932 a third period of activity occurred during which a number of shafts and drives were cut. During this period approximately 960 tons of ore was extracted and drilling, as a follow-up to geophysics, was carried out by the Department of Mines. Details of the drilling are also included in Taylor and Burger (1952).

A fourth period of activity occurred during 1938 when approximately 278 tons of ore was extracted. Further drilling was undertaken by the Department of Mines in 1939–40. Between 1946 and 1948 another phase of mining was undertaken, with 750 tons of ore being mined during 1948. Details of production, values and extent of workings from the different shafts are included in Taylor and Burger (1952).

Taylor and Burger (1952) also noted that the ore bodies generally occurred on the footwall side of the 'gabbroic dykes' or at the lower contact of the 'dykes' with the sedimentary rocks. However, in some areas the ore was enclosed entirely by the 'dyke'.

Silver-lead, zinc occurrences

Within the Cuni area two 'Silver-Lead' mines, the Lead Blocks and McKimmie, have been worked. Both of these mines consisted of vein systems of galena and sphalerite in a gangue of quartz and carbonate. The Lead Blocks workings are recorded as having produced 2180 tons of ore from which was extracted 1420 tons of lead and 120,000 oz of silver. The McKimmie workings produced at least 56 tons of ore from which 35 tons of lead and approximately 3000 oz of silver were obtained (Blissett, 1962).

Platinum Group Element occurrences

Before 1980 the only report of PGE from rocks covered by the Exempt Area was that of platinum and palladium, associated with copper-nickel ore at two separate locations.

The first record was for ore obtained from the Devereaux ore body (Reid, 1925). Samples of ore from this body assayed: 0.1–0.16 oz per ton platinum; 0.02–0.04 oz per ton gold; 1.1–1.4 oz per ton silver; with 13–18% copper and 5–9% nickel.

The second sample was from ore obtained from Munro's Shaft and contains 1–2 dwt/ton platinum and paladium in a medium to fine-grained granule association of magnetite, pyrite, pyrrhotite, pentlandite and chalcopyrite. Spectroscopic analysis indicated that the platinum and palladium were in approximately equal proportions (Stillwell, 1946*b*).

During 1982 and 1984 surface samples were obtained from the Serpentine Hill and Melba Flats areas and analysed for PGE. The results of this study are recorded in Brown *et al.* (1988). Values obtained during this study, and a review of the Tasmanian ultramafic rocks and their PGE values, are included as Appendix 5.

ASBESTOS DEPOSITS ON SERPENTINE HILL

Asbestos has been mined from the ultramafic rocks at Serpentine Hill, on the north-eastern side of the Exempt Area. An overall review of asbestos in Tasmania was carried out by Taylor (1955). This report reviews the Serpentine Hill area as the "Argent Tunnel Prospect" (pp. 80–88). A specific report of the area was written by Knight (1946).

Taylor records that the "...distribution of fibre throughout the various orebodies is so irregular that the only effective way of sampling is to mill large parcels." Mining occurred during the early 1940's and by the end of October 1945 approximately 6141 tons of ore had been processed with a recovery of 360 tons of bagged fibre.

GEOPHYSICAL BACKGROUND

R. G. Richardson

History of geophysical exploration in the Cuni Area.

The first geophysical work in the Cuni area is recorded in the report of the Imperial Geophysical Experimental Survey (Edge and Laby, 1931). Most of the work was conducted in the northern part of the area (fig. 5) and consisted of a reconnaissance equipotential line survey followed by more detailed investigations with the AC potential ratio, high frequency and magnetic methods. The equipotential survey showed three zones of interest, two of them being over known workings. Both the AC potential ratio and high frequency surveys showed a number of small anomalies, whilst the magnetic method showed that the basic dykes were essentially non-magnetic.

A number of areas were recommended for geological follow-up and the Department of Mines trenched or drilled these sites. Minor sulphides were encountered in all localities.

In response to requests from the Department of Mines and an exploration company, the Bureau of Mineral Resources (BMR) carried out self-potential, electromagnetic and magnetic surveys in the Cuni area between May 1952 and March 1953 (Keunecke, 1953). With the exception of one strong self-potential anomaly in the Cuni North area, the self-potential anomalies are limited in extent and are of small amplitude (fig. 6). A number of the anomalies were trenched and found to be due to pyritised shear zones, weak lead-zinc mineralisation, or pyritic and graphitic shales. In the Cuni North area the anomaly is closely associated with a known basic dyke and old workings, and may result from several sources separated by cross-faults.

Electromagnetic measurements were made mainly in the Cuni North area and showed a general picture of the strike and extent of mineralisation. In the Cuni South area the only significant anomalies coincide with the position of the basic dyke. As expected from the results of Edge and Laby (1931), the magnetic survey failed to detect any of the basic intrusive rocks. The BMR selected several drilling targets (fig. 7).

The BMR carried out further self-potential and magnetic surveys in the southern part of the Cuni area at the request of Montana Silver Lead N.L. during October 1956, and from March to May 1957 (Horvath and O'Connor, 1958). Several self-potential anomalies were found, and testing of two of large areal extent showed them to be related to graphitic slate. Several small magnetic anomalies were found, and drilling of one showed low grade nickel and chrome mineralisation associated with magnetite within the serpentine belt.

Following a regional aeromagnetic survey covering much of north-west Tasmania Rio Tinto Australian Exploration selected a variety of sites for further work. In 1960 they carried out magnetic and self-potential surveys over an aeromagnetic anomaly (fig. 9) considered to occur in an environment favourable for Renison Bell-type mineralisation (Mattocks, 1960). The ground magnetic survey showed several anomalies. One having a northerly strike and continuous over several lines was attributed to a near-surface basic intrusive. No definite self-potential anomalies were detected.

The next survey for which data is held was a TURAM survey for the Electrolytic Zinc Company performed by Seigel Associates (Howland-Rose, 1971). The more interesting anomalies generally have limited strike extent and moderate conductivity. The anomaly trends (fig. 8) are similar to those observed previously. Most of the conductors were interpreted to lie between 80 ft (24 m) and

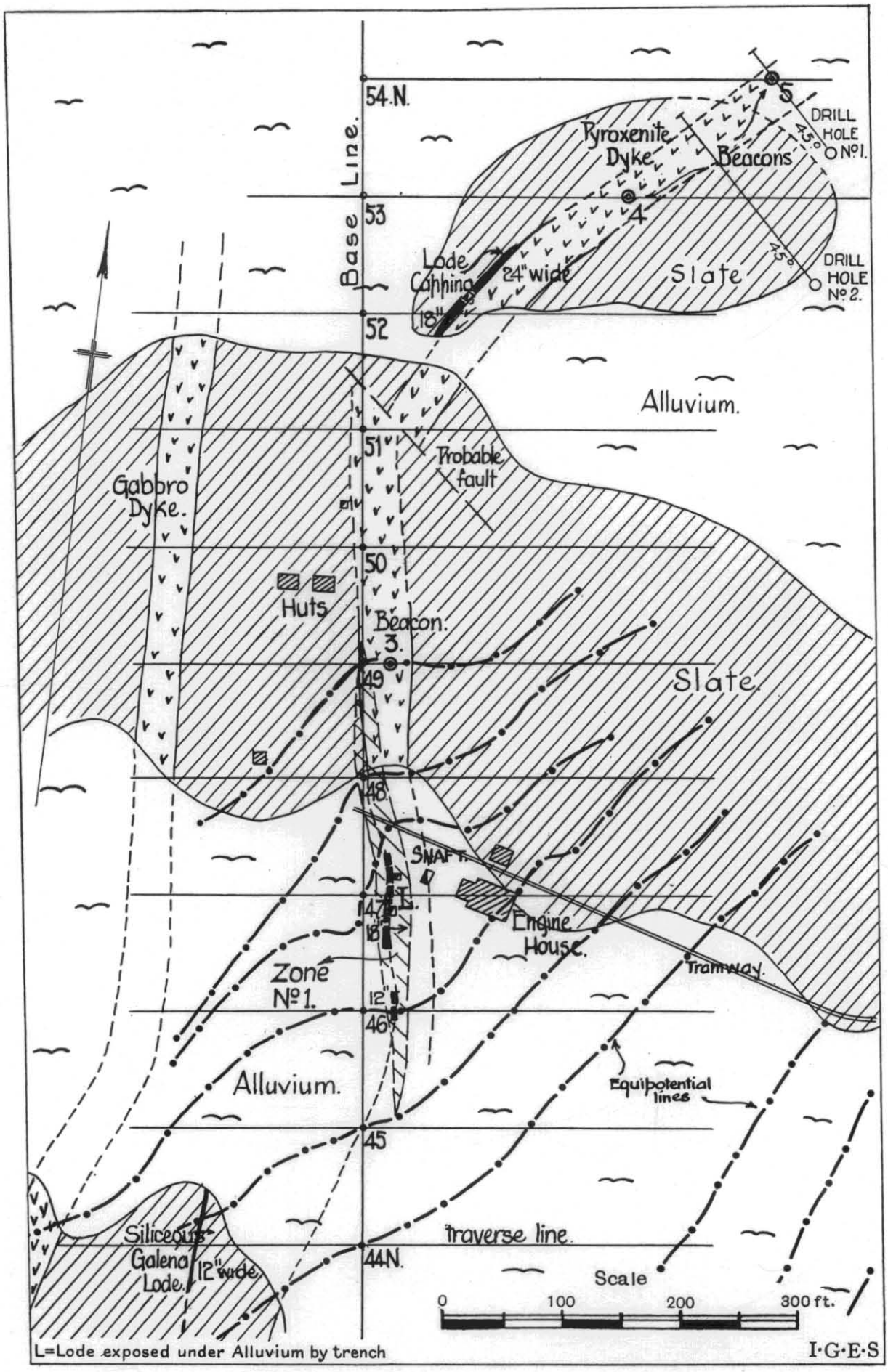

FIGURE 5.
Geological map and equipotential line survey of northern part of copper-nickel field (Edge and Laby, 1931)

5 cm

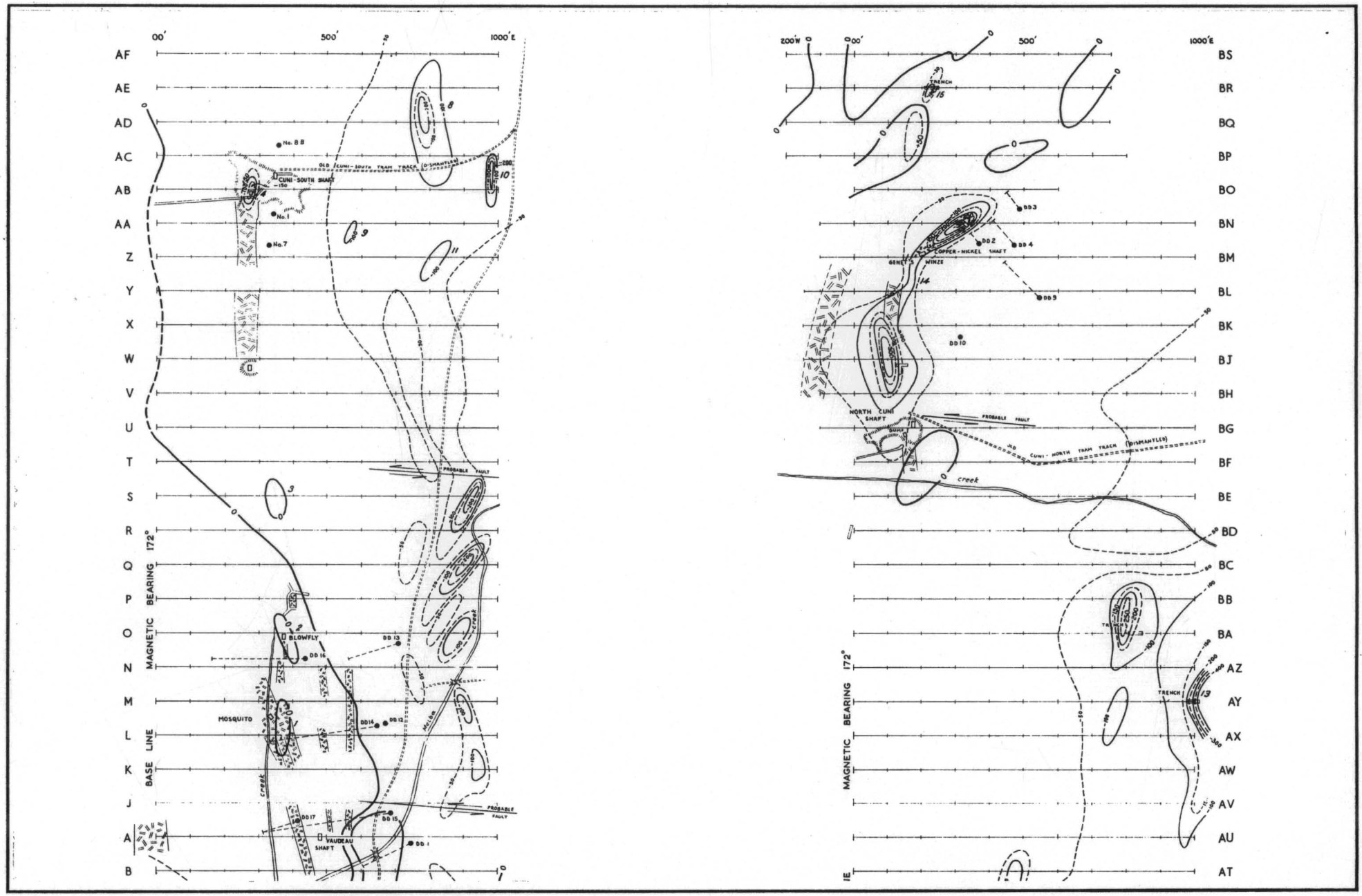
00'
500'
1000'E
200W
AF
AE
AD
AC
AB
AA
Z
Y
X
W
V
U
T
S
R
Q
P
O
N
M
L
K
J
A
B
BS
BR
BQ
BP
BO
BN
BM
BL
BK
BJ
BH
BG
BF
BE
BD
BC
BB
BA
AZ
AY
AX
AW
AV
AU
AT
IE
No. 88
No. 1
No. 7
CUNI - SOUTH SHAFT
OLD CUNI - SOUTH TRAM TRACK (DISMANTLED)
PROBABLE FAULT
BLOWFLY
MOSQUITO
VAUDEAU SHAFT
DD 1
DD 2
DD 3
DD 4
DD 5
DD 9
DD 10
DD 12
DD 13
DD 14
DD 15
DD 16
DD 17
COPPER - NICKEL SHAFT
GENET'S WINZE
NORTH CUNI SHAFT
CUNI - NORTH TRAM TRACK (DISMANTLED)
TRENCH
creek
MAGNETIC BEARING 172°
BASE LINE

5 cm

17/63

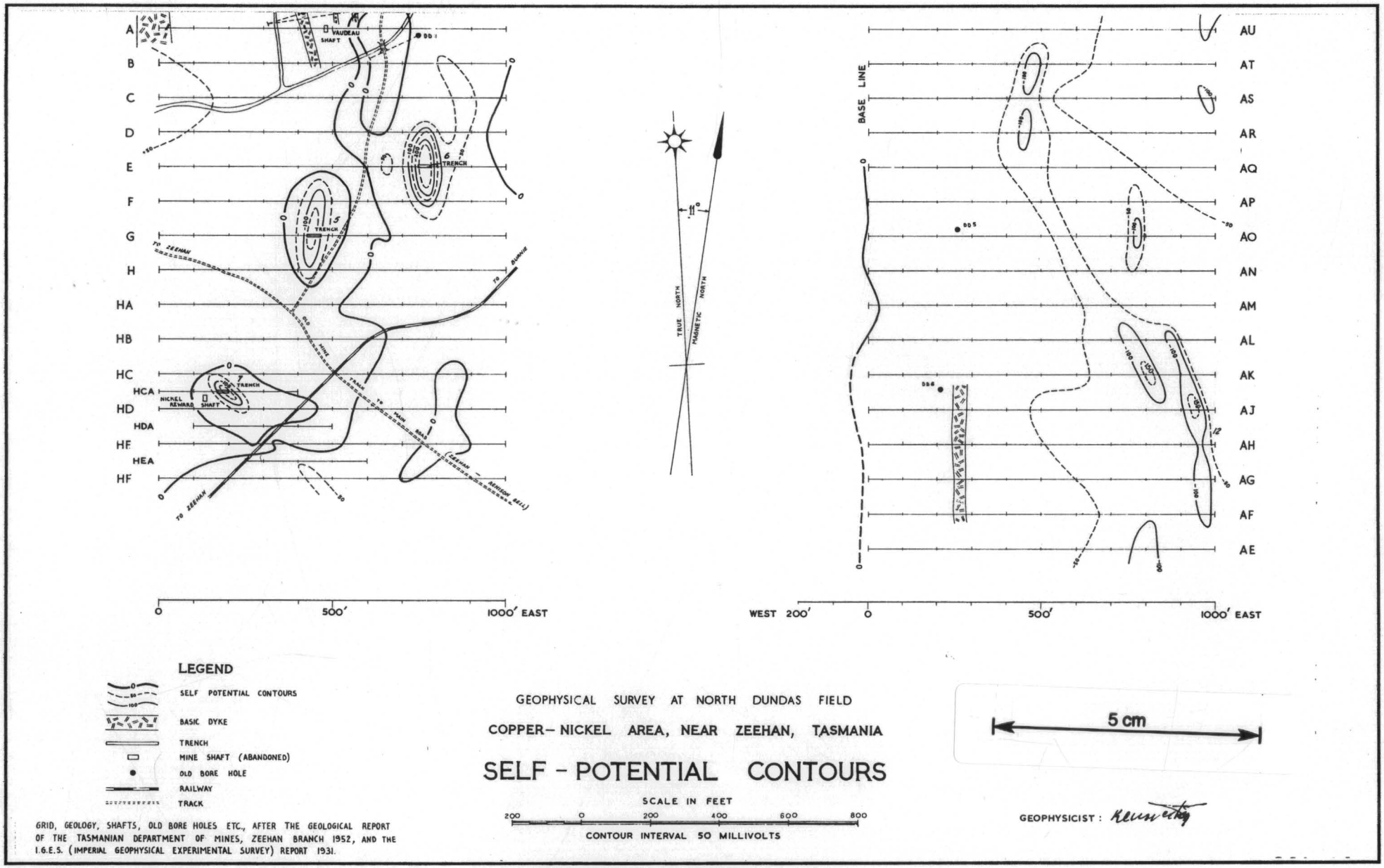

FIGURE 6 (from Keunecke, 1953)

18/63

19/63

GEOPHYSICAL SURVEY AT NORTH DUNDAS FIELD,
COPPER-NICKEL AREA NEAR ZEEHAN, TASMANIA.

ELECTROMAGNETIC AND SELF-POTENTIAL RESULTS AND DRILLING TARGETS, CUNI NORTH AREA

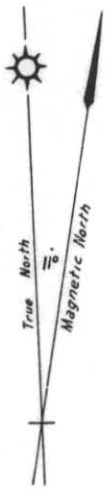

LEGEND

- STRONG
- MEDIUM
- WEAK
- VERY WEAK

} ELECTROMAGNETIC INDICATIONS

- CENTRE OF INDICATION OBTAINED BY SELF POTENTIAL WORK
- BASIC DYKE, POSITION APPROXIMATE
- OLD TRENCH
- ●DDH OLD DIAMOND DRILL HOLE
- ⊕ TARGET POSITION
- ⊙ PROPOSED DIAMOND DRILL SITE

} RECOMMENDATIONS

GRID, GEOLOGY, SHAFTS, OLD BORE HOLE POSITIONS ETC., AFTER THE GEOLOGICAL REPORT OF THE TASMANIAN DEPARTMENT OF MINES, ZEEHAN BRANCH 1952, AND THE I.G.E.S. (IMPERIAL GEOPHYSICAL EXPERIMENTAL SURVEY) REPORT 1931.

FIGURE 7 (from Keunecke, 1953)

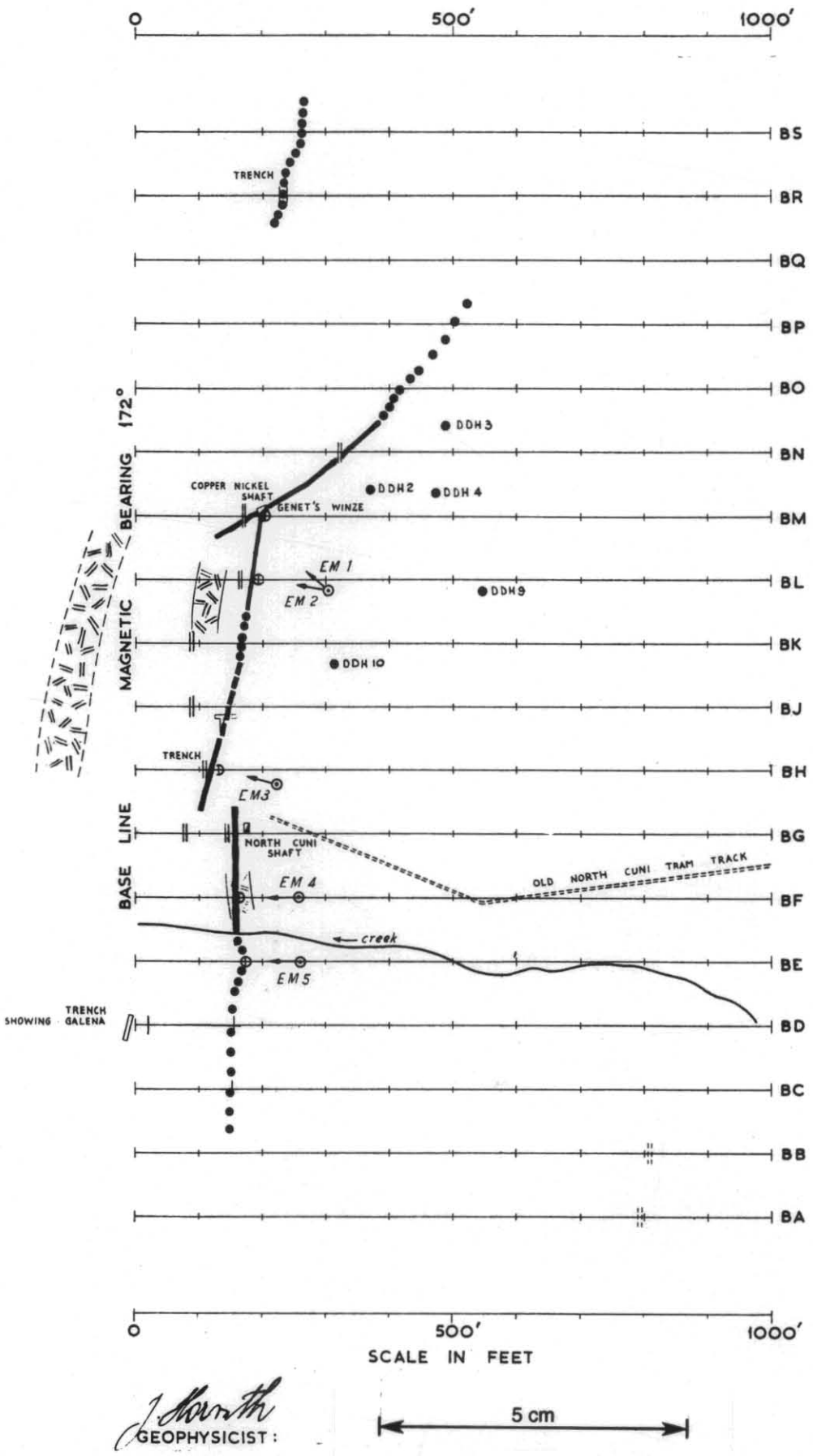
0
500'
1000'
BS
BR
BQ
BP
BO
BN
BM
BL
BK
BJ
BH
BG
BF
BE
BD
BC
BB
BA
TRENCH
172° BEARING
MAGNETIC BASE LINE
COPPER NICKEL SHAFT
GENET'S WINZE
DDH 3
DDH 2
DDH 4
DDH 9
DDH 10
EM 1
EM 2
EM 3
EM 4
EM 5
NORTH CUNI SHAFT
OLD NORTH CUNI TRAM TRACK
creek
TRENCH SHOWING GALENA
0
500'
1000'
SCALE IN FEET
GEOPHYSICIST:
5 cm
Geophysical Section, Bureau of Mineral Resources, Geology & Geophysics
G 32-31

FIGURE 8

TURAM electromagnetic survey data profiles, grid plan, and conductor axis, Cuni Prospect, Zeehan area (from Howland-Rose, 1971)

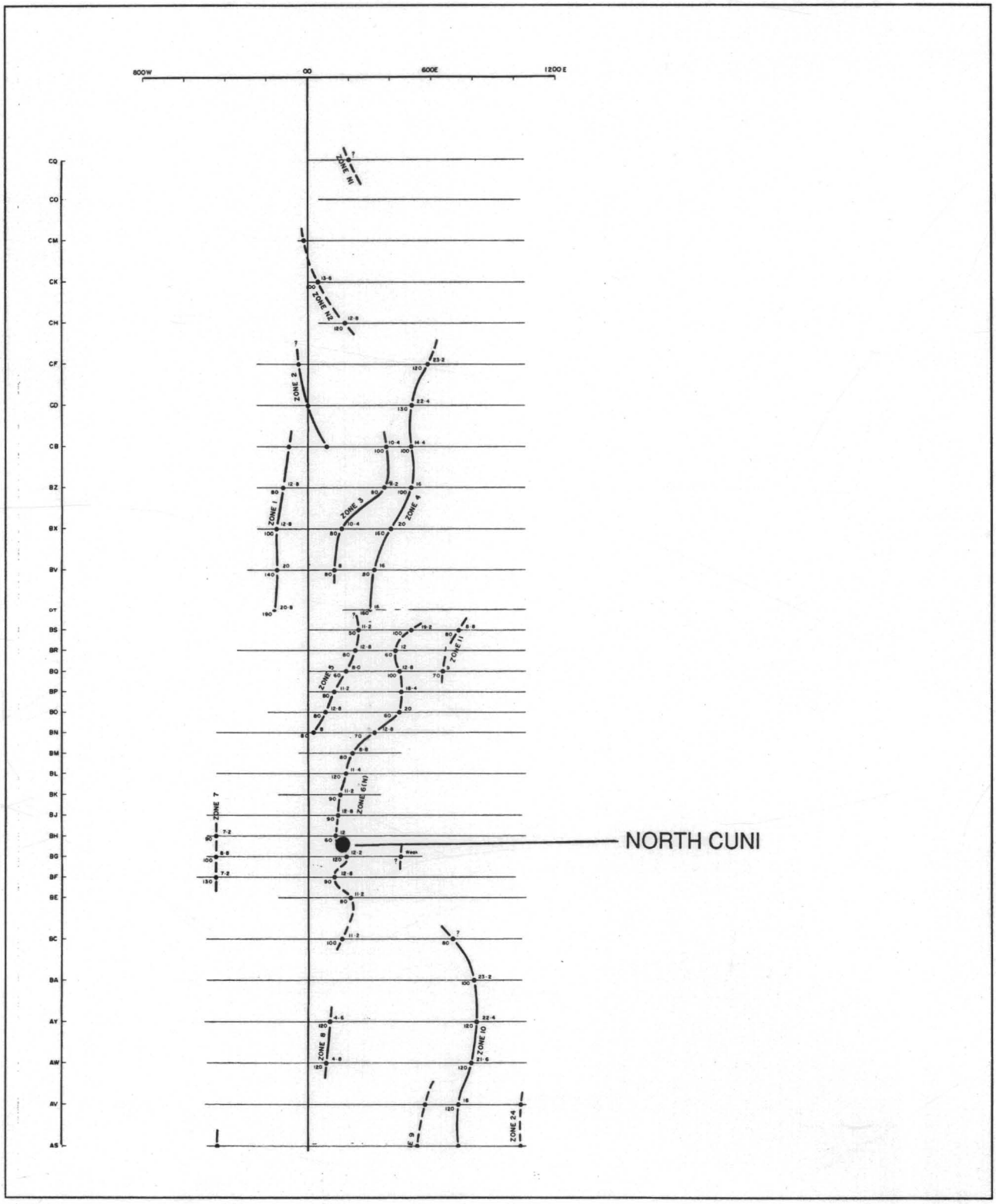

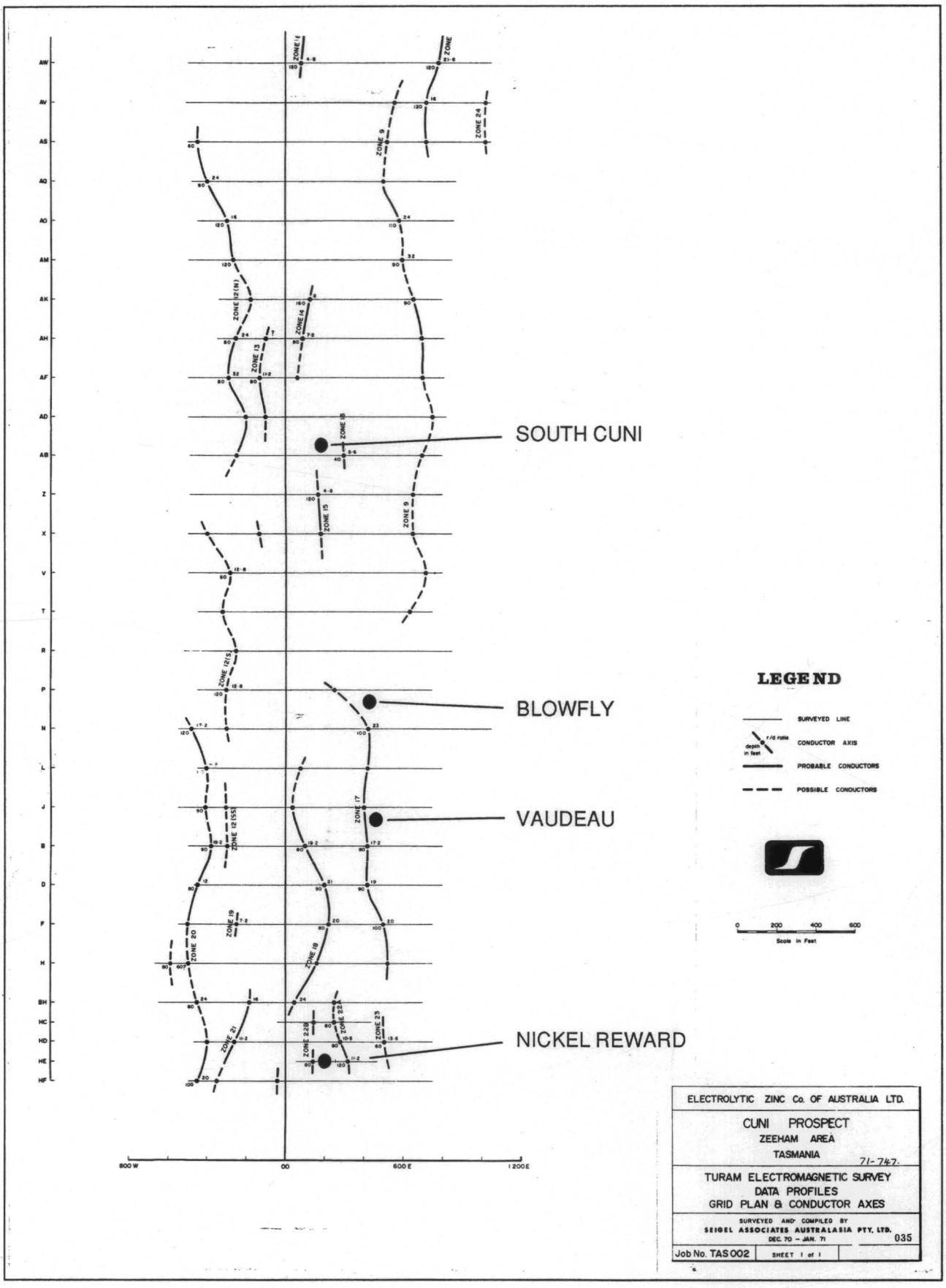
SOUTH CUNI
BLOWFLY
VAUDEAU
NICKEL REWARD
LEGEND
SURVEYED LINE
r/d ratio
depth in feet
CONDUCTOR AXIS
PROBABLE CONDUCTORS
POSSIBLE CONDUCTORS
0 200 400 600
Scale in Feet
800 W
00
600 E
1200 E
ELECTROLYTIC ZINC Co. OF AUSTRALIA LTD.
CUNI PROSPECT
ZEEHAM AREA
TASMANIA
71-747.
TURAM ELECTROMAGNETIC SURVEY
DATA PROFILES
GRID PLAN & CONDUCTOR AXES
SURVEYED AND COMPILED BY
SEIGEL ASSOCIATES AUSTRALASIA PTY. LTD.
DEC. 70 - JAN. 71
035
Job No. TAS 002
SHEET 1 of 1

5 cm

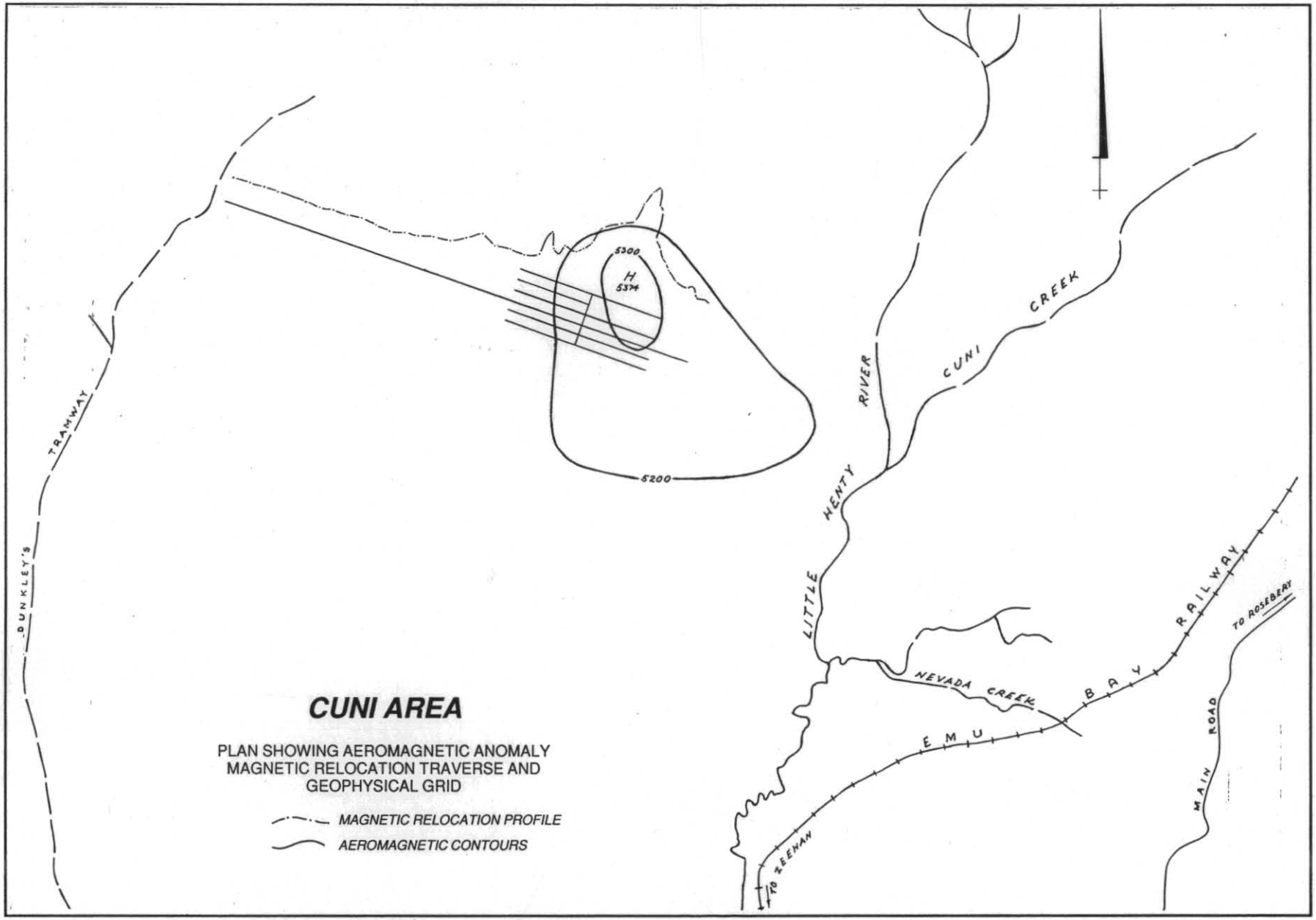

FIGURE 9 (from Mattocks,1960)

100 ft (30 m) depth. Howland-Rose notes a good correlation between the known occurrences of nickel sulphide and the TURAM anomalies.

CSR Minerals held the Cuni area as part of Exploration Licence 15/76, Dundas. Basic data from some of the geophysical surveys carried out early in the term of the licence are not available. Macnamara (1981) presented magnetic susceptibility measurements on core from two drill holes. The 1981 Department of Mines West Tasmania aeromagnetic survey included the Cuni area, and CSR arranged for simultaneous in-fill flying to give a 250 m line spacing coverage of the exploration licence. Original and reprocessed data are presented by Macnamara and Ellis (1983) and Macnamara (1983*a*, *b*). A large subcircular anomaly in the northern Cuni area was modelled and the anomaly is at a depth of 700–800 m (Ellis, 1985). Several secondary anomalies are apparent, and were interpreted to have depths of 250 to 300 metres.

A CSAMT survey along one line over the North Cuni magnetic anomaly confirmed the presence of a deeper body. Additional ground magnetic coverage was obtained, and re-interpretation indicated that the main body was at a depth of 400–600 m (Ellis, 1986). To provide a cost-effective magnetic coverage a detailed (70 m nominal terrain clearance, 100 m line spacing) aeromagnetic survey was flown over the North Cuni area. Four anomalies were considered worthy of drilling (Ellis, 1986) but showed no lithology of economic interest in the drill core. Both magnetic susceptibility and remanence measurements were carried out on the core. Thin sections showed the areas of higher susceptibility to be associated with fine grained opaque minerals, probably magnetite (Ellis, 1987*a*). Gidley presents a comprehensive summary of geophysical exploration in the Cuni area as Appendix 1 of Ellis (1987*b*).

In addition to the surveys outlined above, the Department of Mines has acquired regional (150 m nominal terrain clearance, 500 m line spacing) aeromagnetic and regional (460 m mesh) gravity coverage over the area.

BIBLIOGRAPHY

BELL, G. 1974. *A Review of the Cuni nickel deposits, Zeehan area, Tasmania. Special Prospectors Licence No 127.* G.Bell and Associates Pty Ltd. [TCR 75-1147].

BERRY, R. F. 1988. The tectonic significance of mylonites on the margins of Cambrian mafic-ultramafic complexes in Tasmania, *in:* TURNER, N. J. (ed.). *The geology and evolution of the latest Precambrian to Cambrian rocks in western Tasmania terrane. Abstracts of convention, April 1988.* 12–13. Geological Society of Australia, Tasmanian Division.

BLAKE, F. 1952. Summary report on the copper-nickel deposits of the Five Mile District, Zeehan. *Unpubl. Rep. Dep. Mines Tasm.* 1952:36–43.

BLISSETT, A. H. 1962. One Mile Geological Map Series. K/55-5-50. Zeehan. *Explan. Rep. geol. Surv. Tasm.*

BLISSETT, A. H.; GULLINE, A. B. 1962. One Mile Geological Map Series. K/55-5-50. Zeehan. *Department of Mines, Tasmania.*

BROWN, A. V. 1986. Geology of the Dundas–Mt Lindsay–Mt Youngbuck region. *Bull. geol Surv. Tasm.* 62.

BROWN, A. V. 1989. Orthopyroxene-rich ultramafic-mafic rocks from western Tasmania and their PGE contents. *Rep. Dep. Mines Tasm.* 1989/40.

BROWN, A. V.; JENNER, G. A. 1989. Geological setting, petrology and chemistry of Cambrian boninite and low-Ti tholeiite lavas in western Tasmania, *in:* CRAWFORD, A. J. (ed.). *Boninites and related rocks.* 232–263. Unwin Hyman : London.

BROWN, A. V.; PAGE, N. J.; LOVE, A. H. 1988. Geology and Platinum-Group-Element geochemistry of the Serpentine Hill Complex, Dundas Trough, western Tasmania. *Canadian Mineralogist* 26:161–175.

EDGE, A. B. B.; LABY, J. H. (ed.). 1931. *The principles and practice of geophysical prospecting being the report of the Imperial Geophysical Experimental Survey.* Cambridge University Press : London.

EDWARDS, A. B. 1957. Copper concentrate from Dundas copper-nickel ore, Tasmania. *Mineragr. Invest. CSIRO Aust.* 678.

ELLIS, P. D. 1985. *Renewal report — 1985. Exploration Licence 15/76 Dundas, Tasmania.* CSR Ltd. [TCR 85-2455].

ELLIS, P. D. 1986. *Renewal report — 1986. Exploration Licence 15/76 Dundas, Tasmania.* CSR Ltd. [TCR 86-2584].

ELLIS, P. D. 1987*a*. *Final report — 1987. Exploration Licence 15/76 Dundas, Tasmania.* CSR Ltd. [TCR 87-2679].

ELLIS, P. D. 1987*b*. *Past exploration within the area of Exploration Licence 15/76 Dundas, Tasmania.* CSR Ltd. [TCR 87-2678].

ELLISTON, J.; HUGHES, T. D. 1965. Platinoid deposits of Tasmania, *in:* MCANDREW, J. (ed.). Geology of Australian Ore Deposits. *Publs 8th commonw. min. metall. Congr.* 1:522.

GOSCOMBE, B. D. 1991. Structural analysis of amphibolite zone, Serpentine Hill DDH No. 1 (SH 1). *Rep. Div. Mines Mineral Resour. Tasm.* 1991/09.

HORVATH, J. 1957. The results of diamond drilling of the copper-nickel deposits at North Dundas, near Zeehan, Tasmania. *Rec. Bureau Miner. Resour. Geol. Geophys. Aust.* 1957/98.

HORVATH, J.; O'CONNOR, M. J. 1958. Geophysical investigation (1956–1957) copper-nickel deposits, North Dundas Field, Tasmania. *Rec. Bureau. Miner. Resour. Geol. Geophys. Aust.* 1958/15.

HOWLAND-ROSE, A. W. 1971. *Report on a TURAM electromagnetic survey, Cuni, Rosebery, north-west Tasmania.* Seigel Associates A'Asia Pty Ltd [TCR 71-747].

HUGHES, T. D. 1965. Nickel mineralisation in Tasmania, *in:* MCANDREW, J. (ed.). Geology of Australian Ore Deposits. *Publs 8th commonw. min. metall. Congr.* 1:523–524.

JENNINGS, I. B.; WILLIAMS, E. 1967. Geology and mineral resources of Tasmania. *Bull. geol. Surv. Tas.* 50.

KEUNECKE, O. 1952. Interim report. Geophysical investigation of the copper-nickel deposits, North Dundas Field, near Zeehan, Tasmania. *Rec. Bureau Miner. Resour. Geol. Geophys. Aust.* 1952/71.

KEUNECKE, O. 1953. Geophysical investigation of the copper-nickel deposits, North Dundas Field, near Zeehan, Tasmania. *Rec. Bureau. Miner. Resour. Geol. Geophys. Aust.* 1953/82.

KNIGHT, C. L. 1946. Report on asbestos deposits near Renison Bell tunnel, Zeehan district, Tasmania. *Rec. Bureau. Miner. Resour. Geol. Geophys. Aust.* 1946/6.

MCANDREW, J. 1956. Copper-nickel ore from North Cuni drill hole, near Zeehan, Tasmania *Mineragr. Invest. CSIRO Aust.* 644.

MACNAMARA, P. M. 1981. *Diamond drilling — 1980. Lead Blocks–Cuni Area, EL 15/76, Dundas, Tasmania.* CSR Ltd. [TCR 81-1599].

MACNAMARA, P. M. 1983*a*. *1982 Soil sampling–magnetics–VLF-EM, Nevada Grid, EL 15/76, Dundas.* CSR Ltd. [TCR 83-1988].

MACNAMARA, P. M. 1983*b*. *EL 15/76: Dundas soil sampling–magnetics–VLF-EM, North Cuni Grid.* CSR Ltd. [TCR 83-1989].

MACNAMARA, P. M.; ELLIS, P. D. 1983. *Annual report — 1982. Exploration Licence 15/76 Dundas, Tasmania.* CSR Ltd. [TCR 83-1928].

MATTOCKS, N. G. 1960. *Investigations Cuni Area. Part 1. Geophysical.* Rio Tinto Australian Exploration Pty Ltd. 14/1960. [TCR 60-311].

NYE, P. B.; BLAKE, F. 1938. The geology and mineral deposits of Tasmania. *Bull. geol. Surv. Tasm.* 44:90–92.

REID, A. M. 1925. The Dundas mineral field. *Bull. geol. Surv. Tasm.* 36.

ROBINSON, R. G. 1959. Recent drilling of the Cuni deposits, Zeehan. *Tech. Rep. Dep Mines Tasm.* 3:11–27.

RUBENACH, M. J. 1967. *The Serpentine Hill complex.* B.Sc. (Hons) thesis, University of Tasmania

RUBENACH, M. J. 1974. The origin and emplacement of the Serpentine Hill Complex, western Tasmania. *J. geol. Soc. Aust.* 21:91–106.

SCOTT, J. B. 1931. Report of the State Mining Engineer (Drilling at the Five-Mile, near Zeehan). *Rep. Secr. Mines Tasm.* 1930:20–21.

STILLWELL, F. L. 1946*a*. Flotation tailings from copper nickel ore, Zeehan, Tasmania. *Mineragr. Invest. CSIRO Aust.* 346.

STILLWELL, F. L. 1946*b*. Copper-nickel ore from Zeehan District, Tasmania. *Mineragr. Invest. CSIRO Aust.* 342.

TAYLOR, B. L. 1955. Asbestos in Tasmania. *Miner. Resour. geol. Surv. Tasm.* 9.

TAYLOR, B. L.; BURGER, D. 1952. The Five-Mile Copper-Nickel Deposits. *Unpubl. Rep. Dep. Mines Tasm.* 1952:72–97.

WILLIAMS, K. L. 1957. Two samples of nickel-bearing ore from Tasmania. *Mineragr. Invest. CSIRO Aust.* 711.

WILLIAMS, K. L. 1958. Nickel mineralisaton in Western Tasmania, *in: F. L. Stillwell Aniversary Volume.* 263–302. Australian Institute of Mining and Metallurgy : Melbourne.

[30 June 1991]

APPENDIX 1

Historical background of lease areas in the Five Mile/Cuni area

G. Thomas

NORTH CUNI SHAFT

3231/87M	80 ac.	W. J. Westcott (Silver Lead)	-	07.11.1890 to 19.01.1892
1076/93M	80 ac.	J. McNamara (Minerals)	-	19.05.1896 to 20.12.1898
4495/M	77 ac.	T. H. Vincent & W. Wallace (Copper)	Transfer	17.12.1909 to 17.05.1913
		Dundas Cunic Mining Co Ltd	Transfer	17.05.1913 to 03.12.1924
		D. W. Albury		03.12.1924 to 15.12.1925
10109/M	77 ac.	B. Grabe (Minerals)	Transfer	21.05.1927 to 11.11.1929
		Copper Nickel Mining Co N.L.	Consolidation	11.11.1929 to 27.01.1952
10575/M			Transfer	
		W. Genat		27.01.1932 to 17.05.1952
2M/46	157 ac.	W. M. Murray & S. Nixon (Nickel & Base Metals)		07.01.1946 to 08.08.1947
			Transfer	
		Lead & Nickel Co.	Transfer	08.08.1947 to 27.02.1951
		Montana Silver Lead N.L.		27.02.1951 to 11.01.1961

COPPER-NICKEL SHAFT (GENET'S WINZE)

1142/93M	63 ac.	W. J. Elkin (Silver Copper Lead)		29.05.1896 to 29.12.1896
4385/M	40 ac.	A. D. Sligo (Minerals)		14.11.1909 to 09.12.1913
4427/M	41 ac.	J. Hutton & A. E. Bruce (Silver Lead)		01.12.1909 to 07.02.1911
5927/M	41 ac.	Zeehan Dundas Mines Ltd (Nickel Copper & Co)		25.06.1912 to 22.01.1914
			Transfer	
		The Mt. Zeehan (Tasmania) Silver Lead Mines Ltd		22.01.1914 to 21.12.1920
9005/M	80 ac.	H. Simpson (Copper Nickel Ore)		31.03.1923 to 16.12.1924
10173/M	80 ac.	B. Grabe (Minerals)	Consolidated	19.07.1927 to 07.12.1927
10575/M	157 ac.	Copper Nickel Mining Co. N.L.	Transfer	07.12.1927 to 27.01.1932
		W. Genat		27.01.1932 to 17.05.1932
10935/M	157 ac.	F. Kershaw (Copper Nickel Ore)	Transfer	01.04.1932 to 05.06.1934
		F. F. Doward		05.06.1934 to 10.06.1947
2M/46	157 ac.	W. M. Murray & S. Nixon (Nickel & Base Metals)		07.01.1946 to 27.02.1951
			Transfer	
		Montana Silver Lead N.L.		27.02.1951 to 11.01.1961

BLOWFLY SHAFT – MOSQUITO SHAFT – VAUDEAU SHAFT

1926/91M	80 ac.	J. Dixon (Reward Nickel)	Transfer	20.06.1893 to 03.05.1894
		R. G. King		03.03.1894 to 16.08.1898
4976/93M	80 ac.	The Silver King P.A. N.L. (Minerals)		06.06.1900 to 10.12.1901
4514/M	34 ac.	W. Davie (Copper)	Transfer	23.12.1909 to 27.08.1913
		J. Brandon	Transfer	27.08.1913 to 13.12.1927

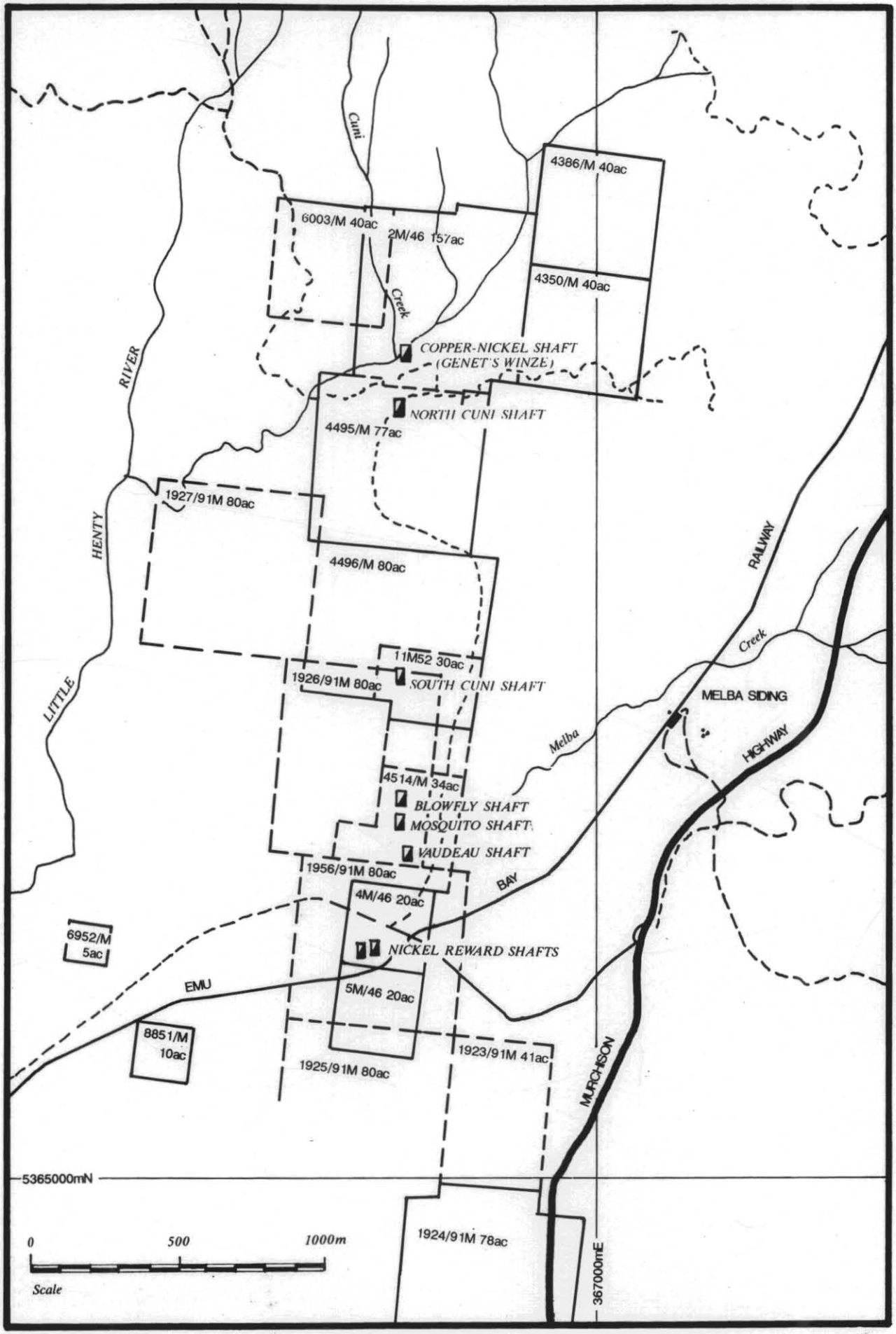

FIGURE 10
Location of historical leases, Cuni area

5 cm

		J. H. S. Munro	Consolidated	13.12.1927 to
10463/M	320 ac.			01.10.1931
10853/M	34 ac.	J. H. S. Munro (Minerals)		15.10.1931 to 15.12.1948
2M/51	34 ac.	R. E. Clarke		07.12.1950 to 05.08.1955

SOUTH CUNI SHAFT (see also 4496/M)

1926/91M	80 ac.	J. Dixon (Nickel)	Transfer	20.06.1893 to 07.09.1893
		E. E. Thomas	Transfer	07.09.1893 to 03.05.1894
		R. G. King		03.05.1894 to 16.08.1898
4976/93M	80 ac.	The Silver King P.A. N.L. (Minerals)		06.06.1890 to 10.12.1901
4604/M	10 ac.	J. Wallace (Copper & C)		23.12.1909 to 12.12.1911
5955/M	10 ac.	J. Wallace (Minerals)		27.07.1912 to 10.12.1918
10138/M	10 ac.	J. H. S. Munro (Minerals)	Consolidated	13.06.1927 to
10463/M	320 ac.			01.10.1931
11935/M	40 ac.	H. E. Sizer (Silver Lead)		21.08.1937 to 24.05.1939
11M/52	30 ac.	Montana Silver Lead NL (Copper Nickel Silver Lead)		14.02.1952 to 06.05.1959

NICKEL REWARD SHAFTS

1956/91M	80 ac.	A. G. & J. Dixon (Reward Nickel)	Transfer	14.07.1893 to 07.09.1893
		E. E. Thomas	Transfer	07.09.1893 to 03.03.1894
		R. G. King		03.03.1894 to 16.08.1898
3510/93M	80 ac.	J. Armstrong (Minerals)		20.08.1898 to 04.12.1900
4603/M	40 ac.	G. Wallace (Copper and c)		23.12.1909 to 12.12.1911
5954/M	32 ac.	W. Davie (Minerals)	Transfer	27.07.1912 to 19.11.1914
		D. V. Allen		19.11.1914 to 09.12.1919
10164/M	40 ac.	J. H. S. Munro (Minerals)	Consolidation	09.07.1927 to 29.04.1929
10463/M	320 ac.			29.04.1929 to 01.10.1931
4M/46	20 ac.	W. M. Murray & S. Nixon (Nickel & Base Metals)	Transfer	07.01.1946 to 08.08.1947
		Lead & Nickel (Zeehan) N.L.		08.08.1947 to 27.02.1951
		Montana Silver Lead N.L.		27.02.1951 to 11.01.1961
1078/93M	73 ac.	J. McNamara & R. A. Dunne (Minerals)		19.05.1896 to 20.12.1898
4496/M	80 ac.	G. & J. Wallace (Copper)	Transfer	18.12.1909 to 17.05.1913
		Dundas Cunic Mining Co. Ltd	Transfer	17.05.1913 to 03.12.1924
		D. W. Albury		03.12.1924 to 15.12.1925
9841/M	10 ac.	T. H. Vincent (Nickel & Copper Ore)		09.09.1926 to 13.12.1927
10137/M	70 ac.	J. H. S. Munro (Minerals)	Consolidated to:	13.06.1927 to 29.04.1929
10463/M	320 ac.			19.04.1929 to 01.10.1931
10272/M	10 ac.	J. H. S. Munro		13.12.1927 to 15.12.1948
1085/M	10 ac.	J. H. S. Munro (Minerals)		06.11.1931 to 15.12.1948
10923/M	20 ac.	F. Kershaw (Copper Nickel Ore)	Transfer	29.03.1932 to 05.06.1934
		F. F. Doward		05.06.1934 to 10.06.1942

3M/46	20 ac.	W. M. Murray & S. Nixon (Nickel & Base Metals)		09.01.1946 to 08.08.1947
			Transfer	
		Lead & Nickel (Zeehan) N.L.	Transfer	08.08.1947 to 27.02.1951
		Montana Silver Lead N.L.		27.02.1951 to 11.01.1961
11M/52	30 ac.	Montana Silver Lead NL (Copper Nickel Silver Lead)		19.02.1952 to 23.02.1960
3285/87M	80 ac.	W. J. Dobbie (Silver Lead)		19.11.1890 to 19.01.1892
1927/91M	80 ac.	R. G. King (Nickel Copper)		22.06.1893 to 16.01.1894
1077/93M	80 ac.	J. McNamara & R. A. Dunne (Minerals)		19.05.1896 to 20.12.1898
4614/M	80 ac.	C. C. Ferguson & R. Hart (Silver Lead Copper)		30.12.1909 to 06.09.1910
2985/87M	79 ac.	Robert J. Sadler (Silver Lead)		16.09.1890 to 06.12.1892
3135/87M		W. Ritchie & Augustus? (Silver)		06.10.1890 to 06.12.1892
3287/87M		E. Allen (Silver Lead)		19.11.1890 to 06.12.1892
964/93M	80 ac.	J. W. Taylor (Minerals)		14.05.1896 to 07.12.1897
1141/93M	80 ac.	W. J. Elkin (Silver Copper Lead)		29.50.1896 to 29.12.1896
3034/M	80 ac.	T. Puckley (Silver Lead)		02.03.1907 to 25.02.1908
4384/M	80 ac.	C. C. Ferguson (Silver Lead)		12.11.1909 to 12.12.1911
6003/M	40 ac.	Zeehan Dundas Mines Ltd (Copper & C)	Transfer	16.09.1912 to 21.01.1914
		The Mount Zeehan (Tas) Silver Lead Mines Ltd		22.01.1914 to 21.12.1920
8851/M	10 ac.	J. C. Deveraux	Transfer	20.04.1922 to 29.03.1923
		H. Simpson		29.03.1923 to 16.12.1924
1923/91M	41 ac.	E. E. Thomas (Copper Nickel)		20.06.1893 to 11.12.1894
514/93M	41 ac.	A. Fencofski & R. Mapley		21.10.1895 to 08.12.1896
4009/93M	80 ac.	J. Armstrong (Silver)		27.04.1899 to 07.06.1899
6371/M) 6372/M)		J. Brandon (Nickel Copper Lead)		10.04.1913 (not proceeded with)
2807/87M	78 ac.	W. Archer (Silver)		08.08.1890 to 26.01.1892
1924/91M	78 ac.	E. E. Thomas (Copper Nickel)		20.06.1893 to 11.12.1894

APPENDIX 2

Details and Core Logs for DDH SH1–6

SERPENTINE HILL DDH 1

Borehole Name/Number:	Serpentine Hill No 1
Easting Co-ordinates:	367 149 mE
Northing Co-ordinates:	5 366 780 mN
Collar height (ASL):	222.4 m
Depth:	106.5 m — originally 671.5 m — final.

DDH-SH1 was sited to test the strike continuity, over 100 m, of the the layer which contained chromitite samples with the elevated PGE values.

The hole was collared in serpentinite, after dunite, with a high disseminated chrome spinel content and pods of chromitite. The site chosen was the position of the sample 22TA84 of Brown *et al.* (1988) which assayed at 1240 ppb Pt, 4 ppb, Pd; 180 ppb, Ru; 54 ppb, Ru; and 70 ppb Ir. Os was not analysed for.

Within the surface outcrop layering, defined by pyroxene and chrome spinel mineral foliations within the dunite, is vertical. However at 8.0 m the layering had a down-dip angle of 40° and at ?? m the collared sequence had been faulted out and a second ultramafic rock sequence encountered. Changes between different ultramafic sequences are recognised by a significant change in chemical compositions of chrome spinel grains within the ultramafic sequence.

Originally 101.5 m was drilled, however because of the revision of the Zeehan geological map sheet, approval was given to deepen the drill hole to 500 m or recognisable basement, in an attempt to define the depth, style and angle of movement of a proposed movement zone along which the ultramafic rocks on the western edge of the Serpentine Hill Complex had been emplaced. The movement zone had been anticipated because the lower 50 m of the original hole contained progressively more foliated amphibolite, after peridotite.

During the second phase of drilling an accident occurred whilst transporting core to the new core store, and nine boxes were upset. Of the nine boxes, it was possible to rebox the core from five boxes into the correct box, although the core was jumbled. Some reassembling was possible. The other four boxes were totally lost. Of the four boxes totally lost, two (box 1 and box 14) had previously been logged, whereas the other two boxes (21 and 22) had not been logged.

The boxes which were saved, but with jumbled core, are:

Box No.	*Depth range (m)*	
4	125.34	131.71
6	138.07	114.27
8	150.60	156.92
10	163.17	169.36
12	177.31	185.62

The boxes which were lost are:

Box No	*Depth range (m)*	
1	106.0	112.67
14	191.0	197.57
21	235.0	242.0
22	242.0	248.0

Core Log with thin section descriptions

From (m)	*To (m)*	*Description*
0.0	0.5	Rubble
0.5	2.0	Green serpentinite with large chrome spinel grains and disseminated sulphide mineralisation. Sample SH1/1, from 0.5–1.5 m, for analysis. In thin section this sample is serpentinite after dunite with a high chrome spinel content. The spinels are deformed along fracture zones.
2.0	10.0	Sheared, light green, massive serpentinite with white and greenish-white calcite and fibrous chrysotile veins.

		Sample SH1/2 — Chromitite lense from 8.0 m for analysis. The lense was 20 mm (true thichness) thick and had a down hole dip of 40°. In thin section the sample is a chromitite with interstitial, partialy serpentinised, orthopyroxene grains.
10.0	31.5	Bluish serpentinite after pyroxene rich peridotite, numerous 5–10 mm shear zones.
		Sample SH1/9, from 11.0 m, in thin section, an altered orthopyroxenite with minor, renmant, chrome diopside grains.
		Sample SH1/10, from 15.0 m, in thin section, dominantly serpentinised orthopyroxenite.
		Sample SH1/3, from 19.5–20.5 m, for analysis. In thin section, altered and partially serpentinised olivine-pyroxenite.
		Sample SH1/11, from 25.0 m, in thin section, highly altered, partially serpentinised, orthopyroxenite.
		Sample SH1/12, from 30.0 m, in thin section, highly altered and deformed serpentinite after pyroxenite.
31.5	35.5	Highly sheared bluish-green serpentinite with iregular calcite veining.
35.5	46.0	Calcite/quartz replacement of brecciated seerpentinite
		Sample SH1/4, from 41.0–42.0 m, quartz-calcite replacement zone. In thin section, quartz, carbonate replacement of peridotite with a high chrome spinel content.
46.0	46.5	Quartz replacement zone
46.5	50.5	Sheared cataclasite with irregular calcite veins
		Sample SH1/13, from 48.0 m, in thin section, partially amphibolitised, deformed and altered serpentinite.
50.5	70.5	Massive, foliated amphibolite, with a foliation dip of 65°.
		Sample SH1/5, from 62.0–63.0 m, banded (on grainsize), amphibolite with remnant, subhedral, chrome spinel grains.
		Sample SH1/14, from 54.0 m, in thin section, foliated amphibolite, along the foliation are zones of remnant chrome spinel grains.
		Sample SH1/15, from 65.0 m, in thin section, massive, foliated amphibolite with grainsize banding.
		Sample SH1/16, from 70.0 m, in thin section, foliated amphibolite.
70.5	71.0	Zone of calcite veining through cataclasite.
71.0	75.2	Foliated serpentinite.
		Sample SH1/17, from 75.0 m, in thin section, quartz-carbonate replacement of serpentinite after peridotite.
75.2	75.7	Serpentinised breccia
75.7	106.5	Foliated serpentinite and amphibolite, dominant foliation dip at 60°.
		Sample SH1/6, from 78.0–79.0 m, serpentinite after dunite with large (2.5–3.5 mm) chrome spinel grains.
		Sample SH1/7, from 92.5–93.5 m for analysis. In thin section, partially amphibolitised serpentinite after peridotite.
		Sample SH1/8, from 104.0–105.0 m, for analysis. In thin section, amphibolite with remnant chrome spinel grains.
		Sample SH1/18, from 85.0 m, in thin section, partially amphibolitised serpentinite after peridotite.
		Sample SH1/19, from 90.0 m, in thin section, partially amphibolitised serpentinite after peridotite.
		Sample SH1/20, from 97.0 m, for thin section, partially amphibolitised serpentinite after peridotite.

Core Log of second phase of drilling

107.0	110.4	Foliated amphibolite, foliation has a dip of 40°.
		Sample Z.342 from 107.5 m. In thin section, the amphibolite contains remnant, subhedral stringers of chrome spinel grains. Post-foliation brecciation and fracturing perpendicular to foliation has occurred with the later fractures being filled with calcite and serpentinite.
110.4	111.0	Breccia Zone with serpentinite, later calcite veining.
111.0	117.5	Foliated amphibolite.

		Sample Z.343 from 114 m. In thin section, the sample is a well foliated amphibolite.
117.5	117.6	Quartz plus 'black' material replacement zone.
117.6	125.4	Foliated banded amphibolite, banding dips at 75°.
		Sample Z.344 from 117.7 m. In thin section the sample is a banded amphibolite. Banding is on millimetre scale and characterised by alternating bands of tremolite/actinolite and tremolite-actinolite intergrown with quartzo-feldspathic material. The dominant foliation is parallel with the banding. Later quartz and calcite fracture filling.
		Sample Z.345 from 123.8 m. Banded amphibolite, on millimetre scale, alternating between foliated amphibolite and cataclastic amphibolite, remnant chrome spinel grains. Later calcite veining.
125.4	127.2	Breccia zone with black matrix.
127.2	187.89	Foliated, banded amphibolite
		Sample Z.346 from 132.25 m. Altered, banded amphibolite. Bands dip at 60°. In thin section some bands contain an altered light pink garnet, other bands have secondary epidote. Calcite and colourless, but anomalous Berlin Blue pleochroic, chlorite-filled fractures.
		Sample Z.347 from 135.62 m. Banded amphibolite, coarse-grained, well laminated. Banding characterised by alternating zones of tremolite-actinolite and tremolite/actinolite and quartzo-feldspathic intergrowth.
		Sample Z.348 from 146.7 m. Banded amphibolite, medium-grained. Similar to Z.347.
		Sample Z.349 from 161.0 m. Banded amphibolite, similar to above but with irregular bands of epidote.
		Sample Z.350 from 170.0 m. Foliated, massive, amphibolite.
		Sample Z.351 from 181.5 m. Fine-grained, banded amphibolite with lenses and irregular bands of epidote. Banding dips at 55°.
		Sample Z.352 from 186.08 m. Banded amphibolite, with alternating, semi-irregular bands and boudinages of amphibolite-quartz-opaque oxide intergrowth; amphibolite; and epidote.
187.89	197.91	Quartz vein
187.91	188.30	Foliated amphibolite
188.30	219.65	Banded, foliated amphibolite. Banding varies between dips of 45° and vertical.
219.65	219.75	Mineralised quartz vein. Pyrhotite and pyrite +(?)
		Sample Z. 581 from 219.68 m.
219.75	220.75	Foliated amphibolite.
220.75	220.85	Mineralised quartz vein.
		Sample Z.582 from 220.95 m
220.85	224.66	Banded, foliated amphibolite
224.66	229.36	Deformed, foliated amphibolite
		Sample Z.583 from 226.05 m
229.36	235.65	Sheared, banded, foliated amphibolite
		Sample Z.584 from 230.01 m
		Sample Z.585 from 234.45 m
		Sample Z.586 from 235.35 m
235.65	**248.26**	**Boxes 21 and 22 Spilt and totally jumbled.**
248.26	250.80	Foliated amphibolite, well developed laminar surface dipping at 60°.
250.80	250.88	Highly sheared zone
250.88	260.65	Foliated amphibolite, well developed laminar surface dipping at 60°.
		Sample Z.353 from 251.5 m, foliated, fine-grained, banded, amphibolite.
		Sample Z.354 from 253.25 m, partially contorted amphibolitised serpentinite after pyroxenite, with secondary carbonate.
		Sample Z.355 from 256.0 m, foliated amphibolite with patches of quartzo-feldspathic material and remnant chrome spinel grains, secondary carbonate.
		Sample Z.356 from 259.7 m, fine-grained, foliated, quartz-chlorite schist.
260.65	261.0	Mineralised, black, carbonaceous mudstone — shear zone — 330 mm core loss
261.00	261.30	Mineralised, black, carbonaceous mudstone
261.30	266.4	Cataclasite (?)

		Sample Z.357 from 264.6 m, brecciated schistose asemblage of quartz, amphibole and opaques with secondary carbonate.
266.4	277.5	Foliated and brecciated gabbro with cross-cutting calcite veins.
		Sample Z.358 from 270.5 m, sheared, partially amphibolitised gabbro.
		Sample Z.359 from 275.0 m, sheared, partially amphibolitised gabbro with later calcite fracture fillings.
277.5	278.1	Foliated, deformed black mudstone
278.1	293.8	Foliated volcanic/wacke with a high calcite content.
		Sample Z.360 from 280.35 m, sheared and brecciated plagioclase and opaque oxide rock with secondary carbonate, chlorite and gunge (possibly hydrogarnet after plagioclase).
		Sample Z.361 from 283.95 m, deformed quartz wacke with minor amounts of feldspar and clastic mica.
		Sample Z.362 from 286.8 m, quartz-carbonate replacement of a brecciated plagioclase/opaque oxide volcanic, with secondary chlorite filled fractures.
		Sample Z.363 from 288.57 m, altered feldspar rich volcanic with large anhedral grains of leucoxene after Fe-Ti oxide.
		Sample Z.364 from 293.32 m, highly altered fine-grained gabbro.
293.80	294.48	Breccia zone with black mudstone and quartz veins
294.48	296.15	Foliated sedimentary rocks
		Sample Z.365 from 295.2 m, bedded mudstone/quartz wacke.
296.60	297.60	Sheared ultramafic with calcite and quartz veins. Veins contain sulphide mineralisation.
		Sample Z.380/2 from 296.05 m — sample of mineralised quartz vein. Polished section reveals sphalerite with inclusions of pyrrhotite and chalcopyrite; galena; fine blebs of pyrrhotite; chalcopyrite; and traces of bornite. Most of the sulphides are intergrown and cogenetic with each other and the host. The sphalerite with pyrrhotite and chalcopyrite is late stage exsolution and/or replacement.(RSB).
297.60	298.80	Thinly bedded, calcareous, mudstone and siltstone. Remnant bedding dips at 70°.
		Sample Z.491 from 297.0 m — mineralisation for analysis.
298.8	???.??	Zone of brecciated black mudstone; bedded, calcareous siltstone and mudstone with minor wacke and brecciated quartz veins with sulphide mineralisation.
		Sample Z.366 from 301.98 m, bedded but deformed mudstone/siltstone/quartz wacke. Most of the larger (sand-grade) quartz grains are derived from a volcanic source. Some of the fragments are of devitrified volcanic glass (snow flake texture).
???.??	307.9	Intrusive gabbro
		Sample Z.367 from 306.82 m, highly altered gabbro.
307.9	310.65	Foliated sedimentary rocks with brecciated zones filled by quartz. Bedding dips at 55°.
		Sample Z.368 from 309.47 m, calcite-sulphide replacement of a quartz wacke with clasts of andesitic/dacitic volcanic rocks, devitrified glass and plagioclase-rich lavas.
310.65	313.2	Fault breccia with quartz infilling
313.2	315.05	Deformed felsic volcanic bearing wacke with quartz and calcite veining.
315.05	323.45	Interbedded black mudstone/siltstone, well foliated with foliation parallel to composition banding — bedding (?). Bedding dips at 55°.
		Sample Z.492 from 319.8 m — mineralisation for analysis.
323.45	325.5	Bedded and foliated wacke with mudstone and siltstone. Intra-bedding slump and soft-sediment folds at 328.5 m. Foliation dips to 60°.
		Sample Z.369 from 324.6 m, well bedded mudstone/siltstone/quartz wacke.
325.5	348.9	Sand-grade units dominate.
		Sample Z.370 from 326.08 m, quartz wacke derived from andesitic/dacitic volcanic source.
		Sample Z.371 from 330.1 m, quartz wacke derived from andesitic/dacitic volcanic source.
		Sample Z.372 from 337.9 m, quartz wacke derived from andesitic/dacitic volcanic source.
		Sample Z.373 from 346.9 m, foliated quartz wacke similar to above.
348.9	350.1	Incoming of purple mudstone with pale green bands.
350.1	353.95	Dominantly felsic wacke, bedding dips at 45° at 352.9 m.
		Sample Z.374 from 350.9 m, foliated quartz wacke.
		Sample Z.587 from 351.80 m (high magnetic susceptibility).

353.95	355.1	Breccia Zone
355.1	369.2	Continuation of wacke dominated succession, good foliation through succession.
		Sample Z.588 from 356.05 m (high magnetic susceptibility).
		Sample Z.375 from 357.34 m, foliated volcanic-quartz wacke from an acid/intermediate volcanic source.
		Sample Z.589 from 358.86 m (high magnetic susceptibility).
		Sample Z.376 from 363.95 m, quartz-volcanic wacke.
		Sample Z.377 from 368.62 m, volcanic wacke, similar to above.
369.2	369.6	Laminated Mudstone and siltstone.
		Sample Z.493 from 369.4 m — mineralisation for analysis.
369.6	376.0	Continuation of wacke dominated succession units, dips to 40° at 365.6 m.
		Sample Z.378 from 373.4 m, fine-grained volcanic wacke.
376.0	385.5	Brecciated black mudstone. Dominant parting dips at 45° at 380.5 m.
		Sample Z.494 from 377.2 m — mineralisation for analysis.
		Sample Z.380/1 from 381.5 m — Black mudstone for XRD. XRD analysis gave ~50% amorphous carbon; ~20% mica; ~15% quartz; ~5% kaolin; ~5% calcite; and ~5% dolomite/ankerite.
385.5	492.60	Brecciated, schistose carbonate and black mudstone with disseminated sulphide.
		Sample Z.495 from 389.2 m — mineralisation for analysis.
390		Hole Surveyed: Direction — 82° dip to 270°.
		Sample Z.379 from 392.15 m, pyritic, carbonaceous mudstone.
492.60	399.0	Calcareous mudstone.
		Sample Z.496 from 393.2 m — mineralisation for analysis.
399.0	422.5	Gabbro
422.5	428.5	Mudstone
		Sample Z.497 from 425.3 m — mineralisation for analysis.
428.5	433.0	Gabbro
433.0	481.0	Sheared and mineralised mudstone with wacke blocks. Dip of shearing varies between 60 and 30°.
		Sample Z.381 from 452.9 m — quartz-carbonate intergrowth within an altered volcanic-quartz wacke.
		Sample Z.498 from 444.2 m — mineralisation for analysis.
		Sample Z.499 from 453.0 m — mineralisation for analysis.
		Sample Z.382 from 463.5 m — mineralised mudstone.
		"Black shale, strongly replaced and veined by carbonate and sulphides. The shale itself is strongly graphitic, but the graphite is mostly very fine-grained. Fine- to medium-grained sulphides are disseminated throughout. These consist predominantly of pyrrhotite with minor to rare sphalerite and chalcopyrite. The grains appear epigenetic or vein-related. Some fine- to medium-grained cassiterite is also present, as is rare leucoxene.
		The veins are mostly carbonate with rare quartz and micas, and minor to abundant sulphide grains. The dominant sulphide is again pyrrhotite, but sphalerite and pyrite are more abundant. The pyrite is porous and appears to be replacing pyrrhotite, as is minor fine-grained marcasite. The sphalerite is iron-rich and contains inclusions of pyrrhotite and chalcopyrite. Galena is very rare and fine grained." (RSB).
		Sample Z.383 from 464.0 m — Wacke
481.0	485.5	Bedded sequence of wacke and mudstone.
		Sample Z.384 from 481.65 m — Mudstone/carbonate
		Sample Z.385 from 481.80 m — Mudstone/carbonate. An XRD analysis gave calcite; dolomite; chlorite; talc; and quartz.
		Sample Z.386 from 481.90 m — Mudstone/carbonate
		Sample Z.387 from 482.60 m — Mudstone/carbonate
		Sample Z.500 from 484.9 m — mineralisation for analysis.
485.8	509.5	Dominantly black mudstone with minor carbonate units. Bedding contorted, quartz veining and sulphide mineralisation. Breccia zones between 489.5 m and 490.5 m and 503.5 to 505.5 m.

		Sample Z.501 from 492.2 m — mineralisation for analysis.
		Sample Z.502 from 504.0 m — mineralisation for analysis.
		Sample Z.388 from 507.8 m — brecciated and mineralised carbonate.
509.5	511.66	Incoming of wacke units.
		Sample Z.389 from 509.7 m — Wacke/mudstone.
		Sample Z.390 from 510.7 m — Wacke.
511.66	515.0	Dominantly mudstone.
515.0	517.0	Breccia zone.
517.0	526.94	Wacke units, tuffaceous.
		Sample Z.391 from 518.7 m — Wacke.
		Sample Z.392 from 523.9 m — Wacke.
		Sample Z.393 from 525.9 m — Wacke.
526.94	530.80	Dominantly wacke with minor mudstone.
		Sample Z.394 from 527.8 m — Wacke.
530.80	535.50	Brecciated zone, dominantly mudstone and carbonate with minor wacke.
535.50	540.5	Dominantly wacke with minor mudstone.
		Sample Z.395 from 539.1 m — Wacke.
540.50	545.00	Honfelsed, pyrite bearing, mudstone and carbonate.
545.00	558.3	Interbedded volcanic wacke and mudstone.
		Sample Z.396 from 551.5 m — Wacke.
		Sample Z.503 from 543.8 m — mineralisation for analysis.
		Sample Z.397 from 554.4 m — Wacke.
558.30	671.5	Interbedded volcanic wacke and mudstone.
		Sample Z.504 from 590.5 m — mineralisation for analysis.
		Sample Z.505 from 607.1 m — mineralisation for analysis.
		Sample Z.506 from 612.1 m — mineralisation for analysis.
		Sample Z.507 from 642.4 m — mineralisation for analysis.
		Sample Z.508 from 670.6 m — mineralisation for analysis.
671.0		Hole Surveyed: Direction — 82° to 275°.

END OF HOLE

SERPENTINE HILL DDH 2 (SH2)

Borehole Name/Number:	Serpentine Hill No 2
Easting Co-ordinates:	367 850 mE
Northing Co-ordinates:	5 366 199 mN
Collar height (ASL):	263.2 m
Depth:	150 m

This hole was drilled in low-Ti basalt, which is part of the Serpentine Hill Ultramafic Complex. The hole was drilled to 150 m depth, as the first 50 m of core was considered too weathered for analysis.

Core Log

From (m)	*To (m)*	*Description*
0.0	14.0	Yellow-red clay
14.0	29.0	Fractured, highly-weathered, pale-green basalt and basalt breccia.
29.0	43.0	Fault/rubble zone, broken, highly weathered basalt.
43.0	62.0	Highly weathered, volcanic agglomerate.
62.0	67.0	Brecciated, vesicular lava.
		Sample SH2/1 — 62 m, basaltic breccia.
67.0	77.5	Brecciated, quenched lava.
77.5	91.0	Brecciated, volcanic wacke/basalt.
91.0	96.0	Volcanic agglomerate.
		Sample SH2/2, quenched basalt.
96.0	100.5	Fine- to medium-grained basalt with calcite veins and disseminated sulphide mineralisation.
100.5	101.0	Zone of sulphide mineralisation.
		Sample SH1/6 — 100.5–101.0 m, mineralised basalt.
101.0	113.0	Massive to brecciated basalt with calcite veins and disseminated sulphide mineralisation.
113.0	114.0	Fine-grained basalt with zone of sulphide mineralisation.
		Sample SH2/3, mineralised, fine-grained basalt.
114.0	122.0	Massive to brecciated basalt with calcite veining and disseminated sulphide mineralisation.
122.0	123.0	Volcanic conglomerate.
123.0	150.0	Massive to brecciated basalt with calcite veining and disseminated sulphide mineralisation.
		Sample SH2/4 — 132 m, vesicular basalt.
		Sample SH2/5 — 148 m, massive, fine-gained basalt.

END OF HOLE

SERPENTINE HILL DDH 3 (SH3)

Borehole Name/Number:	Serpentine Hill No 3
Easting Co-ordinates:	367 914 mE
Northing Co-ordinates:	5 367 011 mN
Collar height (ASL):	235.5 m
Depth:	140 m

This hole was drilled into the two-pyroxene gabbro associated with the low-Ti tholeiitic basalt. Because the top 45 m consisted of clay and a small amount of kernels of gabbro, the hole was taken to 140 metres.

Grain sizes used:	Fine-grained	<1 mm
	Medium-grained	1–3 mm
	Coarse-grained	3–5 mm
	Pegmatitic	>5 mm

Note — Grain size can vary markedly over 100–500 mm.

Log of Core

From (m)	*To (m)*	*Description*
0.0	25.0	Clay and small kernels of gabbro from a spheroidally weathered zone — only 3.5 m core recovery.
25.0	40.0	Clay and small kernels of gabbro from a spheroidally weathered zone — only 4.0 m core recovery.
40.0	45.0	Clay and small kernels of gabbro from a spheroidally weathered zone — only 1.5 m core recovery.
45.0	50.0	Fine- to medium- grained gabbro.
		Sample SH3/1 — 46.5 m, medium-grained gabbro.
50.0	50.65	Pegmatitic zone, some crystals 50 mm.
50.65	52.70	Fine- to medium-grained gabbro.
52.70	52.85	Pegmatitic zone, some crystals 50 mm.
52.85	72.20	Fine- to medium-grained gabbro.
		Sample SH3/2 — 67.0 m, medium-grained gabbro.
72.20	72.40	200 mm wide quartz vein.
72.40	88.60	Fine- to medium-grained gabbro.
88.60	89.90	Pale-grey, highly-weathered, gabbro.
89.00	99.0	Fine- to medium-grained gabbro.
		Sample SH3/3 — 91.5 m, medium-grained gabbro.
99.0	102.0	Dominantly pegmatitic gabbro.
102.0	110.0	Dominantly coarse-grained.
110.0	110.80	Pegmatitic gabbro.
110.8	116.5	Fine- to medium-grained gabbro.
		Sample SH3/4 — 114.5 m, medium-grained gabbro.
116.5	117.0	Pegmatitic gabbro.
117.0	125.0	Medium- to coarse-grained gabbro.
125.0	125.3	Pegmatitic gabbro.
125.3	132.0	Dominantly medium-grained gabbro.
132.0	140.0	Dominantly-coarse grained gabbro.
		Sample SH3/5 — 138.5 m, coarse-grained gabbro.

END OF HOLE

38/63

SERPENTINE HILL DDH 4 (SH4)

Borehole Name/Number:	Serpentine Hill No 4
Easting Co-ordinates:	368 298 mE
Northing Co-ordinates:	5 367 516 mN
Collar height (ASL):	335.1 m
Depth:	101.5 m
Inclination:	60° to 270°

Log of Core

From (m)	*To (m)*	*Description*
0.0	53.20	Serpentinised peridotite, in places plagioclase-bearing, in places with thin gabbroic dykes.
		Sample SH4/1 — 15.5 m, serpentinised peridotite.
		Sample SH4/2 — 33.0 m, serpentinised peridotite.
		Sample SH4/3 — 47.0 m, gabbroic zone.
53.20	55.00	Fault zone — core loss — only 500 mm core recovery.
55.0	83.10	Serpentinised peridotite with carbonate replacement zones between 72.0–74.3 m, and 76.3–79.1 m; and shear zones, between 83.1–83.7 m and 89.0–90.5 m.
		Sample SH4/4 — 65.0 m, serpentinised peridotite.
		Sample SH4/5 — 78.5 m, carbonate replacement zone.
83.10	101.5	Light-green, highly sheared, serpentinite with fibrous chrysotile and magnetite schlieren.
		Sample SH4/6 — 92.0 m, serpentinised peridotite.
		Sample SH4/7 — 100.0 m, serpentinised peridotite.

END OF HOLE

SERPENTINE HILL DDH 5 (SH5)

Borehole Name/Number:	Serpentine Hill No 5
Easting Co-ordinates:	368 289 mE
Northing Co-ordinates:	5 367 464 m
Collar height (ASL):	331.5 m
Depth:	101.5 m
Inclination:	60° to 270°

Log of Core

From (m)	*To (m)*	*Description*
0.0	48.6	Serpentinised peridotite, in places plagioclase-bearing, in places with thin cross-cutting gabbroic dykes with reaction zones.
		Sample SH5/1 — 22.5 m, serpentinised peridotite.
		Sample SH5/2 — 41.5 m, serpentinised peridotite.
48.6	50.8	Gabbro
50.8	60.5	Serpentinised peridotite, in places plagioclase-bearing, in places with thin cross-cutting gabbroic dykes with reaction zones.
		Sample SH5/2 — 41.5 m, serpentinised peridotite.
		Sample SH5/3 — 54.5 m, serpentinised peridotite.
60.5	63.5	Gabbro.
63.5	68.2	Serpentinised peridotite with disseminated sulphide mineralisation.
		Sample SH5/4 — 66.0 m, serpentinised peridotite.
86.2	78.8	Serpentinised peridotite, in places plagioclase-bearing, in places with thin cross-cutting gabbroic dykes with reaction zones.
78.8	90.0	Serpentinised, coarse-grained, orthopyroxenite-bearing peridotite — in places oikocrystic, in places with a mosaic texture, in places with post-cumulate plagioclase.
		Sample SH5/5 — 86.5 m, serpentinised, plagioclase-bearing peridotite.
90.0	91.0	Rubble zone — core loss, 500 mm recovery, dominantly orthopyroxene-bearing peridotite.
91.0	101.5	Light-green, highly sheared, serpentinite with fibrous chrysotile and magnetite schlieren.
		Sample SH5/6 — 100.5 m, serpentinite.

END OF HOLE

40/63

SERPENTINE HILL DDH 6 (SH6)

Borehole Name/Number:	Serpentine Hill No 6
Easting Co-ordinates:	368 281 mE
Northing Co-ordinates:	5 367 416 mN
Collar height (ASL):	325.6 m
Depth:	101.5 m
Inclination:	60° to 270°

Log of Core

From (m)	*To (m)*	*Description*
0.0	59.90	Serpentinised peridotite, in places plagioclase-bearing, in places with thin cross-cutting gabbroic dykes with reaction zones.
		Sample SH6/1 — 11.5 m, serpentinised peridotite.
		Sample SH6/2 — 34.5 m, serpentinised peridotite.
		Sample SH6/3 — 47.5 m, serpentinised peridotite.
59.0	63.3	Reaction zone between peridotitic and gabbroic rocks.
		Sample SH6/4 — 62.5 m, reaction zone.
63.3	88.5	Serpentinised peridotite, in places plagioclase-bearing, in places with thin cross-cutting gabbroic dykes with reaction zones.
		Sample SH6/5 — 81.5 m, serpentinised peridotite.
88.5	89.8	Alteration zone with disseminated sulphide mineralisation.
89.8	90.0	Sheared serpentinite.
90.0	101.5	Serpentinised peridotite, in places with pyroxene oikocrysts.
		Sample SH6/6 — 101.0 m, serpentinised, oikocryst-bearing peridotite

END OF HOLE

41/63

APPENDIX 3

Chemical analyses of whole rock samples from the diamond drill holes

TABLE 4

Analyses of basalt samples from hole SH2 and gabbro samples from hole SH3

Field No.	SH2/1	SH2/2	SH2/3	SH2/4	SH2/5	SH2/6	SH3/1	SH3/2	SH3/3	SH3/4	SH3/5
Anal. No.	884612	884613	884614	884615	884616	884617	884618	884619	884620	884621	884622
SiO_2	57.11	43.21	55.68	48.24	57.35	48.87	49.17	47.60	46.09	49.86	47.72
TiO_2	0.14	0.16	0.25	0.23	0.29	0.22	0.11	0.05	0.04	0.14	0.03
Al_2O_3	13.54	12.18	11.01	14.50	12.45	12.48	13.23	13.38	12.05	14.77	15.76
Fe_2O_3	1.46	1.38	5.47	1.31	2.36	2.48	1.13	1.01	1.29	0.83	1.04
FeO	9.52	12.56	7.82	8.67	6.77	9.35	8.15	7.92	7.60	5.34	5.21
MnO	0.08	0.38	0.16	0.17	0.11	0.19	0.18	0.18	0.18	0.15	0.14
MgO	9.80	8.56	3.82	6.16	3.74	7.00	12.05	10.72	13.17	10.85	10.82
CaO	0.07	6.58	5.59	7.63	5.09	6.09	11.14	11.53	10.47	12.93	13.27
Na_2O	0.70	1.28	2.74	3.01	3.76	2.15	1.06	1.69	1.47	2.04	2.09
K_2O	0.50	0.09	0.34	0.12	0.15	0.05	0.09	0.11	0.21	0.12	0.11
P_2O_5	0.03	0.09	0.07	0.26	0.24	0.26	0.28	0.06	0.05	0.08	0.09
SO_3	0.06	0.21	1.32	0.18	0.90	3.86	0.31	0.04	0.04	0.10	0.02
CO_2	0.05	5.09	2.64	3.32	3.14	2.47	0.25	1.10	1.48	0.12	0.29
H_2O^+	7.08	7.45	3.43	7.00	3.72	4.26	3.74	4.15	5.21	2.91	3.41
Total	100.14	99.22	100.59	100.80	100.07	99.73	100.89	99.54	99.35	100.24	100.00
Cr	870	310	91	160	135	230	760	460	1000	610	540
Ni	170	115	34	66	45	120	185	145	210	165	200
Co	57	57	67	52	38	98	68	58	67	46	39
Sc	43	45	49	47	32	44	46	39	46	41	39
V	250	260	420	290	200	280	160	140	130	150	115
Cu	45	115	610	150	310	6300	230	41	31	22	15
Pb	<11	<11	<11	<11	<11	<11	<11	<11	<11	<11	<11
Zn	140	230	53	45	27	55	43	41	53	28	28
Rb	21	26	31	22	19	28	28	27	48	28	26
Sr	7	61	110	90	98	110	150	125	140	210	190
Ta	0.42	-	0.35	-	0.30	-	0.35	-	0.36	-	0.60
Hf	0.26	-	0.34	-	0.20	-	0.22	-	0.23	-	0.21
Zr	13	17	27	23	29	26	27	23	24	33	29
Y	5	3	7	6	8	3	<2 (1)	<2 (1)	2	<2 (1)	<2 (1)
La	0.17	-	0.28	-	0.34	-	0.11	-	0.07	-	0.09
Ce	0.88	-	0.83	-	1.00	-	0.40	-	0.40	-	0.40
Nd	1.00	-	1.20	-	1.50	-	0.35	-	0.35	-	0.35
Sm	0.40	-	0.54	-	0.63	-	0.12	-	0.14	-	0.11
Eu	0.09	-	0.17	-	0.21	-	0.17	-	0.17	-	0.17
Tb	0.15	-	0.20	-	0.25	-	0.07	-	0.07	-	0.07
Ho	0.27	-	0.40	-	0.49	-	0.10	-	0.10	-	0.10
Yb	1.07	-	1.03	-	1.39	-	0.24	-	0.31	-	0.24
Lu	0.17	-	0.21	-	0.24	-	0.14	-	0.04	-	0.04

TABLE 5

Analyses of ultramafic rocks from hole SH1 Melba Flats and ultramafic rocks from hole SH4 from east of the highway at Serpentine Hill

Field No.	SH1/1	SH1/3	SH1/5	SH1/6	SH1/7	SH1/8	SH4/1	SH4/2	SH4/3	SH4/4	SH4/5	SH4/6	SH4/7
Anal No.	884604	884606	884608	884609	884610	884611	884623	884624	884625	884626	884627	884628	884629
SiO_2	38.59	45.80	43.86	40.50	41.05	43.98	40.51	39.46	47.69	35.65	31.57	34.65	33.34
TiO_2	0.01	0.01	0.58	0.19	0.16	0.39	0.01	0.04	0.05	<0.01	0.01	<0.01	<0.01
Al_2O_3	2.83	1.81	13.34	7.06	6.71	12.20	4.13	3.98	9.39	0.68	0.05	0.01	0.01
Fe_2O_3	5.36	2.49	1.39	2.46	3.60	2.14	5.11	4.49	0.91	8.42	2.63	4.56	4.26
FeO	2.31	4.99	8.29	6.33	6.05	7.65	4.14	4.20	7.66	2.28	3.54	1.03	0.61
MnO	0.08	0.19	0.17	0.14	0.16	0.17	0.12	0.11	0.20	0.07	0.11	0.08	0.07
MgO	36.09	31.10	14.54	27.87	27.45	17.82	31.59	33.53	19.01	38.28	35.08	41.75	42.64
CaO	0.19	0.65	8.75	3.93	4.52	9.67	2.94	1.23	7.82	0.64	0.78	1.01	0.83
Na_2O	1.09	1.71	1.96	0.41	0.46	1.25	0.43	0.35	1.09	0.28	0.23	0.25	0.25
K_2O	0.15	0.17	0.57	0.05	0.06	0.18	0.03	0.02	0.05	0.01	0.06	0.08	0.01
P_2O_5	0.05	0.06	0.15	0.22	0.04	0.10	0.02	0.18	0.07	<0.01	0.03	0.01	0.03
SO_3	0.08	0.03	0.09	0.23	0.13	0.11	0.05	0.06	0.02	0.04	0.06	0.03	0.02
CO_2	0.28	0.85	1.40	1.38	0.38	0.08	0.28	0.07	0.06	1.26	18.43	1.89	1.59
H_2O^+	12.16	9.40	4.22	9.18	8.64	3.71	10.09	12.04	5.69	11.92	6.59	14.20	15.32
Total	99.27	99.26	99.34	99.95	99.41	99.45	99.45	99.76	99.71	99.54	99.17	99.56	98.99
Cr	7600	5000	1400	4900	3700	1750	3300	3500	2100	7400	2000	2100	2500
Ni	1950	680	500	1650	1200	630	1550	1750	320	1500	1800	1950	1800
Co	115	81	75	100	100	81	105	99	63	100	70	89	92
Sc	<8	18	44	24	22	44	19	14	33	7	<5	<5	<5
V	16	43	210	105	110	200	61	54	135	25	5	5	4
Cu	6	6	135	65	29	98	9	7	22	9	<4	<4	<4
Pb	<11	<11	<11	<11	<11	<11	<11	<11	<11	<11	<11	<11	<11
Zn	34	36	57	46	40	45	30	30	42	39	49	36	36
Rb	17	18	44	21	19	30	21	21	25	20	15	12	12
Sr	<8	13	92	17	25	50	6	<5	93	<5	<5	18	<5
Zr	6	9	39	13	16	30	7	7	19	9	6	6	7
Y	<6	<6	8	7	6	14	<6	<6	<6	<6	<6	<6	<6

TABLE 6

Analyses of samples from holes SH5 and SH6 — both within ultramafic rocks, east of the highway at Serpentine Hill

Field No.	SH5/1	SH5/2	SH5/3	SH5/4	SH5/5	SH5/6	SH5/13	SH6/1	SH6/2	SH6/3	SH6/4	SH6/5	SH6/6
Anal No.	884630	884631	884632	884633	884634	884635	884636	884637	884638	884639	884640	884641	884642
SiO_2	37.54	37.53	37.51	38.97	47.58	33.25	39.10	39.21	38.29	35.42	42.19	36.71	40.84
TiO_2	0.01	0.01	0.02	0.05	0.08	0.03	0.05	0.04	0.05	0.04	0.16	0.04	0.02
Al_2O_3	2.69	2.20	2.31	2.07	5.99	0.47	3.98	2.64	3.52	2.82	15.74	2.63	5.24
Fe_2O_3	5.45	6.36	5.92	4.12	1.02	6.71	4.82	5.53	5.02	6.33	0.70	6.30	2.89
FeO	3.90	3.00	2.97	3.99	6.88	1.80	4.72	3.74	3.95	3.45	2.51	2.59	5.40
MnO	0.09	0.08	0.10	0.18	0.18	0.06	0.11	0.13	0.12	0.11	0.22	0.09	0.11
MgO	35.99	36.87	36.96	36.14	26.03	43.56	34.66	35.18	35.23	39.65	11.41	37.35	31.74
CaO	0.15	0.04	0.05	0.05	4.70	0.03	2.30	0.71	1.04	0.07	21.78	0.11	2.71
Na_2O	0.28	0.24	0.25	0.25	0.27	0.36	0.25	0.29	0.127	0.24	0.32	0.25	0.06
K_2O	0.02	0.01	0.01	0.01	0.20	0.01	0.02	0.02	0.02	0.02	0.14	0.01	0.02
P_2O_5	0.01	0.02	0.02	0.16	0.20	0.16	0.19	0.16	0.18	0.16	0.17	0.15	0.08
SO_3	0.02	0.06	0.05	0.11	0.02	0.06	0.03	0.04	0.07	0.06	0.02	0.08	0.11
CO_2	0.08	0.04	<0.01	0.01	0.07	0.34	0.13	0.08	0.16	0.06	0.31	0.12	0.03
H_2O^+	12.22	12.26	12.44	13.07	7.53	13.44	10.81	11.87	12.34	12.53	4.57	12.55	10.11
Total	98.45	98.72	98.62	99.18	100.55	100.28	101.17	99.64	100.26	100.96	100.24	98.98	99.36
Cr	5300	4800	5800	4800	3800	5700	3400	6900	7100	6900	256	6600	5500
Ni	1800	2000	1750	1700	560	1350	1550	1550	1800	1900	410	2100	1150
Co	99	100	100	92	62	100	105	110	110	105	33	99	93
Sc	12	10	11	9	25	8	16	14	13	12	41	9	14
V	51	39	51	40	73	19	54	61	54	59	140	50	54
Cu	7	6	<4	6	<4	13	6	9	7	8	14	6	9
Pb	<11	<11	<11	<11	<11	<11	<11	<11	<11	<11	<11	<11	<11
Zn	38	34	33	31	33	46	32	40	38	239	29	27	35
Rb	16	15	14	18	13	16	17	15	16	16	40	14	19
Sr	<8	<8	<8	<8	<8	<8	<8	<8	<8	<8	33	<8	<8
Zr	<6	6	7	7	<6	<6	7	6	7	<6	14	6	6
Y	<6	<6	<6	<6	<6	<6	<6	<6	<6	<6	<6	<6	<6

APPENDIX 4

Structural Analysis of Amphibolite Zone, Serpentine Hill Drill Hole SH1

Tasmania Department Of Resources and Energy

Division of Mines and Mineral Resources — Report 1991/09

Structural analysis of amphibolite zone, Serpentine Hill DDH No. 1 (SH 1)

by B. D. GOSCOMBE

CHRONOLOGY OF DEFORMATION AND METAMORPHISM

An interpretive time sequence of tectonic events recognised in thin section in the different lithologies is presented in Table 1. The lithologies and deformational features recognised in specific samples are summarised with respect to depth in the core in Figure 1.

The majority of the section of core studied (0–280 m) is amphibolite and banded epidote-amphibole rock (fig. 1). Both types of amphibolites are metamorphic rocks which have a fine-grained to medium-grained polygonal texture consisting largely of well aligned (foliated) pale green amphibole laths. As such the texture of these rocks is that of an annealed shear fabric (S_2, see Table 1). In other words, grain margins are straight and appear to have been thermally annealed either during and/or subsequent to ductile shearing. Thermal annealing of the shear fabric is supported by the general paucity of shearing, boudinage, kinking and undulose extinction of the individual amphibole grains. Consequently the mineral phases constituting the shear fabric define a metamorphic assemblage labelled M_2.

M_2 assemblages include the following in amphibolite:

- pale green amphibole-plagioclase-sphene-opaque-orange biotite.

The assemblages of the different domains in banded epidote-amphibole rock are:

- pale green amphibole-plagioclase-sphene-chlorite-opaque ± epidote,
- epidote-sphene-scapolite-chlorite-pale green amphibole,
- pale green amphibole-scapolite-plagioclase-biotite,
- biotite-epidote-plagioclase.

The assemblage in the pelitic ultra-mylonite at 260 m is:

- quartz-calcite-chlorite-plagioclase-biotite.

The mineral proportions and mineral assemblages are consistent with the protolith of the two amphibolite rock types having been basalts metamorphosed to the lower amphibolite facies (i.e. approximately 400–500°C).

The aligned granoblastic texture of these amphibolites is the typical fabric expression as a result of ductile shear of amphibolites (Goscombe, 1990). The texture is strongly foliated in most samples and is mylonitic in nature. Development of this strong foliation by shear is supported by this foliation enclosing augen of pre-existing coarse-grained amphibole and plagioclase. Biotite laths are also strongly aligned, and both enclose and abut the fine-grained S_2 amphibole grains. In most amphibolite samples 90–100 % of the rock is amphibole, and the only variations in the S_2 foliation are domains of finer grainsize. In some samples a second planar element is recognised as very thin planes of significantly finer grainsize at low angles to the S_2 foliation. The S_2 foliation swings into these planes, which are interpreted as thin zones of relatively high strain, that is C-planes (Simpson, 1984). In some samples these zones of relatively high strain (i.e. marked grainsize reduction) are thought to parallel the S_2 foliation. In the banded amphibolites the S_2 foliation not only parallels a pre-existing compositional layering (2–8 mm thick) but also excentuates this and gives rise to a finer scale (1–2 mm thick) differentiated layering.

Amphibolite samples Z358 and Z359, from 270.5 m and 275 m respectively, have 30–40 % of the sample being a much coarser grained metamorphic assemblage of augen which are enclosed by the M_2 ductile shear fabric described above. The earlier coarse-grained augen assemblage consists of pale green amphibole and plagioclase, and has been labelled M_1. Similarly the epidote-rich layers in the banded amphibolites are enclosed and boudinaged by the ductile shear fabric (S_2), thus these layers may also represent M_1 domains. Consequently it is felt that both M_1 and M_2 have similar lower amphibolite facies assemblages, except for the presence of biotite in the S_2 shear fabric.

Apart from the amphibolite facies metamorphic rocks recognised in the first 280 m of core (fig. 1), there is a component of distinctly different igneous rocks. The first 48 m consists largely of retrogressed (serpentinised and actinolitised to varying degrees) orthopyroxenite. There are also two slivers of serpentinite after orthopyroxenite at

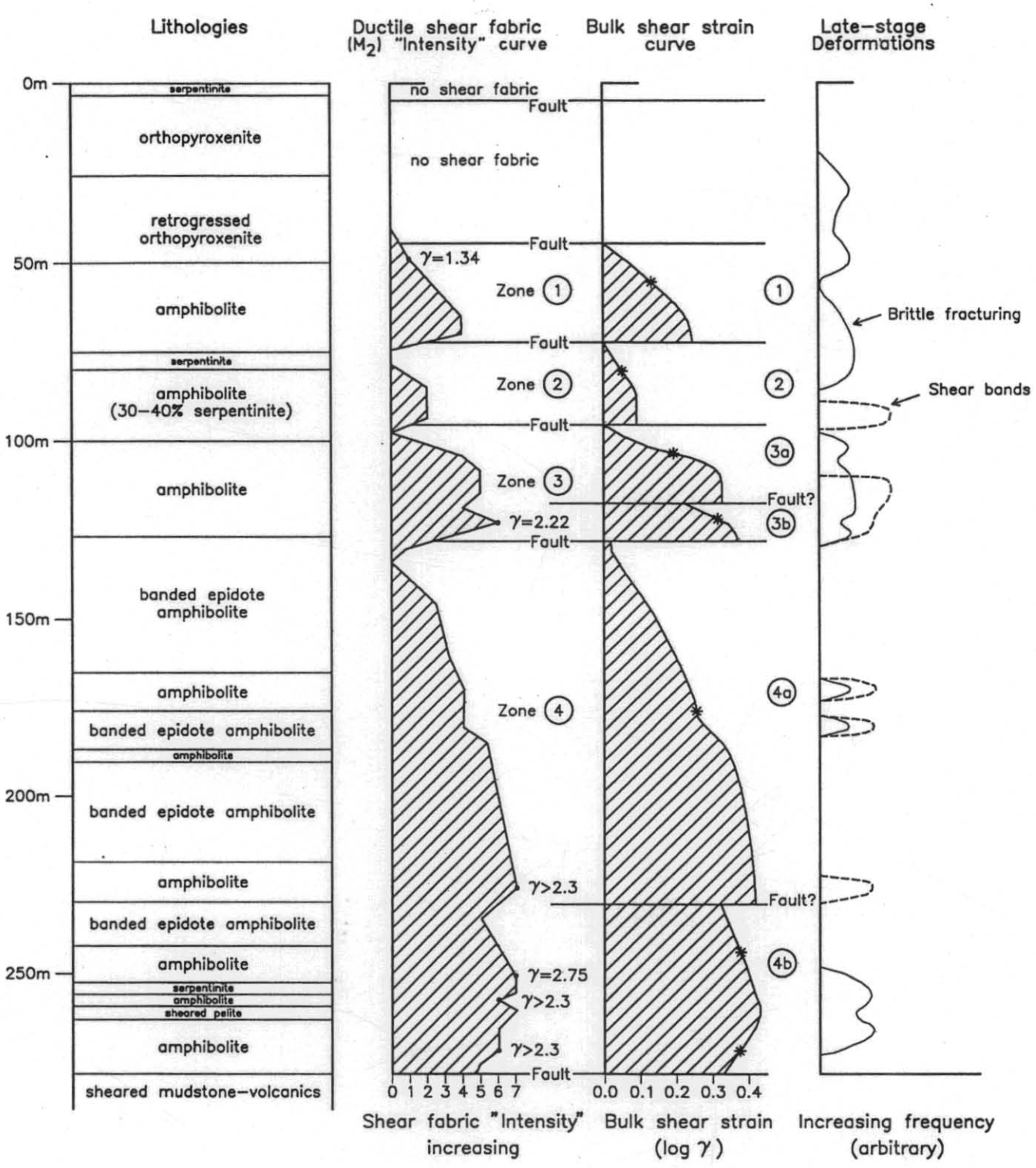
Lithologies
Ductile shear fabric (M_2) "Intensity" curve
Bulk shear strain curve
Late–stage Deformations
0m
50m
100m
150m
200m
250m
serpentinite
orthopyroxenite
retrogressed orthopyroxenite
amphibolite
serpentinite
amphibolite (30–40% serpentinite)
amphibolite
banded epidote amphibolite
amphibolite
banded epidote amphibolite
amphibolite
banded epidote amphibolite
amphibolite
banded epidote amphibolite
amphibolite
serpentinite
amphibolite
sheared pelite
amphibolite
sheared mudstone–volcanics
no shear fabric
Fault
no shear fabric
Fault
γ=1.34
Zone 1
Fault
Zone 2
Fault
Zone 3
γ=2.22
Fault
Zone 4
γ>2.3
Fault?
γ=2.75
γ>2.3
γ>2.3
Fault
1
2
3a
Fault?
3b
4a
4b
Brittle fracturing
Shear bands
0 1 2 3 4 5 6 7
0.0 0.1 0.2 0.3 0.4
Shear fabric "Intensity" increasing
Bulk shear strain (log γ)
Increasing frequency (arbitrary)

Figure 1.

5 cm

78.5 m and 253 m (fig. 1). The amphibolites which occur throughout the bulk of the core do not have assemblages (except for the presence of high Cr-spinel in some samples) consistent with their formation by metamorphism of serpentinised orthopyroxenite. It is thought that the orthopyroxenite and amphibolites are two distinct rock types, not the amphibolites being the metamorphic equivalent of the other. It is felt that both the serpentinisation of the igneous orthopyroxenite and the early amphibolite facies metamorphism (M_1) of the basalts occurred prior to the ductile shear fabric (S_2). As a consequence M_1 metamorphism and the serpentinisation event may be unrelated.

A multitude of late-stage (largely brittle and hydrous-carbonic) deformational features overprint and reactivate the earlier ductile shear fabric (S_2). These are listed below in an approximate chronological order of formation (oldest to youngest). However it is felt that these are not discrete deformational episodes, as the timing of these features do overlap.

1. The earliest features are thin (<1 mm), discrete, foliated shear bands consisting of very fine-grained phases such as serpentinite, carbonate, chlorite, actinolite and quartz. These most commonly reactivate the earlier ductile fabric (S_2) as discrete zones of very marked grainsize reduction parallel to S_2, but also form at high angles to it.

2. Closely associated with thin shear bands, but also forming in isolation from them, are brittle fractures filled with the same mineral phases but of a much coarser grainsize and no foliation development. Fracture planes are random in orientation but are largely at high angles to the early ductile shear fabric (S_2). In some samples a high spatial density of these fractures and shear bands has formed brecciated domains. Some blocks, of the earlier S_2 fabric, within the breccia are rounded and so imply movement associated with the brittle fracturing episode. Movement along individual fractures is also shown by rotation and offsetting of the S_2 foliation. Some fractures are irregular and non-planar, similarly not all fractures are filled with the retrogressive minerals.

3. Thin (<<1 mm), discrete, laterally persistent and straight planes of movement displace (<1 mm) the chlorite-serpentinite-calcite-quartz filled fractures.

4. The last generation of brittle fractures are filled with coarse-grained quartz and/or calcite only, and these are not associated with any lateral displacements.

Brittle fracturing and fracture filling are recognised in many samples throughout the first 280 m of core, but particularly so in the intervals; 20–80 m, 100–123 m and 250–270 m (fig. 1). Thin, discrete shear bands are less common but are strongly correlated with the inferred fault-thrust planes (fracturing is also) which are discussed below and marked in Figure 1. Consequently these brittle-hydrous-carbonic features may be associated with late-stage reactivation of discrete sharp thrust? planes which may have formed during the earlier ductile shear episode (S_2).

Two late-stage faults (thrusts?) are inferred at the boundaries between the vertical, 40° and 60° dipping foliation zones at the top of the drill core. Dip of the foliation down the drill core is collated in Table 2. Consequently the two inferred faults are at approximately 7 m and 45 m. No ductile shear fabric (i.e. S_2) is recognised in the two uppermost zones of serpentinite (fig. 1). Consequently it is felt that the serpentinite did not experience S_2 ductile shear (Table 1) and thus formed extraneous to the amphibolite sequence, with the result that both rock types were later brought into fault (thrust?) juxtaposition after S_2 ductile shearing of the amphibolites. This juxtaposition possibly occured during the late-stage discrete thrusting? and brittle episodes (Table 1).

ESTIMATES OF SHEAR STRAIN AND DISPLACEMENTS

The "intensity" of the early ductile mylonitic fabric (S_2) has been arbitrarily graded into seven catagories (fig. 1). The "intensity" of the fabric is based on the following:

1. Degree of parallel alignment of amphibole laths and biotite plates.

2. The aspect ratios (i.e. length vs. width) of amphibole laths.

3. The degree of grainsize reduction experienced.

4. The proportion of the sample that has developed a mylonitic fabric. In most cases this is essentially 90–100 % (except for the samples listed in Table 2).

The variation in shear fabric "intensity" with bore hole depth is plotted in Figure 1. It is noted that there is a general increase in shear fabric "intensity" with depth. Furthermore, there are four broad zones between 45 m and 280 m. Within each zone the shear fabric "intensity" increases gradually from 0 at the top of the zone to a maximum value at or immediately before the base of the zone (fig. 1). Thus, within each of these zones there is an asymmetry of strain partitioning, with most of the strain being partitioned in the base. The boundaries between the high strain base of one zone and the absense of strain at the top of the next zone down the hole is very sharp. Consequently these boundaries are considered faults (possibly thrusts?). This is supported by distinct lithological changes at these boundaries. It is proposed that these four zones are in fact a packet of ductile shear zones which over-rode each other along sharp planes (thrusts?) of relatively high shear strain. In addition, further zones are defined by distinct drops in fabric "intensity", although not to zero values.

Quantitative estimates of bulk shear strain were made in seven samples (Table 2) by measuring the acute angle between the S_2 foliation (S-plane) and discrete, thin planes of relatively high shear strain which formed coevally with S_2 (C-plane). The relationship between bulk shear strain (γ) and the angle between C-S planes (ψ) is given as;

$$\tan 2\psi = 2/\gamma \text{ (Ramsay \& Graham, 1970).}$$

Mylonites with co-planar C-S planes are generally thought to have shear strains of >2.3 (Burg and Laurent, 1978). The

few approximate bulk shear strain estimates obtained are used to very roughly calibrate the fabric "intensity" curve data and so produce the shear strain curve presented in the middle of Figure 1 (with log γ axis).

The bulk shear strain curve has been used to derive estimates of the ductile shear displacement (parallel to S_2 foliation) within each delimited zone. These estimates do not incorporate possibly very large displacements along the discrete planes (thrusts?) between these zones. Displacements parallel to the shear fabric (S_2) are calculated by the following:

Assuming a vertical drill hole, the real width of the zone measured orthogonal to its margin (W) is given by;

$$W = L \cdot \cos \theta$$

where L = length of zone intersected by the core.
θ = dip from horizontal of the S_2 foliation.

The angle of rotation (due to S_2 ductile shearing) of a line originally orthogonal to S_2 (ψ) is given by the following two relationships;

$$\psi = \tan (D/W)$$

and

$$\psi = \tan \gamma$$

where D = displacement parallel to S_2
γ = bulk shear strain.

Consequently, displacement parallel to S_2 due to ductile shear is given by;

$$D = L \cdot \gamma \cdot \cos \theta$$

Maximum displacements are calculated using the maximum bulk shear strain estimate in the respective zone (Table 3). The median displacements are calculated using the average bulk shear strains (marked as a star on the shear strain curve in Figure 1). These displacement estimates and the relevant data are tabulated in Table 3. The estimates of total displacement by ductile (S_2) shear accross the packet of ductile shear zones between 45 m and 280 m are 256 m maximum displacement and 198 m average (or minimum) lateral displacement. The real total displacement across all these zones is not known because displacements due to the discrete bounding thrusts? are not known. Displacements along these discrete thrust? planes could potentially be in the order of kilometres.

CONCLUSIONS

Berry (1988) reports from the region that the foliation in the amphibolites dip to the east, and that the sense of shear is SE over NW along steeply plunging amphibole mineral lineations. Thus the 116 m wide (orthogonal to S_2 foliation) packet of ductile shear zones in amphibolites in the Serpentine Hill core involved a bare minimum of 256–198 m of over-thrusting to the NW. Further displacements were involved along discrete thrust planes within and bounding the amphibolite ductile shear zones, and in the highly sheared black muds and volcanic rocks (not discussed in this report) below the amphibolites. These un-quantified displacements were presumably large (kilometres scale) to emplace these medium-grade metamorphic rocks and cumulate ultramafic rocks in the upper crust.

The late-stage, more brittle and retrogressive deformational features may represent either of the following.

1. Brittle deformational expressions may have resulted from thrusting along the discrete thrust planes proposed by this study. These thrust planes may have formed in the final stages of S_2 ductile shear, either due to an increase in the strain rate or as a result of the body of rock moving upwards (to shallower crustal levels) into progressively less ductile deformational regimes (i.e. lower temperature and confining pressure).

2. Alternatively the more brittle deformations may be due to a totally unrelated shearing episode which reactivated parts of the S_2 ductile shear zone at lower crustal levels and at a later date than S_2–M_2.

REFERENCES

BERRY, R. F. 1988. The tectonic significance of mylonites on the margins of Cambrian mafic-ultamafic complexes in Tasmania, *in:* TURNER, N. J. (ed.). *The geology and evolution of the latest Precambrian to Cambrian rocks in the western Tasmania terrane. Abstracts of convention, April 1988.* 12–13. Geological Society of Australia, Tasmanian Division.

BERTHE, D.; CHOUKROUNE, P.; JEGOUZO, P. 1979. Orthogneiss, mylonite and non coaxial deformation of granites; the example of the South Armorican shear zone. *J. Struct. Geol.* 1:31–42.

BURG., J. P.; LAURENT, Ph. 1978. Strain analysis of a shear zone in a granodiorite. *Tectonophysics* 47:15–42.

GOSCOMBE, B. D. 1990. Tectonic evolution of an annealed ductile shear zone activated during the Alice Springs Orogeny. *Abst. geol. Soc. Aust.* 25. 188.

RAMSAY, J. G.; GRAHAM, R. H. 1970. Strain variation in shear belts. *Can. J. Earth. Sci.* 7:786–813.

[13 June 1991]

TABLE 1

Time sequence of tectono-thermal episodes recognised in the Serpentine Hill core. Time progresses down the page.

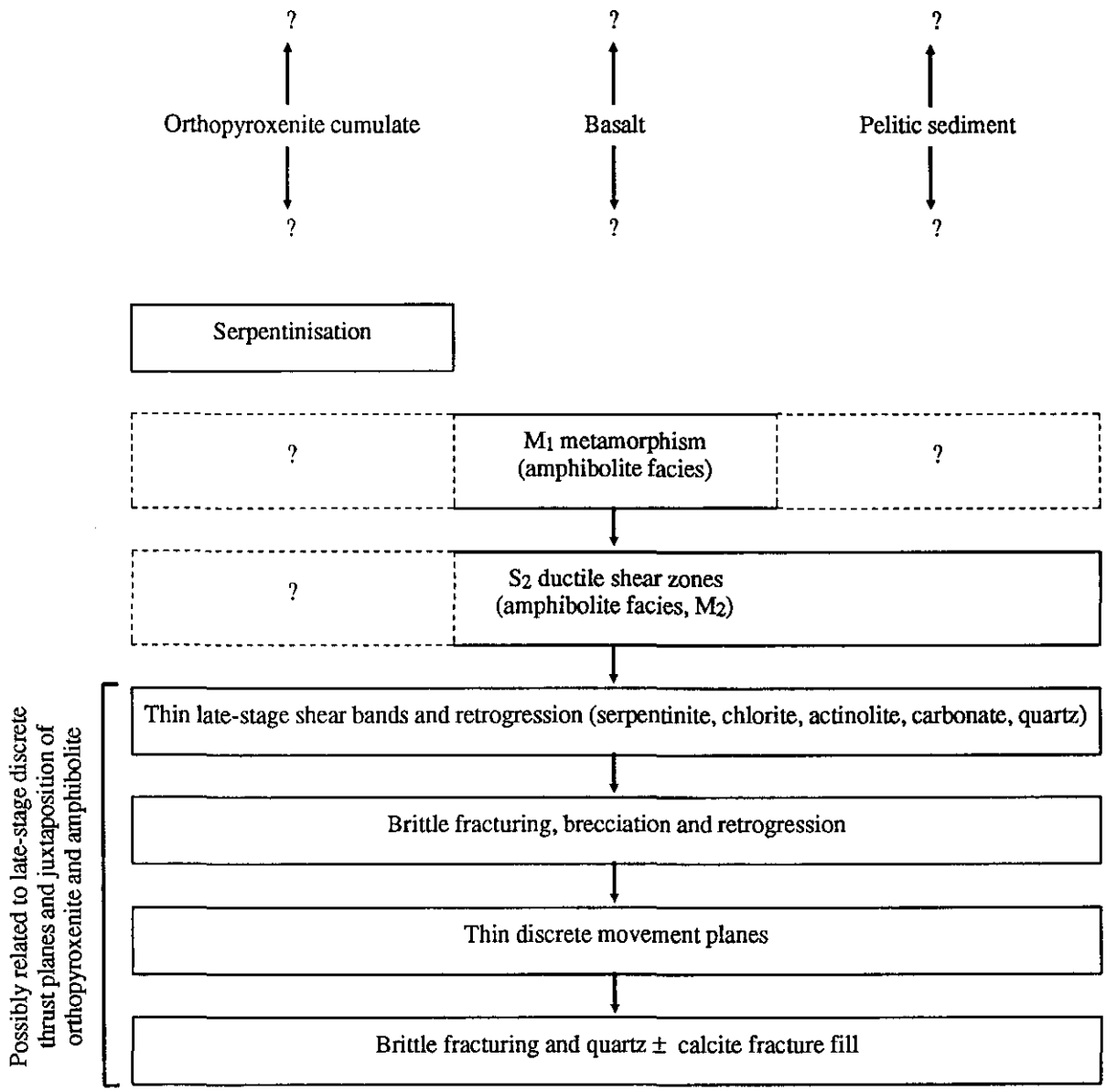

TABLE 2

Estimates of bulk shear strains (after Ramsay and Graham, 1970) from Type-1 (Berthe *et al.*, 1979) S-C amphibolite mylonites in Serpentine Hill core. * value after arguments of Burg and Laurent (1978).

Drill core depth (m)	Sample	Proportion of S_2 in sample (%)	Angle between C-S planes	Bulk shear strain (γ)
48	13	20	28°	1.34
123.8	45	90–100	21°	2.22
226	83	90–100	28°	1.34
251.5	2353	90–100	18°	2.75
251.5	2353	90–100	parallel	>2.3*
256	2355	90–100	parallel	>2.3*
270.5	2358	70	parallel	>2.3*
275	2359	60	-	-

TABLE 3

Estimates of displacement parallel to S_2 foliation due to ductile shear only in the amphibolite mylonites. Displacements are for the individual zones delimited in Figure 1. Calculations by method discussed in text.

Shear zone label	1	2	3a	3b	4a	4b	Total
Vertical thickness of zone — L (m)	27.5	23	22	10	102	47.5	232
True thickness of zone — W (m)							116
Dip of S_2 foliation — θ	65°	60°	60°	75°	60°	60°	
Maximum γ	1.78	1.2	2.13	2.29	2.51	2.69	
Average γ	1.35	1.09	1.58	2.09	1.82	2.29	
Maximum displacement — D (m)	20.7	13.8	23.4	5.9	128	64	255.8
Median displacement — D (m)	16	12.5	17.4	5.4	93	54	198.3

APPENDIX 5

Orthopyroxene-rich ultramafic-mafic rocks from western Tasmania and their PGE contents.

Tasmania Department of Mines—Report 1989/40

Orthopyroxene-rich ultramafic-mafic rocks from western Tasmania and their PGE contents

by A .V. Brown

Abstract

Ultramafic rocks from western Tasmania have been subdivided into three different successions on field criteria and/or mineral chemical data. Two of the three successions have whole-rock PGE values. Chondrite-normalised PGE plots define a negative slope distribution (Os-Pd) with an anomalous high Pt peak.

INTRODUCTION

This report combines the data used for a poster display presented at the Fifth International Platinum Symposium, Espoo, Finland (August 1–3, 1989), and a poster display to be presented at the Tenth Australian Geological Congress, Hobart, February 4–9, 1990.

Within western Tasmania there are fifteen separate areas of ultramafic–mafic rocks (fig. 1). The areas are usually fault-bounded, and consist of rocks belonging to one or more of three different ultramafic successions, which can be distinguished by field criteria and/or mineral chemical data (Brown, 1986).

The three associations are:–

- Layered Dunite-Harzburgite (LDH) succession
- Layered Pyroxenite-Dunite (LPD) succession
- Layered Pyroxenite-Peridotite and Associated Gabbro (LPG) succession

PGE Distribution

Whole-rock samples from all three of the Tasmanian ultramafic–mafic successions have detectable PGE concentrations.

A chondrite-normalised PGE diagram containing the 'average Tasmanian whole-rock sample' (average of 42 samples) shows that the plot for the Tasmanian 'sample' has a similar slope to samples from so called 'ophiolite' bodies but, in comparison to these, the Tasmanian 'sample' has anomalously high Pt values (fig. 2).

Work to date on Tasmanian samples indicates that PGE values are higher in rocks with a high chrome-spinel content. So far only Os–Ir–Ru alloy and laurite grains have been observed in polished sections. No Pt–Pd–Rh sulphide or alloy minerals have been observed, indicating that these elements are probably dispersed throughout the silicate phases and were not concentrated by a sulphide phase.

LDH SUCCESSION

The LDH succession consists of interlayered dunite, orthopyroxene-bearing dunite, and harzburgite. The rock types depend on the amount of orthopyroxene within any specific layer. Rocks within this succession contain olivine, enstatite and chrome spinel. The chemical range of these minerals is very restricted, irrespective of which area a sample comes from. Olivine grains have the composition of Fo_{93} to Fo_{94}; enstatite, En_{93} and En_{94}, with a calcium content of less than 0.5 wt%, indicating an original clinoenstatite composition. Chrome spinel grains have a 100×Cr/Cr+Al ratio (Cr*) of 87–93 (fig. 4). Late-stage, coarse-grained orthopyroxenite contains enstatite crystals of En_{93-94}, chrome spinel grains with a Cr* of 92 to 94, and minor olivine of Fo_{86-89}. This succession is considered to have been formed at high temperatures and low pressures as the magma chamber product of a boninitic magma.

Areas of the LDH succession occur on the western side of the Heazlewood River Complex (No. 3, fig. 1); as the whole of the Mt Stewart Complex (No. 4); the major part of the Huskisson and Wilson River Complexes (No. 5 & 6; Plates 1 and 2); a large part of the Adamsfield and Boyes River Complexes (No. 13 & 14); and at Rocky Boat Harbour (No. 15).

PGE Contents

Os–Ir–Ru alloy grains have been mined from alluvial and eluvial deposits associated with all areas of LDH succession. Records show that between 1880 and 1980, just over 880 kg of "osmiridium" had been recovered from the four main areas — Adamsfield (No. 14); Heazlewood (No. 3); Mt Stewart (No. 4) and Wilson River (No. 5). Smaller amounts are known to have been obtained from the Boyes River (No. 13) and Rocky Boat Harbour (No. 15). Compositions of PGE minerals from the Adamsfield area are listed in Table 1*a* and plotted in Figure 3. Further analyses of "osmiridium" parcels from Adamsfield are given in Table 1*b*.

LPD SUCCESSION

The LPD succession consists of thin (<5 mm–200 mm), uniform layers of orthopyroxenite, olivine orthopyroxenite and dunite. Harzburgite layers have not been found in this succession. Orthopyroxene grains range in composition from En_{85} to En_{89}, and have calcium contents varying between 0.6 and 2.0 wt%. Olivine grains vary between Fo_{87} and Fo_{90}. Minor chrome-diopside has a very limited composition with an average Ca:Mg:Fe = 47:49:4. Chrome-spinel grains have an average Cr* of 64 (fig. 4).

Areas of the LPD succession occur as fault-bounded blocks intermixed with areas of the LDH succession in the northern (Harman River) and southern (Riley Knob; Plate 3) parts of the Wilson River Complex (No. 5); in the Heazlewood River and Huskisson River Complexes (No.

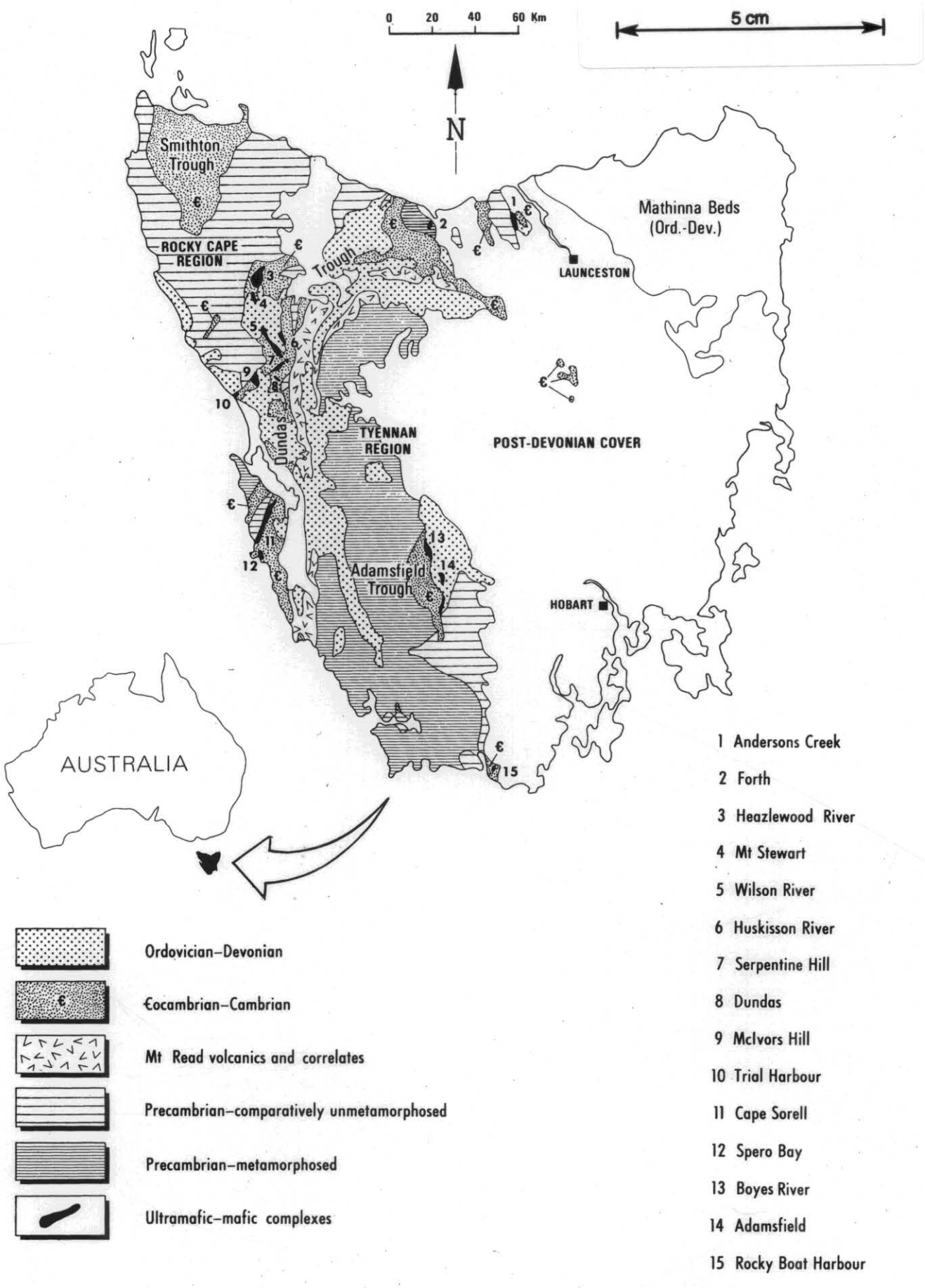

Figure 1. *Schematic geological map of Tasmania showing locations of ultramafic–mafic complexes. Rock distribution after 1:500 000 Geological Map of Tasmania (1976).*

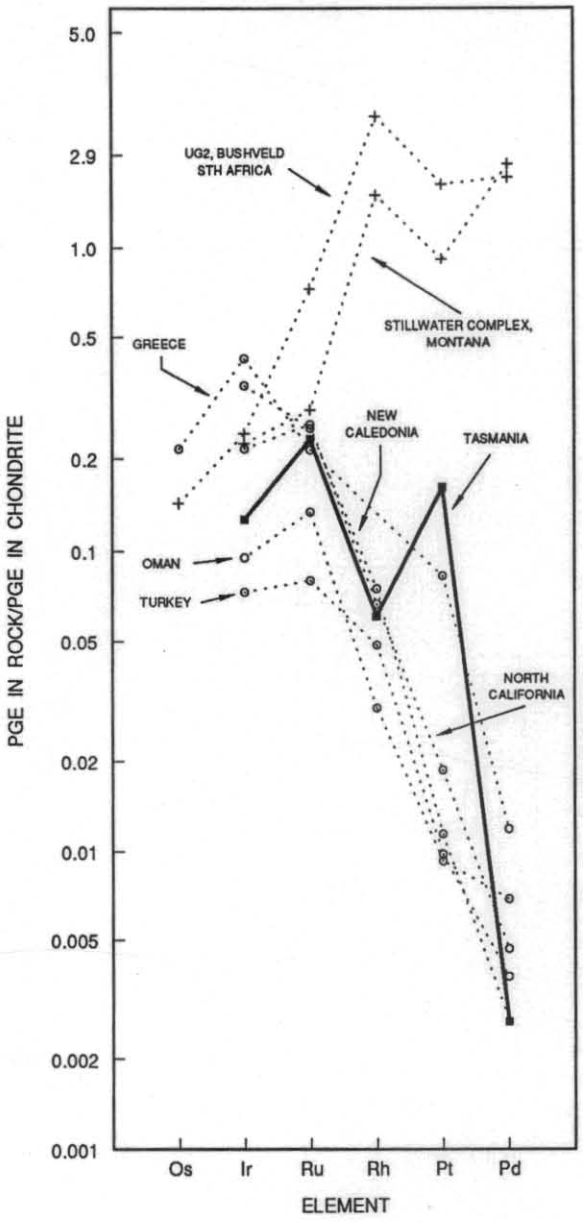

Figure 2. *Chondrite-normalised platinum-group element data (after Page et al., 1984) showing average data for 42 samples (after Brown et al., 1988)*

3 & 6); form the Colebrook Hill and Dundas bodies (No. 8); and at Adamsfield (No. 14; Plate 4), where rafts of the succession, surrounded by serpentinitic sheaths, are fault juxtaposed against areas of the LDH succession.

PGE Contents

So far no PGE minerals have been recorded associated with areas of LPD succession rocks. The average values for whole-rock samples from three different areas of this succession, the southern parts of the Heazlewood River (No. 3), Wilson River (No. 5), and Huskisson River (No. 6) Complexes, are listed in Table 2.

LPG SUCCESSION

The LPG succession is a multi-phase ultramafic-mafic succession. It consists of two ultramafic phases and a later intrusive phase of gabbro.

At Serpentine Hill the LPG succession consists of fault-disrupted blocks of what was originally a layered, plagioclase-bearing, orthopyroxene-rich sequence of pyroxenite, olivine pyroxenite, harzburgite and dunite, with numerous sedimentary-like structures. This sequence was later intruded and dismembered by a second magma which formed a layered, plagioclase-bearing, olivine-rich succession, which incorporated blocks of the first sequence and contains zones rich in chrome-spinel. Both of the ultramafic sequences were later intruded by a magma phase, or phases, which formed a massive, two-pyroxene gabbro. Although the mineral chemistry of the constituent mineral phases of the LPG succession have a similar chemical range to those in the LPD succession, the LPG succession contains plagioclase as a pervasive post-cumulus phase, and contains different rock types and layering characteristics to the LPD and LDH successions. The LPG succession is considered to have formed as the magma chamber product of a low-titanium, tholeiite magma (Brown and Jenner, 1989).

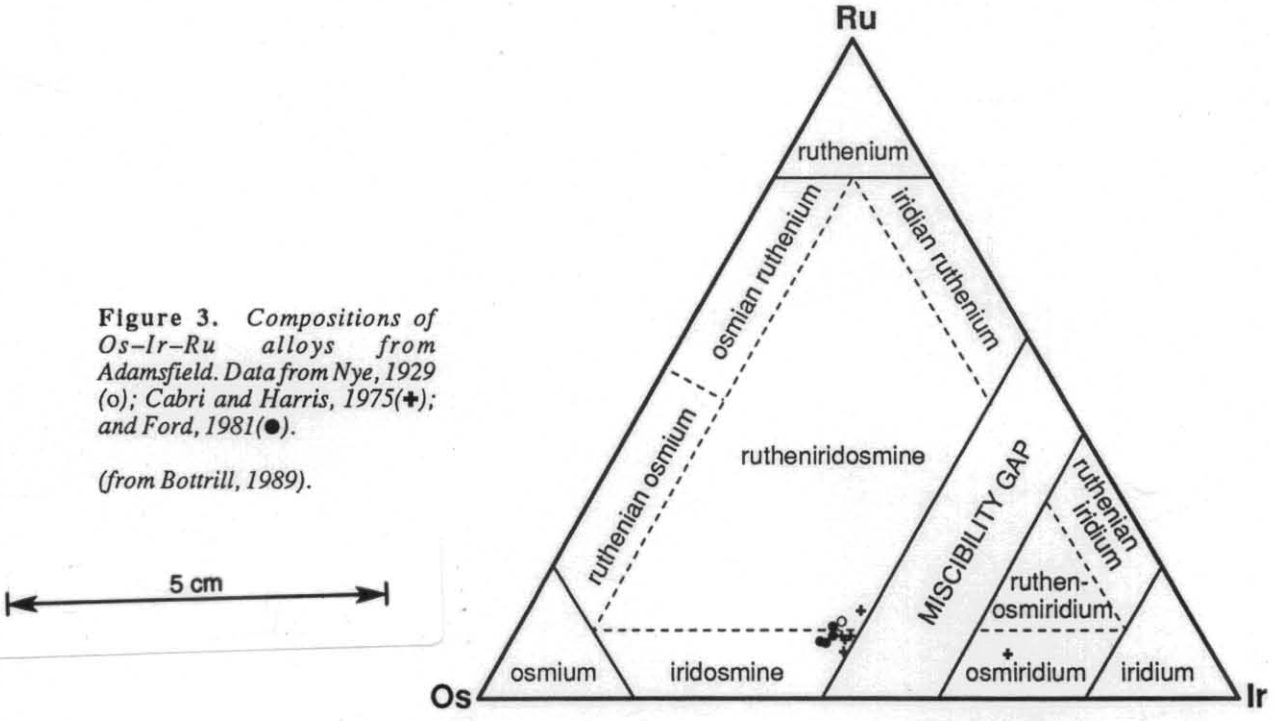

Figure 3. *Compositions of Os–Ir–Ru alloys from Adamsfield. Data from Nye, 1929 (o); Cabri and Harris, 1975(+); and Ford, 1981(●).*

(from Bottrill, 1989).

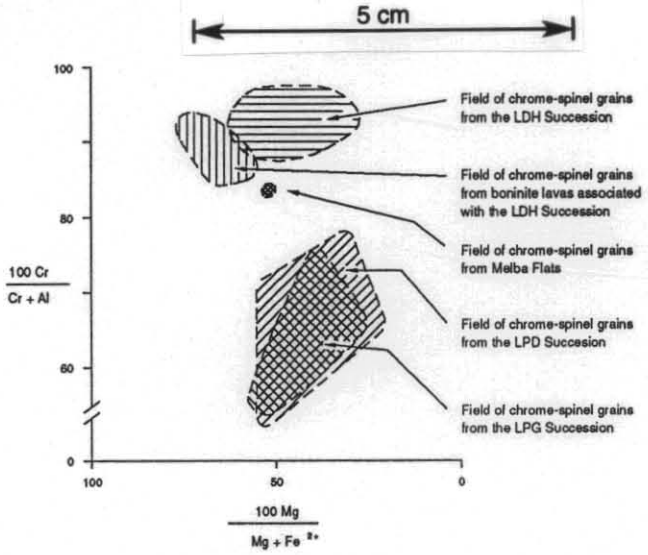

Figure 4. *Fields of chrome-spinel grains from Tasmanian ultramafic rocks.*

Areas of the LPG succession occur at Serpentine Hill (No. 7; Plates 5 and 6); McIvors Hill (No. 9); and as part of the Heazlewood River Complex (No. 3).

PGE Contents

A study of the LPG succession at Serpentine Hill (Brown *et al.*, 1988) showed that all the different parts of the succession contained whole-rock PGE values. Surface whole-rock samples were analysed by fire-assay / atomic absorption for Pt, Pd and Rh, and by fire-assay / spectographic technique for Ir and Ru, at the USGS Laboratories, Lakewood, Colorado, USA. Average values for these samples for the various sequences within the LPG succession at Serpentine Hill are listed in Table 3.

Because of the results obtained in the surface sampling programme, a follow-up programme of six, 100 m drill holes was undertaken on the different lithologies of the LPG succession at Serpentine Hill. The purpose of the holes was to obtain the distribution of PGE values across a stratigraphic distance in areas where PGE values had previously been obtained. Five samples were taken from each drill hole, at approximately 20 m spacings, for analysis.

Three holes were placed in the olivine-rich layered sequence to intersect the chromite-rich zone which had been defined by surface mapping in the original study. The dominant rock type intersected in these holes was serpentinite, after pyroxene-bearing dunite. The serpentinite has a high percentage of disseminated chrome-spinel which has a Cr* around 66. Chromitite lenses were not intersected by any of the drill holes, indicating that the zone defined by surface mapping is discontinuous down dip.

The fourth hole was drilled at Melba Flats, at the site of the sample which gave the Pt reading of 1244 ppb in the earlier study. The resultant core was dominantly sheared serpentinite with disseminated chrome spinel. The top ten metres of the drill hole, and the zone between 75 and 85 m, contained chrome-spinel with a Cr* around 84, whereas the rest of the core contained chrome-spinel with a Cr* around 60 (fig. 4). The fifth hole was drilled into the associated two-pyroxene gabbro, and the sixth into the low-titanium basalt.

Samples obtained from drill core were prepared by fire assay–NiS collection and analysed by INAA techniques at Becquerel Laboratories, Lucas Heights, Sydney, Australia.

The analyses obtained from the drill hole samples do not reflect the results obtained from grab samples of surface outcrop. At Melba Flats, with the exception of one 50 mm thick chromitite band encountered at 18 m, none of the samples gave PGE values greater then detection limit values.

Element	Au	Ir	Os	Pd	Pt	Ru
Detection limit (ppb)	1	0.5	5	10	20	20
Melba Flats chromitite sample	20	51	58	<10	32	320

Samples from the three holes drilled into the olivine-rich sequence Pt, Pd, Os and Ru were all below detection limits. Ir values ranged between 0.9 and 5.0 ppb, with an average of 2.3 ppb for ten samples. However the fifteen samples from the three holes averaged 25 ppb gold, and small Ni-Fe-Co sulphide grains were ubiquitous throughout the samples.

All PGE were below detection limits for the samples of two-pyroxene gabbro. Gold averaged 28 ppb across the section. The low-titanium basalt recorded an average of 21.5 ppb for Pd, and below detection limits for other PGE. Gold averaged 86 ppb across the 100 m section.

Individual grains of PGE alloys or PGM are rarely found in polished sections. Two PGM grains which were found occurred within chrome spinel grains which were obtained from areas of high spinel concentration within the olivine-rich sequence. The first grain (Plate 7) was an Os-Ir-Ru alloy with subsiduary amounts of Cr, Fe, As and S. The amount of PGE's in the analysis was 80.81 wt% in the proportions $Os_{0.554}$:$Ir_{0.322}$:$Ru_{0.124}$. The grain is 10 µm long by 9 µm wide. The second grain (Plate 8) is a rectangular grain of laurite, 15 µm long by 7 µm wide. The analysis, with a total of 100.81 wt%, gave a formula of $(Ru_{1.003}, Os_{0.055}, Ir_{0.032})_{1.09}\ S_2$.

This follow-up study to Brown *et al.* (1988), shows that

- Platinum Group Elements and/or minerals are not distributed evenly over stratigraphic depth;
- the chromitite zone defined by surface mapping is discontinuous at depth as well as along strike;
- grab samples from surface outcrop are not necessarily representative of a continuous section through a specific unit;
- when dealing with low level PGE contents, different parts of a specific whole-rock sample do not necessarily give repeatable PGE values.

REFERENCES

BOTTRILL, R. S. 1989. Economic Geology, *in:* BROWN, A. V. *et al.* Geological atlas 1:50 000 series. Sheet 73 (8112N). Huntley. *Explan. Rep. geol. Surv. Tasm.*

BROWN, A. V. 1986. Geology of the Dundas–Mt Lindsay–Mt Youngbuck region. *Bull. geol. Surv. Tasm.* 62.

BROWN, A. V.; PAGE, N. J.; LOVE, A. H. 1988. Geology and Platinum-Group-Element geochemistry of the Serpentine Hill Complex, Dundas Trough, Western Tasmania. *Can. Mineral.* 26:161–175.

BROWN, A. V.; JENNER, G. A. 1989. Geological setting, petrology and chemistry of Cambrian boninite and low-Ti tholeiite lavas in western Tasmania, *in:* CRAWFORD, A. J. (ed). *Boninites and related rocks*. Allen & Unwin: London.

CABRI, L. J.; HARRIS, D. C. 1975. Zoning in Os-Ir alloys and the relation of the geological and tectonic environment of the source rocks to the bulkPt:Pt+Ir+Co ratio for placers. *Can. Mineral.* 13:266–274.

FORD, R. J. 1981. Platinum-group minerals in Tasmania. *Econ. Geol.* 76:408–186.

NYE, P. B. 1929. The osmiridium deposits of the Adamsfield district. *Bull. geol. Surv. Tasm.* 39.

PAGE, N. J.; ENGIN, T.; SINGER, D. A.; HAFFTY J. 1984. Distribution of Platinum-Group Elements in the Bati Kef chromite deposit, Guleman–Elazig areas, Eastern Turkey. *Econ. Geol.* 79:177–184.

REID, A. M. 1921. Osmiridium in Tasmania. *Bull. geol. Surv. Tas.* 32.

[3 November 1989]

Table 1 (a)

COMPOSITIONS OF PGE MINERALS FROM ADAMSFIELD

	mass %									atomic %						
No.	Os	Ir	Ru	Rh	Pt	Pd	Fe	Ni	Totals	Os	Ir	Ru	Rh	Pt	Fe	Mineral
1	45.51	41.65	6.40	0.29	1.12	tr	na	na	94.97	46.08	41.73	12.19	...	...	...	Bulk sample
2	48.40	44.70	5.60	0.61	0.67	0.05	1.40	0.27	101.70	46.91	42.88	10.21	...	...	...	Rutheniridosmine
3	49.10	46.50	5.30	0.60	0.75	nd	0.07	0.01	102.33	46.72	43.79	9.49	...	...	...	Iridosmine
4	47.90	46.50	5.40	0.66	0.96	nd	0.29	0.04	101.75	46.02	44.21	9.76	...	...	...	Iridosmine
5	26.50	65.30	3.70	0.53	5.00	nd	0.45	0.10	101.58	27.02	65.88	7.10	...	...	...	Osmiridium
6	44.70	46.40	7.60	0.49	1.00	0.05	0.56	0.09	100.89	42.61	43.77	13.63	...	...	...	Rutheniridosmine
7	49.80	46.30	4.20	0.49	0.67	nd	0.28	0.05	101.79	48.11	44.26	7.63	...	...	...	Iridosmine
8	50.46	42.97	6.42	0.00	0.00	na	0.49	na	100.34	48.03	40.47	11.50	...	...	...	Rutheniridosmine
9	51.41	43.13	5.44	0.43	0.00	na	0.54	na	100.95	49.28	40.91	9.81	...	...	...	Iridosmine
10	52.24	42.52	5.18	0.42	0.00	na	0.56	na	100.92	50.20	40.43	9.36	...	...	...	Iridosmine
11	50.81	42.54	4.95	0.67	0.00	na	0.43	na	99.40	49.71	41.18	9.11	...	...	...	Iridosmine
12	50.09	43.03	5.60	0.00	0.00	na	0.58	na	99.30	48.53	41.26	10.21	...	...	...	Rutheniridosmine
13	2.96	7.41	6.10	8.36	72.24	na	3.81	na	100.88	2.45	6.08	9.51	12.81	58.39	10.75	Rhodium iron platinum
14	0.00	1.29	0.00	4.94	86.35	na	7.07	na	99.65	0.00	1.08	0.00	7.70	70.95	20.28	Iron platinum

Analyses: 1 – from Nye, 1929 (the average of 31 concentrates); 2-7 – from; Cabri and Harris, 1975; 8-14 – from Ford, 1981.

tr = trace, nd = not detected, na = no analysis given

Table 1 (b)

ANALYSES OF OSMIRIDIUM FROM ADAMSFIELD (from Nye, 1929)

	mass %							
No.	Ir	Os	Ru	Pt	Rh	Pd	Au	Remarks
1	40.80	46.10	8.00	2.00	0.80	tr	...	From Eames and Scoles' Claim
2	39.20	50.20	6.50	2.00	1.00	tr	...	Hansen's Claim
3	38.40	47.00	9.80	1.60	1.60	tr	...	H. Tudor's Claim
4	36.30	47.25	10.60	2.20	1.60	tr	...	General sample
5	40.12	44.89	6.50	1.02	0.18	...	...	From 60 oz parcels
6	40.48	44.14	6.54	1.00	0.20	...	...	
7	40.02	43.96	6.67	1.16	0.20	...	...	
8	44.35	45.74	6.46	...	tr	...	tr	
9	41.43	43.50	5.35	1.10	0.16	...	0.007	Samples from 50 oz parcels
10	42.33	43.86	5.97	1.06	0.17	...	0.03	
11	42.70	46.28	5.54	1.04	0.18	...	0.003	
12	41.37	46.84	5.29	1.01	0.16	...	0.005	
13	42.80	47.10	5.52	0.48	0.14	...	0.002	
14	42.22	46.30	6.03	0.92	0.14	...	0.005	
15	43.21	45.88	5.81	1.04	0.14	...	0.003	
16	42.39	44.96	6.75	1.25	0.17	...	nil	
17	41.25	43.92	6.59	1.27	0.21	...	nil	
18	42.85	44.10	6.47	1.21	0.19	...	0.007	Samples from 75 oz parcels
19	42.82	44.30	6.12	1.36	0.22	...	nil	
20	43.58	44.36	5.81	0.50	0.14	...	nil	
21	42.11	45.70	6.16	0.56	0.10	...	nil	
22	42.03	45.92	5.73	0.52	0.16	...	nil	50 oz parcel
23	42.62	43.31	6.43	1.14	0.14	...	nil	75 oz parcel
24	41.45	46.80	6.13	1.12	0.16	...	nil	75 oz parcel
25	42.53	44.36	6.02	1.24	0.18	...	nil	50 oz parcel
26	41.66	43.35	6.48	1.34	0.12	...	nil	75 oz parcel
27	42.02	46.22	5.30	1.21	0.11	...	nil	75 oz parcel
28	41.85	46.64	5.49	0.92	0.12	...	nil	50 oz parcel
29	41.76	45.74	6.79	1.14	0.19	...	nil	75 oz parcel
30	42.20	45.83	6.35	1.26	0.18	...	nil	75 oz parcel
31	42.28	46.50	6.31	1.20	0.18	...	nil	50 oz parcel
Average	41.65	45.51	6.40	1.12	0.29	...	0.002	

Analysts:

Samples 1-4. Department of Mines Laboratory, Launceston
Samples 5-7. Daniel C. Griffith & Co., London
Sample 8. Mathey's, London
Samples 9-31. Daniel C. Griffith & Co., London

Table 2

AVERAGE PGE VALUES FOR SAMPLES FROM THE LPD SUCCESSION (from Brown et al., 1988)

Rock type	No. of samples	Pt	Pd	Rh	Ru	Ir
		(ppb)				
Pyroxenite	6	25	1	<1	<100	<20
Peridotite	6	20	<1	<1	<100	<20

Table 3

AVERAGE PGE VALUES FOR SAMPLES FROM VARIOUS PARTS OF THE LPG SUCCESSION AT SERPENTINE HILL (from Brown et al., 1988)

Rock type and sequence	Pt	Pd	Rh	Ru	Ir
	(ppb)				
Orthopyroxene-rich layered sequence	36.0 (4)	1.7 (3)	2.0 (3)	<100	<20
Olivine-rich layered sequence					
a) Dunite with a high chrome spinel content	22.3 (6)	1.0 (3)	<1	<100	<20
b) Chromitite lenses in dunite	44.5 (6)	3.4 (5)	6.2 (6)	270 (6)	68.3 (6)
Melba Flats—chromitite lense	1240	4	54	180	70
Two-pyroxene gabbro	36.0 (4)	10.3 (4)	<1	<100	<20
Low-titanium tholeiite	37	25	<1	<100	<20

(number of samples, if greater than one, in parentheses)

(Surface whole-rock samples analysed by fire-assay/atomic absorption for Pt, Pd and Rh, and by fire assay/spectrographic technique for Ir and Ru, at the USGS Laboratories, Lakewood, Colorado, USA. See Brown *et al.* (1988)

Plate 1.

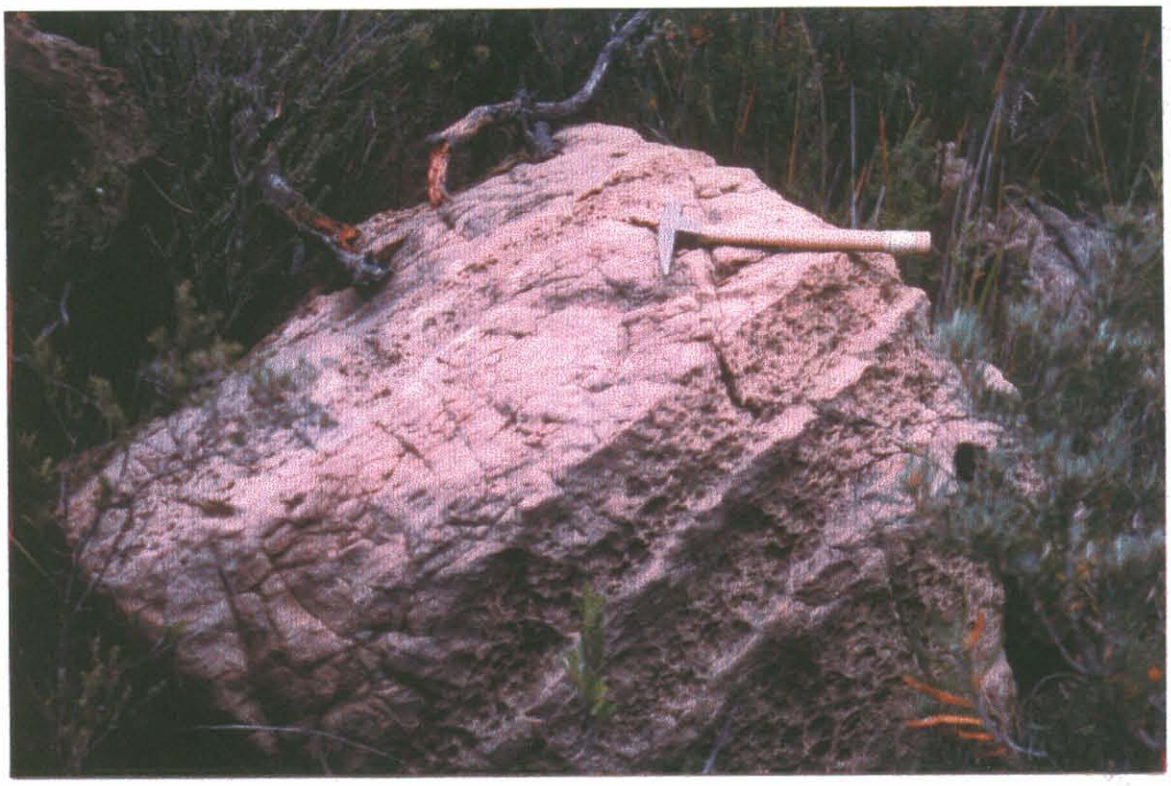

Plate 2.

Plates 1 and 2. *Typical layering within the LDH succession. The smooth textured layers are dunite, and the 'pock-marked' textured layers either orthopyroxne-bearing dunite or harzburgite. Location: Harman River area.*

5 cm

Plate 3.

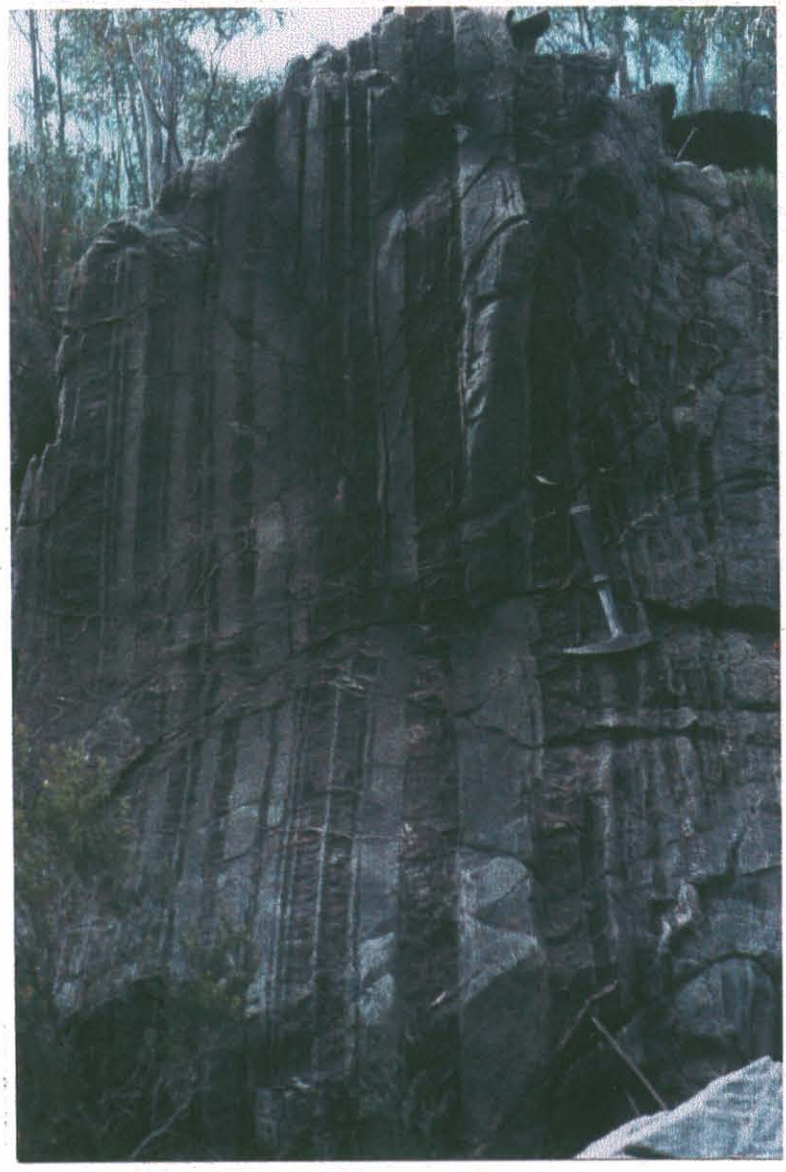

Plates 3 and 4. *Typical layering within the LPD Succession. The smooth-textured, light grey layers are dunite; the relatively smooth light brown layers are olivine-bearing orthopyroxenite; and the rough-textured, brown layers are orthopyroxenite.*

Locations: Plate 3 Rileys Knob; Plate 4 Adamsfield.

5 cm

Plate 4.

62/63

Plate 5. *Layer types in orthopyroxenite-rich sequence. Smooth areas are olivine-rich, rough areas are orthopyroxene-rich. In the middle of the plate is a typical dunite → harzburgite → orthopyroxenite graded layer.*

Plate 6. *Unconformity in orthopyroxenite-rich sequence. Mineralogy is the same as Plate 5.*

Plates 5 and 6. *Typical layering within the LPG Succession, Serpentine Hill.*

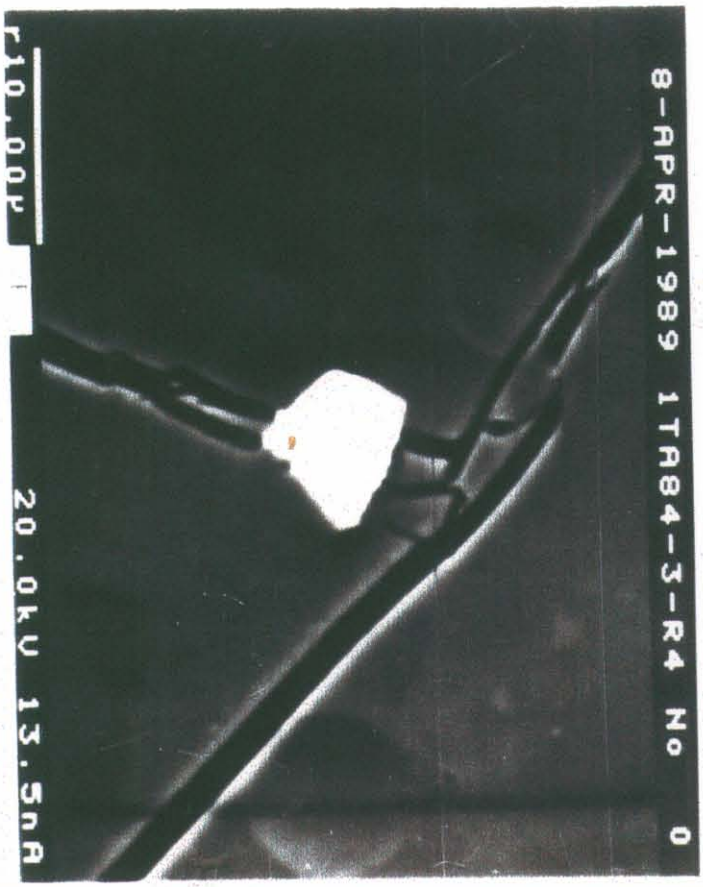

Plate 7. *A grain of Os-Ir-Ru alloy in a chrome-spinel crystal from a chromitite lense in LPG succession rocks, Serpentine Hill.*

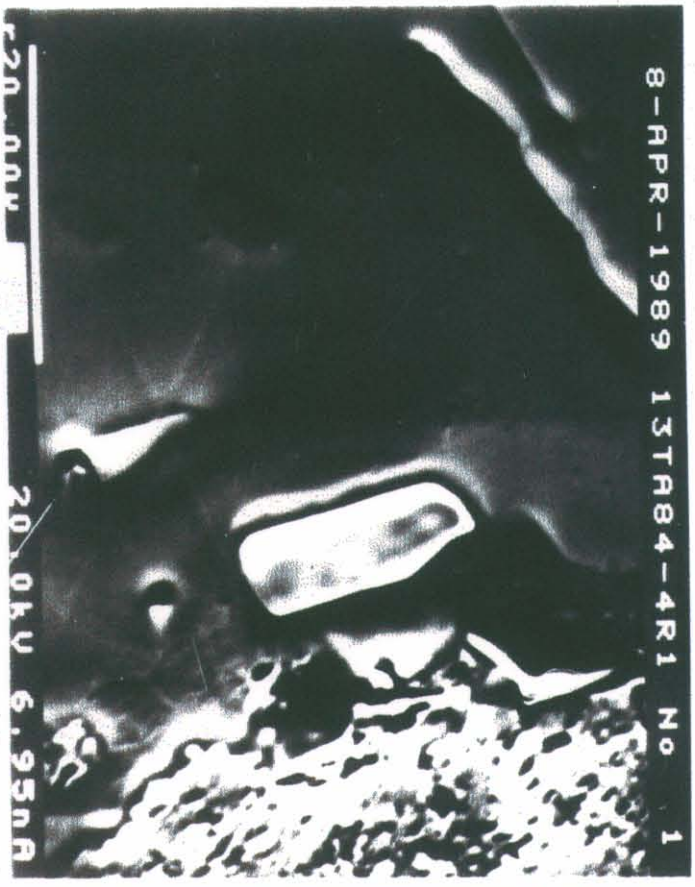

Plate 8. *A laurite grain in a chrome spinel crystal from a chromitite lense in LPG succession rocks, Serpentine Hill.*

5 cm